

Systems metabolic engineering of *Escherichia coli* for
production of
violacein and deoxyviolacein

Dissertation zur Erlangung des Grades
eines Doktors der Ingenieurwissenschaften (Dr.-Ing.)
der Naturwissenschaftliche-Technischen Fakultät III Chemie, Pharmazie,
Bio- und Werkstoffwissenschaften
der Universität des Saarlandes

von
André Luis Rodrigues

Saarbrücken
2014

Tag des Kolloquiums:	14. November 2014
Dekan:	Prof. Dr.-Ing. Dirk Bähre
Berichterstatter:	Prof. Dr. Christoph Wittmann Prof. Dr. Rolf Müller
Vorsitz:	Prof. Dr. Gert-Wieland Kohring
Akademischer Mitarbeiter:	Dr. Björn Becker

“Reality is merely an illusion, albeit a very persistent one.”

Albert Einstein

Peer-reviewed publications

Partial results of this work have been published in advance authorized by the Institute of Biochemical Engineering (Technische Universität Braunschweig) and the Institute of Systems Biotechnology (Universität des Saarlandes) represented by Prof. Dr. Christoph Wittmann.

Rodrigues, A. L., Becker, J., Lima, A. O. S., Porto, L. M., Wittmann, C., 2014. Systems metabolic engineering of *Escherichia coli* for gram scale production of the antitumor drug deoxyviolacein from glycerol. *Biotechnology and Bioengineering*. 111, 2280-2289.

Rodrigues, A. L., Trachtmann, N., Becker, J., Lohanatha, A. F., Blotenberg, J., Bolten, C. J., Korneli, C., Lima, A. O. S., Porto, L. M., Sprenger, G. A., Wittmann, C., 2013. Systems metabolic engineering of *Escherichia coli* for production of the antitumor drugs violacein and deoxyviolacein. *Metabolic Engineering*. 20, 29-41.

Poblete-Castro, I., Binger, D., Rodrigues, A. L., Becker, J., Dos Santos, V., Wittmann, C., 2013. In-silico-driven metabolic engineering of *Pseudomonas putida* for enhanced production of poly-hydroxyalkanoates. *Metabolic Engineering*. 15, 113-123.

Rodrigues, A. L., Göcke, Y., Bolten, C. J., Brock, N. L., Dickschat, J. S., Wittmann, C., 2012. Microbial production of the drugs violacein and deoxyviolacein – analytical development and strain comparison. *Biotechnology Letters*. 34, 717-720.

Conference contributions - lectures

Rodrigues, A. L., Göcke, Y., Bolten, C. J., Brock, N. L., Dickschat, J. S., Porto, L. M., Lima, A. O. S., Trachtmann, N., Sprenger, G. A., Wittmann, C., 2012. Systems metabolic engineering of *Escherichia coli* for production of violacein and deoxyviolacein. VAAM International Workshop. 27-29 September, Braunschweig, Germany.

Rodrigues, A. L., Göcke, Y., Bolten, C. J., Brock, N. L., Dickschat, J. S., Porto, L. M., Lima, A. O. S., Trachtmann, N., Sprenger, G. A., Wittmann, C., 2013. Systems metabolic engineering of *Escherichia coli* for production of violacein and deoxyviolacein. 1. MINAS Symposium. 20-21 June 2013, Warberg, Germany.

Conference contributions - Posters

Rodrigues, A. L., David, F., Wucherpfennig, T., Eslahpazir, M., Korneli, C., Krull, R., Wittmann, C., 2012. Pharmaceutical engineering research at the institute of biochemical engineering. Research Colloquium on Pharmaceutical Engineering, 7 May, Braunschweig, Germany.

Rodrigues, A. L., Göcke, Y., Bolten, C. J., Brock, N. L., Dickschat, J. S., Porto, L. M., Lima, A. O. S., Trachtmann, N., Sprenger, G. A., Wittmann, C., 2012. Systems-wide pathway engineering for production of violacein and deoxyviolacein in recombinant *Escherichia coli*. ProcessNet-Jahrestagung und 30. DECHEMA-Jahrestagung der Biotechnologen, 10-13 September, Karlsruhe, Germany.

Rodrigues, A. L., Bolten, C. J., Bergmann, S., Korneli, C., Porto, L. M., Lima, A. O. S., Wittmann, C., 2011. Production of violacein and derivatives in *Escherichia coli*. 2ND Summer School – Biotransformations, 22-25 August, Bad Herrenalb, Germany.

Acknowledgements

Coming to Germany was really a nice experience. Beyond knowing a new culture, this time abroad has enabled me to have another perspective of my own country. Now I have experimental proof that it is possible to play soccer under $-10\text{ }^{\circ}\text{C}$. I would like to thank Prof. Christoph Wittmann for giving me the opportunity of conducting this work under his supervision, for the nice work together, for the possibility of knowing Germany, and especially for his patience during my studies since our first meeting in Curitiba. I am also thankful to Prof. André O. S. Lima and friends at Vale do Itajaí University for everything that I have learnt during my time in Itajaí, and also for the after-work time skateboarding or surfing on the Praia Brava beach. To Prof. Luismar M. Porto (and the intelLab team) I would like to thank for the wonderful time in Florianópolis and, in addition to Prof. André O. S. Lima, for the possibility of continuing to work on the violacein project in Germany. I would like to express gratitude to Prof. Dr. Rolf Müller and Prof. Dr. Gert-Wieland Kohring for accepting the invitation to participate as members of the evaluation committee. I would like to thank my wife Franciane Moretti for joining me during this time. I am happy that she could adapt and was able to pursue her professional aspirations. In spite of being skeptical about the fact that, according to the German Academic Exchange Service (DAAD), learning to speak German in six months is possible, now I know that this goal is indeed achievable, at least in part. Despite being able to use the *Konjunktiv II der Vergangenheit mit Modalverben*, sometimes mimicry skills can help the life a lot in daily tasks. To all people of ibvt, I would like to thank for the help, hospitality, team work, and for the nice parties and barbecues. I am particularly thankful to Dr. Christoph J. Bolten and Dr. Judith Becker for helping me to get started at ibvt; Dr. Claudia Korneli, Dr. Juan Carlos Sigala Alanís, Dr. Sven Bergmann, Yvonne Göcke, for the help with equipments and techniques; and M.Sc. Jana Blotenberg and Dr. Ignacio Poblete Castro for the team work. I thank also my office colleagues for the wonderful time together and for the mutual diet sabotages by bringing cookies and all other kinds of candies to avoid glucose limitation while working in the office. As the ibvt soccer team could see, there are in fact Brazilians that can not play soccer so well, but I will keep trying. I also thank Prof. Georg A. Sprenger, Dr. Natalie Trachtmann for the nice time spent in Stuttgart and for the collaboration; and Dr. Jeroen S. Dickschat, and

M.Sc. Nelson L. Brock for the support. I would like to thank Prof. John Pemberton for the kind donation of plasmids. To DAAD, I would like to express gratitude for providing the means to support my studies, as well as the nice time spent together in the meetings. Financial support from Max-Buchner Foundation and the Coordenação de Aperfeiçoamento de Pessoal de Nível Superior (CAPES) is also gratefully acknowledged. I would like also to express gratitude to my students Ananta Fabian Lohanatha and Thomas Krieg, for the fun time working together. Finally, I would like to thank my family and friends for their support along the last years. Nothing that we have accomplished here would have been possible without you.

Table of Contents

LIST OF FIGURES	I
LIST OF TABLES	V
SUMMARY	1
ZUSAMMENFASSUNG	2
1 INTRODUCTION	3
1.1. VIOLACEIN AND DEOXYVIOLACEIN	3
1.1.1. <i>Biotechnological and therapeutic potential of violacein and deoxyviolacein</i>	3
1.2. E. COLI AS INDUSTRIAL PRODUCTION HOST.....	7
1.3. PHYSIOLOGY AND METABOLISM OF E. COLI.....	8
1.3.1. <i>Transport and metabolism of glucose, L-arabinose and glycerol</i>	10
1.3.2. <i>Metabolic pathways of the central metabolism</i>	14
1.3.3. <i>Anapleurotic reactions</i>	20
1.3.4. <i>L-Tryptophan biosynthesis</i>	21
1.4. ESCHERICHIA COLI AS HOST FOR VIOLACEIN AND DEOXYVIOLACEIN PRODUCTION	24
1.4.1. <i>Tools for genetic engineering</i>	25
1.4.2. <i>Heterologous production of violacein and deoxyviolacein</i>	27
2 MATERIALS AND METHODS	31
2.1. DEVELOPMENT OF METHODS FOR SEPARATION AND QUANTIFICATION OF VIOLACEIN AND DEOXYVIOLACEIN.....	31
2.1.1. <i>Organisms and growth conditions</i>	31
2.1.2. <i>Preparation of pure violacein and deoxyviolacein</i>	31
2.1.3. <i>Quantification of violacein and deoxyviolacein</i>	32
2.1.4. <i>Estimation of extinction coefficients</i>	32
2.2. SYSTEMS METABOLIC ENGINEERING OF ESCHERICHIA COLI FOR PRODUCTION OF VIOLACEIN AND DEOXYVIOLACEIN FROM L-ARABINOSE	32
2.2.1. <i>Strains and plasmids</i>	32
2.2.2. <i>Construction of the violacein production plasmid</i>	33
2.2.3. <i>Construction of the deoxyviolacein production plasmid</i>	36
2.2.4. <i>Genomic integration of the vioD gene</i>	37
2.2.5. <i>Transduction of target constructs</i>	37
2.2.6. <i>Growth media</i>	39
2.2.7. <i>Cultivation in shake flasks</i>	40
2.2.8. <i>Fed-batch production in bioreactor</i>	40
2.2.9. <i>Quantification of cell concentration</i>	41
2.2.10. <i>Quantification of violacein and deoxyviolacein</i>	41
2.2.11. <i>Quantification of sugars and organic acids</i>	42
2.2.12. <i>Intracellular amino acids</i>	42

2.2.13. <i>Extraction and crystallization of violacein</i>	43
2.3. SYSTEMS METABOLIC ENGINEERING OF <i>ESCHERICHIA COLI</i> FOR PRODUCTION OF DEOXYVIOLACEIN FROM GLYCEROL	43
2.3.1. <i>Strains and plasmids</i>	43
2.3.2. <i>Genetic engineering</i>	44
2.3.3. <i>Growth media</i>	45
2.3.4. <i>Microplate cultivation</i>	46
2.3.5. <i>Shake flask cultivation</i>	47
2.3.6. <i>Fed-batch cultivation</i>	47
2.3.7. <i>Quantification of cell concentration</i>	47
2.3.8. <i>Quantification of sugars, glycerol and acetate</i>	48
2.3.9. <i>Quantification of deoxyviolacein</i>	48
2.3.10. <i>Purification of deoxyviolacein</i>	48
2.3.11. <i>GC-MS labelling analysis</i>	48
3 RESULTS	50
3.1. HPLC-BASED SEPARATION AND QUANTIFICATION OF VIOLACEIN AND DEOXYVIOLACEIN.....	50
3.1.1. <i>Evaluation of photometric measurement of crude violacein</i>	50
3.1.2. <i>Development of an HPLC method for quantification of violacein and deoxyviolacein</i> ..	51
3.1.3. <i>Quantification of violacein and deoxyviolacein in microbial cultures</i>	52
3.2. SYSTEMS METABOLIC ENGINEERING OF <i>ESCHERICHIA COLI</i> FOR PRODUCTION OF VIOLACEIN AND DEOXYVIOLACEIN.....	53
3.2.1. <i>Construction of a basic strain for deoxyviolacein production</i>	53
3.2.2. <i>Evaluation of deoxyviolacein and violacein analytics</i>	55
3.2.3. <i>Impact of temperature and chaperone co-expression on deoxyviolacein production by recombinant E. coli</i>	57
3.2.4. <i>Quantification of intracellular precursor availability by targeted metabolite analysis</i>	58
3.2.1. <i>Design of feedback-resistant enzymes in supporting pathways</i>	60
3.2.2. <i>Metabolic engineering of tryptophan supply</i>	60
3.2.3. <i>Metabolic engineering of the chorismate supply</i>	62
3.2.4. <i>Metabolic engineering of erythrose 4-phosphate supply</i>	63
3.2.5. <i>Metabolic engineering of serine supply</i>	63
3.2.6. <i>Evaluation of the capacity of carbon core metabolism and the heterologous deoxyviolacein pathway</i>	64
3.2.7. <i>Fed-batch production of deoxyviolacein in E. coli dVio-6 from L-arabinose as carbon source</i>	64
3.2.8. <i>Elimination of L-arabinose metabolism in producing E. coli</i>	65
3.2.9. <i>Verification of deletion of the gene of the tryptophan repressor, TrpR</i>	68
3.2.10. <i>Evaluation of deoxyviolacein production on different carbon sources</i>	68
3.2.11. <i>Investigation of remaining L-arabinose turnover in E. coli ΔaraBAD using ¹³C labeling experiments</i>	69
3.2.12. <i>Glycerol-based fed-batch production of deoxyviolacein by E. coli dVio-8</i>	71

3.2.13. Extension of the product spectrum to violacein	72
3.2.14. Production performance of the designed violacein mutant in a fed-batch process.....	73
4 DISCUSSION	75
4.1.1. HPLC method for quantification of violacein and deoxyviolacein.....	75
4.1.2. The synthetic <i>E. coli</i> based producers enable efficient and safe production of violacein and deoxyviolacein	75
4.1.3. Systems metabolic engineering of supporting pathways drives secondary metabolite production	76
4.1.4. The arabinose-inducible system mediates stable expression of the heterologous pathway.....	76
4.1.5. The comparative evaluation of deoxyviolacein and violacein production should consider the analytical method used.....	77
4.1.6. Production of deoxyviolacein using glycerol as carbon source.....	78
5 CONCLUSIONS AND OUTLOOK.....	81
6 REFERENCES	83
7 APPENDIX	98
7.1. SUPPLEMENTARY INFORMATION	98
7.1.1. Construction of strains TRP1 to TRP6	98
7.1.2. Cloning of vector pJNNmod.....	107

List of Figures

FIGURE 1. CENTRAL METABOLISM OF <i>E. COLI</i> AND L-TRYPTOPHAN PATHWAY. COMPOUND NAMES: G6P (GLUCOSE 6-PHOSPHATE), F6P (FRUCTOSE 6-PHOSPHATE), GAP (GLYCERALDEHYDE 3-PHOSPHATE), 3PG (3-PHOSPHOGLYCERATE), PEP (PHOSPHOENOLPYRUVATE), PYR (PYRUVATE), ACCOA (ACETYL-CoA), OAA (OXALOACETATE), IND (INDOLE), RUL5P (RIBULOSE 5-PHOSPHATE), XYL5P (XYLULOSE 5-PHOSPHATE), RIB5P (RIBOSE 5-PHOSPHATE), SED7P (SEDOHEPTULOSE 7-PHOSPHATE), E4P (ERYTHROSE 4-PHOSPHATE), SER (L-SERINE), DAHP (3-DEOXY-D-ARABINO-HEPTULOSONATE-7-PHOSPHATE), CHO (CHORISMATE), ANTH (ANTHRANILATE), TRP (L-TRYPTOPHAN), IPA (INDOLE-3-PYRUVIC ACID IMINE), PDVA (PROTODEOXYVIOLACEINIC ACID), AND AC (ACETATE).	9
FIGURE 2. STRUCTURE OF THE ARAC PROTEIN AND MECHANISM OF ACTIVATION AND REPRESSION OF THE <i>ARABAD</i> PROMOTER. A) DOMAINS OF THE ARAC MONOMER AND THE ACTIVATOR AND REPRESSOR FORMS OF THE ARAC DIMMER. B) ORGANIZATION OF THE P _{BAD} AND P _C PROMOTERS. C) MECHANISM OF REPRESSION AND ACTIVATION OF THE <i>ARABAD</i> PROMOTER IN THE PRESENCE AND ABSENCE OF L-ARABINOSE AND THE CRP PROTEIN. THIS FIGURE WAS MODIFIED FROM (MOAT ET AL., 2003).	13
FIGURE 3. OVERVIEW OF GENETIC MODIFICATION USING THE RECOMBINEERING METHODOLOGY FOLLOWED BY MARKER REMOVAL.	26
FIGURE 4. BIOSYNTHETIC PATHWAYS FOR VIOLACEIN AND DEOXYVIOLACEIN.	28
FIGURE 5. ANALYSIS OF VIOLACEIN AND DEOXYVIOLACEIN: EXTINCTION COEFFICIENTS FOR MIXTURES OF VIOLACEIN AND DEOXYVIOLACEIN (A), HPLC ANALYSIS OF VIOLACEIN (B), DEOXYVIOLACEIN (C) AND A MIXTURE (D) ON A C18 COLUMN WITH 50% (v v ⁻¹) ETHANOL AS MOBILE PHASE. THE SAMPLES REFLECT STANDARD SOLUTIONS OF 6.0 MG L ⁻¹ VIOLACEIN (B), 19.5 MG L ⁻¹ DEOXYVIOLACEIN (C) AND 1:1 (v v ⁻¹) MIX OF BOTH (D). THE RESPECTIVE UV-VIS SPECTRUM IS PRESENTED FOR EACH PEAK. FOR MEASUREMENT OF EXTINCTION COEFFICIENTS, THE PIGMENTS WERE DISSOLVED IN ETHANOL AND ANALYZED AT $\lambda = 575$ NM.	50
FIGURE 6. VIOLACEIN AND DEOXYVIOLACEIN PRODUCTION PROFILES OF <i>J. LIVIDUM</i> DSM 1522 CULTIVATED IN LB MEDIUM WITH 1% (w v ⁻¹) GLYCEROL AT 25 °C.	52
FIGURE 7. CONTROL OF THE DEOXYVIOLACEIN PRODUCTION IN <i>E. COLI</i> dVio-1, USING THE ARAC SYSTEM AND L-ARABINOSE AS INDUCER FOR <i>vioABCE</i> EXPRESSION: PLATE-GROWN CELLS ON COMPLEX LB MEDIUM WITH KANAMYCIN (A) AND ON COMPLEX LB MEDIUM WITH KANAMYCIN AND L-ARABINOSE (B).	53
FIGURE 8. GROWTH AND PRODUCTION PROFILE OF RECOMBINANT <i>E. COLI</i> dVio-1 (A), dVio-6 (B), AND TRP11 (C) IN MINERAL MEDIUM CONTAINING 10 G L ⁻¹ L-ARABINOSE AS CARBON AND ENERGY SOURCE. N=3.....	54
FIGURE 9. HPLC BASED ANALYSIS OF VIOLACEIN AND DEOXYVIOLACEIN. THE CHROMATOGRAMS DISPLAY A PURIFIED DEOXYVIOLACEIN STANDARD (A), AN EXTRACT FROM THE CULTURE BROTH OF <i>E. COLI</i> dVio-1 (B), A PURIFIED VIOLACEIN STANDARD (C), AND AN EXTRACT FROM THE CULTURE BROTH OF <i>E. COLI</i> Vio-4 (D). THE ELUTING COMPOUNDS REPRESENT VIOLACEIN (1) AND DEOXYVIOLACEIN (2).	55

FIGURE 10. EFFECT OF CHAPERONE CO-EXPRESSION ON DEOXYVIOLACEIN PRODUCTION BY RECOMBINANT <i>E. COLI</i> DVIO-1 AT 30 °C. THE EXPRESSED CHAPERONES CORRESPOND TO THE DIFFERENT PLASMIDS (TABLE 2) USED, I.E. PGRO7 (<i>GROES GROEL</i>). THEIR EXPRESSION WAS INDUCED BY ADDITION OF TETRACYCLINE (TET) AND/OR L-ARABINOSE (ARA). THE DASHED LINE MARKS THE LEVEL OF THE BASIC PRODUCER AT 20 °C. N=3.	57
FIGURE 11. DEOXYVIOLACEIN TITER (A) AND INTRACELLULAR LEVELS OF TRYPTOPHAN (B) AND SERINE (C) IN THE PARENT STRAIN <i>E. COLI</i> NC (CONTROL), THE RECOMBINANT PRODUCERS DVIO-1 THROUGH DVIO-6, AND THE TRYPTOPHAN PRODUCER TRP11 (TABLE 2) IN L-ARABINOSE MINERAL MEDIUM. N=3.	59
FIGURE 12. SYSTEMS METABOLIC ENGINEERING OF VIOLACEIN AND DEOXYVIOLACEIN PRODUCTION IN <i>ESCHERICHIA COLI</i> . BOLD, GREEN ARROWS MARK REACTIONS THAT WERE AMPLIFIED BY OVEREXPRESSION OF THE ENCODING GENES AND DE-REGULATION OF FEEDBACK CONTROLLED REACTION STEPS. ELIMINATED REACTIONS OR CONTROL MECHANISMS, OBTAINED BY GENE DELETION ARE MARKED IN RED COLOR. COMPOUND NAMES: G6P (GLUCOSE 6-PHOSPHATE), F6P (FRUCTOSE 6-PHOSPHATE), GAP (GLYCERALDEHYDE 3-PHOSPHATE), 3PG (3-PHOSPHOGLYCERATE), PEP (PHOSPHOENOLPYRUVATE), PYR (PYRUVATE), ACCOA (ACETYL-COA), OAA (OXALOACETATE), IND (INDOLE) RUL5P (RIBULOSE 5-PHOSPHATE), XYL5P (XYLULOSE 5-PHOSPHATE), RIB5P (RIBOSE 5-PHOSPHATE), SED7P (SEDOHEPTULOSE 7-PHOSPHATE), E4P (ERYTHROSE 4-PHOSPHATE), SER (SERINE), DAHP (3-DEOXY-D-ARABINO-HEPTULOSONATE-7-PHOSPHATE), CHO (CHORISMATE), ANTH (ANTHRANILATE), TRP (TRYPTOPHAN), IPA (INDOLE-3-PYRUVIC ACID IMINE), PDVA (PROTODEOXYVIOLACEINIC ACID), AND AC (ACETATE).....	61
FIGURE 13. FED-BATCH PRODUCTION OF DEOXYVIOLACEIN IN <i>E. COLI</i> DVIO-6. THE DASHED LINE MARKS THE BEGINNING OF THE FEED PHASE. THE FEED RATE WAS ADJUSTED TO A CONSTANT GROWTH RATE OF 0.011 h ⁻¹ , BASED ON GROWTH PARAMETERS (M _{MAX} = 0.018 h ⁻¹ , Y _{X/S} = 0.235 g g ⁻¹) PREVIOUSLY OBTAINED (RODRIGUES ET AL., 2013).	65
FIGURE 14. VALIDATION OF GENETIC MODIFICATIONS IN DEOXYVIOLACEIN PRODUCING <i>E. COLI</i> DVIO-8: DELETION OF <i>ARABAD</i> (A) AND OF <i>TRPR</i> (B). LANES 1-3 SHOW PCR PRODUCTS FOR VALIDATION OF <i>ARABAD</i> DELETION IN STRAINS MG1655 (1), Δ <i>ARABAD</i> (2), AND DVIO-8 (3). LANES 4-6 SHOW PCR PRODUCTS FOR VALIDATION OF <i>TRPR</i> DELETION IN STRAINS MG1655 (4), Δ <i>ARABAD</i> (5), AND DVIO-8 (6).....	66
FIGURE 15. GROWTH OF <i>E. COLI</i> STRAINS DVIO-6 (A) AND DVIO-8 (B) IN MINERAL MEDIUM WITH L-ARABINOSE AS SINGLE CARBON SOURCE. CULTIVATIONS WERE PERFORMED IN SHAKEN FLASKS (N=3).	67
FIGURE 16. <i>E. COLI</i> DVIO-8 IS GROWN ON LB AGAR PLATES WITH L-ARABINOSE AS INDUCER OF GENE EXPRESSION OF THE BIOSYNTHETIC DEOXYVIOLACEIN PATHWAY. PIGMENTATION OF THE COLONIES VERIFIES SUCCESSFUL INDUCTION OF THE HETEROLOGOUS OPERON.....	67
FIGURE 17. IMPACT OF FRUCTOSE (A) AND GLYCEROL (B) AS CARBON SOURCE ON GROWTH AND DEOXYVIOLACEIN PRODUCTION IN <i>E. COLI</i> DVIO-8. DIFFERENT LEVELS OF L-ARABINOSE (10-500 MG L ⁻¹) WERE TESTED TO IDENTIFY OPTIMUM INDUCING CONDITIONS FOR DEOXYVIOLACEIN PRODUCTION (C). CULTIVATIONS WERE PERFORMED IN MICROPLATES (N=3).	69

FIGURE 18. ELUCIDATION OF L-ARABINOSE CATABOLISM IN <i>E. COLI</i> DVIO-6 (A) AND DVIO-8 (B). STRAINS WERE CULTURED IN MEDIA CONTAINING NON-LABELED OR 99% L-[1- ¹³ C] ARABINOSE, RESPECTIVELY. METABOLIZATION OF L-ARABINOSE WAS ASSESSED BY ¹³ C LABELING ANALYSIS OF AMINO ACIDS FROM THE CELL PROTEIN.	70
FIGURE 19. FED-BATCH PRODUCTION OF DEOXYVIOLACEIN IN <i>E. COLI</i> DVIO-8. THE ARROW INDICATES THE TIME POINT OF GLUCOSE DEPLETION, AT WHICH THE REACTOR WAS COOLED FROM 37°C TO 20°C AND THE CARBON SOURCE WAS SWITCHED TO GLYCEROL. THE DASHED LINE MARKS THE BEGINNING OF THE FEED PHASE.	71
FIGURE 20. VALIDATION OF PURITY OF DEOXYVIOLACEIN AFTER EXTRACTION FROM CULTURE BROTH AND PURIFICATION BY FLASH CHROMATOGRAPHY. THE SIGNALS OF THE SAMPLE REFLECT THE DEAD VOLUME OF THE COLUMN (1) AND THE TARGET COMPOUND DEOXYVIOLACEIN (2). THE PEAK AREAS REVEAL A PURITY OF > 99.5%. ANALYSIS WAS CONDUCTED WITH HPLC AND DETECTION WITH A DIODE ARRAY DETECTOR.	72
FIGURE 21. FED-BATCH PRODUCTION OF VIOLACEIN BY RECOMBINANT <i>E. COLI</i> VIO-4. THE VALUES, GIVEN FOR FEED-BATCH PHASE ARE NORMALIZED BY THE INITIAL MEDIUM VOLUME TO ACCOUNT FOR DILUTION OF THE MEDIUM.	73
FIGURE 22. PURIFICATION OF VIOLACEIN: CRYSTALLIZED VIOLACEIN (A) AND CHROMATOGRAM OF THE VIOLACEIN CRYSTALS, SOLUBILIZED IN ETHANOL (B).	74
FIGURE 23. SYSTEMS METABOLIC ENGINEERING STRATEGY FOR DEOXYVIOLACEIN PRODUCTION IN <i>E. COLI</i> DVIO-8, USING GLYCEROL AS CARBON SOURCE AND L-ARABINOSE AS INDUCER. COMPOUND NAMES: G6P (GLUCOSE 6-PHOSPHATE), F6P (FRUCTOSE 6-PHOSPHATE), GAP (GLYCERALDEHYDE 3-PHOSPHATE), 3PG (3-PHOSPHOGLYCERATE), PEP (PHOSPHOENOLPYRUVATE), PYR (PYRUVATE), ACCOA (ACETYL-CoA), OAA (OXALOACETATE), IND (INDOLE), RUL5P (RIBULOSE 5-PHOSPHATE), XYL5P (XYLULOSE 5-PHOSPHATE), RIB5P (RIBOSE 5-PHOSPHATE), SED7P (SEDOHEPTULOSE 7-PHOSPHATE), E4P (ERYTHROSE 4-PHOSPHATE), SER (L-SERINE), DAHP (3-DEOXY-D-ARABINO-HEPTULOSONATE-7-PHOSPHATE), CHO (CHORISMATE), ANTH (ANTHRANILATE), TRP (L-TRYPTOPHAN), IPA (INDOLE-3-PYRUVIC ACID IMINE), PDVA (PROTODEOXYVIOLACEINIC ACID), AND AC (ACETATE).	79
SUPPL. FIGURE 1. MAPS OF PLASMIDS pCO1CATFRT AND pCO1KANFRT WITH RELEVANT FEATURES FOR THE PRESENT STUDY. BOTH PLASMIDS ARE BASED ON VECTOR PJF119EH (FÜRSTE ET AL., 1986). NOTI RESTRICTION SITES (CUSTOM-SYNTHEZED BY GENEART, REGENSBURG, GERMANY) WERE INTRODUCED BY SITE-DIRECTED MUTAGENESIS 5' UPSTREAM OF THE P _{TAC} PROMOTER AND 3' DOWNSTREAM OF THE TRANSCRIPTION TERMINATOR SEQUENCE, 5SRRNBT1T2 TO OBTAIN VECTOR PF113. CM ^R AND KM ^R GENE CASSETTES, RESPECTIVELY, WERE EQUIPPED ON BOTH ENDS WITH FRT SITES AND HINDIII RESTRICTION SITES, RESPECTIVELY (DEGNER AND SPRENGER, UNPUBLISHED RESULTS).	98
SUPPL. FIGURE 2. DELETION OF <i>TRPL</i> GENE AND MUTAGENESIS OF <i>TRPE</i> GENE IN THE CHROMOSOME OF STRAIN BW25113. THE STRAIN TRP2 (BW25113 Δ <i>TRPE</i> :: <i>FRT-KM-FRT</i>) WAS CONSTRUCTED USING THE λRED RECOMBINATION METHOD (DATSENKO AND WANNER, 2000). DISRUPTION OF THE <i>TRPE</i> GENE WAS BY INSERTION OF AN AMPLIFIED KM ^R CASSETTE FROM PLASMID pCO1KANFRT (SUPPL. FIGURE 1; DEGNER AND SPRENGER, UNPUBLISHED RESULTS) AND PRIMERS 28 AND 29.	101

SUPPL. FIGURE 3. CHROMOSOMAL INTEGRATION OF <i>E. COLI AROFBL</i> GENES AS AN ARTIFICIAL OPERON UNDER CONTROL OF A P _{TAC} PROMOTER (ORF AND BONGAERTS, UNPUBLISHED RESULTS) REPLACING THE RESIDENT <i>LACIZYA</i> GENE CLUSTER. FOR THE DNA SEQUENCE OF THE RESPECTIVE REGION SEE SUPPL. FIGURE 4 AND TEXT.	103
SUPPL. FIGURE 4. DNA SEQUENCE OF CHROMOSOMAL P _{TAC} <i>ARO</i> <i>FBL</i> REGION.	105
SUPPL. FIGURE 5. MAP OF PLASMID PJNNMOD. THE PLASMID IS BASED UPON PJF119EH (FÜRSTE ET AL., 1986). THE MULTIPLE CLONING SITE HAS BEEN CHANGED TO CONTAIN RESTRICTION SITES FOR THE FOLLOWING ENZYMES: NDEI-KPNI-BAMHI-XBAI-SPHI-HINDIII. (TRACHTMANN AND SPRENGER, UNPUBLISHED RESULTS).	107

List of Tables

TABLE 1. PRECURSOR METABOLITES REQUIRED FOR THE BIOSYNTHESIS OF THE BUILDING BLOCKS.	19
TABLE 2. STRAINS AND PLASMIDS.....	33
TABLE 3. PRIMERS USED FOR GENETIC CONSTRUCTION WORK.....	37
TABLE 4. STRAINS AND PLASMIDS USED IN THE PRESENT WORK.	44
TABLE 5. PRIMERS USED FOR DELETION OF <i>ARABAD</i> IN <i>E. COLI</i>	45
TABLE 6. PRODUCTION OF VIOLACEIN AND DEOXYVIOLACEIN BY DIFFERENT STRAINS CULTIVATED ON LB AGAR FOR 2 WEEKS.....	52
TABLE 7. REVISION OF ANALYTICAL APPROACHES FOR THE QUANTIFICATION OF DEOXYVIOLACEIN. THE EVALUATION INVESTIGATED PURE STANDARD SOLUTIONS OF THE ANALYTE WITH ABSOLUTE CONCENTRATIONS OF 3.7 MG L ⁻¹ (STANDARD 1), 7.7 MG L ⁻¹ (STANDARD 2) AND 38.3 MG L ⁻¹ OF DEOXYVIOLACEIN AND ONE EXTRACT FROM THE CULTIVATION BROTH OF THE RECOMBINANT PRODUCER <i>E. COLI</i> dVIO-6, WHICH WERE ANALYZED IN PARALLEL BY HPLC (RODRIGUES ET AL., 2012) AND PHOTOMETRICAL MEASUREMENT AT A WAVELENGTH OF 560 NM (JIANG ET AL., 2012). THE LATTER RECRUITED THE REPORTED EXTINCTION COEFFICIENT OF $E_{560} = 15.955 \text{ L (G CM)}^{-1}$ TO ESTIMATE THE DEOXYVIOLACEIN CONTENT. CONCENTRATIONS GIVEN ARE MEAN VALUES AND DEVIATIONS FROM THREE REPLICATES.....	56
TABLE 8. REVISION OF ANALYTICAL APPROACHES FOR THE QUANTIFICATION OF VIOLACEIN. THE EVALUATION INVESTIGATED PURE STANDARD SOLUTIONS OF THE ANALYTE WITH ABSOLUTE CONCENTRATIONS OF 3.2 MG L ⁻¹ (STANDARD 1), 6.4 MG L ⁻¹ (STANDARD 2) AND 12.8 MG L ⁻¹ OF VIOLACEIN AND ONE EXTRACT FROM THE CULTIVATION BROTH OF THE RECOMBINANT PRODUCER <i>E.</i> <i>COLI</i> VIO-4. THESE WERE ANALYZED IN PARALLEL BY HPLC (RODRIGUES ET AL., 2012) AND BY PHOTOMETRY AT 570 NM WITH $E_{570} = 10.955 \text{ L (G CM)}^{-1}$ (PHOTOMETRY 1, (WANG ET AL., 2009)), AT 575 NM WITH $E_{575} = 56.010 \text{ L (G CM)}^{-1}$ (PHOTOMETRY 2, (MENDES ET AL., 2001)), AND AT 575 NM WITH $E_{575} = 29.700 \text{ L (G CM)}^{-1}$ (PHOTOMETRY 3, (DURÁN ET AL., 2007)). CONCENTRATIONS GIVEN ARE MEAN VALUES AND DEVIATIONS FROM THREE REPLICATES. THE CORRELATION FACTORS (FROM LEFT TO RIGHT) RELATE HPLC TO THE DIFFERENT PHOTOMETRICAL ASSAYS.....	56
SUPPLEMENTARY TABLE 1. PRIMERS USED.	99

Summary

Violacein and deoxyviolacein are promising therapeutics against pathogenic bacteria and viruses as well as tumor cells. In the present work, systems-wide metabolic engineering was applied to *Escherichia coli* for heterologous production of these high-value products. First, a high performance liquid chromatography method for accurate separation and quantification of violacein and deoxyviolacein was developed. Afterwards, a basic producer, *E. coli* dVio-1, that expressed the *vioABCE* cluster from *Chromobacterium violaceum* under control of the *araBAD* promoter and induction by L-arabinose, was constructed. Targeted intracellular metabolite analysis then identified bottlenecks in pathways that supply tryptophan, the major product building block of the natural products of interest. This was used for systems-wide engineering of serine, chorismate and tryptophan biosynthesis and the non-oxidative pentose-phosphate pathway, followed by elimination of L-arabinose catabolism. Transferred to a glycerol-based fed-batch process, *E. coli* dVio-8 surpassed the gram scale and produced 1.6 g L⁻¹ deoxyviolacein (> 99.5% purity). The created chassis of a high-flux tryptophan pathway was complemented by genomic integration of the *vioD* gene of *Janthinobacterium lividum*, which enabled exclusive production of violacein (710 mg L⁻¹ with 99.8% purity). This demonstrates the potential of *E. coli* as a platform for production of tryptophan based therapeutics.

Zusammenfassung

Violacein und Deoxyviolacein sind vielversprechende Therapeutika gegen pathogene Bakterien und Viren als auch Tumorzellen. In der vorliegenden Arbeit wurde *Escherichia coli* zur heterologen Produktion dieser hochwertigen Produkte untersucht. Zuerst wurde eine HPLC-Methode für eine genaue Trennung und Quantifizierung von Violacein und Deoxyviolacein entwickelt. Anschließend wurde einer Basisstamm von *E. coli*, die die *vioABCE* Operon aus *Chromobacterium violaceum* unter der Kontrolle des *araBAD*-Promotor, konstruiert. Gezielte intrazelluläre Stoffwechselanalysen identifizierten dann Engpässe in den zuliefernden Routen der Biosynthese von Tryptophan, dem zentralen Baustein für das Produkt. Dieses Wissen wurde für die rationale Stammoptimierung genutzt. Durch die aufeinanderfolgende Optimierung von Serin-, Tryptophan- und Chorismat-Biosynthese sowie des nicht-oxidativen Pentose-Phosphat-Weges konnte eine umfassende Optimierung des Stoffflusses zum Zielprodukt erreicht werden. In einem Glycerin-basierten Fed-Batch-Verfahren, hat *E. coli* dVIO-8 den Gramm-Maßstab übertroffen (1,6 g L⁻¹ Deoxyviolacein, >99,5% Reinheit). Das metabolische Chassis von *E. coli* mit einem High-Flux-Tryptophan-Weg wurde durch genomische Integration des *vioD* Genes aus *Janthinobacterium lividum* zur gezielten Produktion (710 mg L⁻¹, 99,8% Reinheit) von Violacein weiterentwickelt. Die Ergebnisse zeigen darüber hinaus das große Potential von *E. coli* als Plattform für die Produktion Tryptophan-basierter Therapeutika.

1 Introduction

1.1. *Violacein and deoxyviolacein*

Violacein and deoxyviolacein are secondary metabolites produced by a diverse group of microorganisms. The pigments were firstly described in 1882 when the compounds were extracted with ethanol and the spectrophotometric properties of the obtained solutions were analyzed (Boisbaudran, 1882). These molecules present blue/violet color, which facilitates the isolation of natural producer strains for further research and enable its use as a bio-dye that provides good color tone and stability (Shirata et al., 2000). Their biological role was studied using bacterial strains isolated from the environment (Matz et al., 2008). In order to analyze growth and survival rates of bacterivorous nanoflagellates, isolates of the violacein and deoxyviolacein producer strains *Janthinobacterium lividum* and *Chromobacterium violaceum* were used to feed these organisms. It was demonstrated that the uptake of less than three pigmented bacterial cells caused cell death in less than 20 min to these microorganisms. The results of the study suggest that the production of the pigments is related to a defense mechanism against predation. In another study, it has been determined that the presence of *J. lividum* on the skin of the salamander species *Plethodon cinereus* increased the survival rates of this amphibian when exposed to the fungus *Batrachochytrium dendrobatidis*, the causative agent of the disease chytridiomycosis one of the causes for the decline in amphibian populations (Becker et al., 2009b). A threshold concentration of about 18 μM violacein prevented mortality caused by *B. dendrobatidis*. Due its biological properties, violacein and deoxyviolacein draw attention of researchers as possible candidate compounds for the development of drugs for cancer treatment among other biotechnological and medical applications.

1.1.1. Biotechnological and therapeutic potential of violacein and deoxyviolacein

Violacein and deoxyviolacein extracted from *J. lividum* are effective against *Rosellinia necatrix*, which is responsible for white root rot of mulberry. The use of

violacein and deoxyviolacein against this phytopathogenic fungi, demonstrated the fungicide potential of these compounds (Shirata et al., 2000).

It was observed that a mixture of violacein and deoxyviolacein is effective against many gram-positive strains of microorganisms and to some extent against gram-negative. They are active against bacteria such as *Bacillus licheniformis*, *Bacillus subtilis*, *Bacillus megaterium*, *Staphylococcus aureus*, and *Pseudomonas aeruginosa* in concentrations ranging from 10-15 mg L⁻¹. Depending on the concentration tested, the pigment mixture was able to cause growth inhibition to cell death (Nakamura et al., 2003; Nakamura et al., 2002). Particularly in the case of *S. aureus*, which is an opportunistic pathogen frequently involved in infections, alternative antibiotics for human treatment are in demand due to the increasing development of resistance against the current medicines available. The treatment of *S. aureus* human infections is done using antibiotics, such as methicillin or vancomycin. Strains resistant to methicillin have been described that could be treated with vancomycin; however, strains of *S. aureus* resistant to methicillin and vancomycin up to serum concentrations of 9.4 mg L⁻¹ (Howe et al., 1998) were isolated, bringing concern to the medical community due to the lack of effective antibiotic alternatives for treatment (Sieradzki et al., 1999). Violacein loaded nanoparticles presented two to five times reduction of the minimal inhibitory concentration compared to the free form of the pigment against strains of *S. aureus* (Martins et al., 2011).

Tuberculosis is a world-wide disease caused by *Mycobacterium tuberculosis*. In 2011, 8.7 million new cases were estimated and 1.4 million died, 430,000 of which were also infected with HIV (WHO, 2012a). Conventional medication for treatment of tuberculosis is becoming ineffective, as occurrence of multidrug-resistant variants of *Mycobacterium tuberculosis* is increasing and reached 60,000 cases world-wide in 2011 (WHO, 2012a). Violacein exhibited activity against *Mycobacterium tuberculosis* (Mojib et al., 2010). The minimum inhibitory concentration of violacein extracted from *Janthinobacterium* sp. was 34.4 mg L⁻¹ for the virulent strain H₃₇Rv demonstrating the potential of violacein for the treatment of tuberculosis.

Experiments conducted to test the effect of violacein and deoxyviolacein mixtures in concentrations above 50 mg L⁻¹ presented no growth inhibition or cell death against *Escherichia coli* HB 101 (Nakamura et al., 2003). Even when

violacein was loaded in polymeric poly-(D,L-lactide-co-glycolide) nanoparticles to improve solubility in water, no significant antibacterial activity occurred against *E. coli* in concentrations up to 68.5 mg L⁻¹ (Martins et al., 2011). The ability of *E. coli* to cope with high violacein and deoxyviolacein concentrations is an important parameter regarding the potential utilization of this microorganism for production purposes, as further discussed below.

Poliomyelitis is a highly infectious viral disease that can cause paralysis (Bonnet and Dutta, 2008) and affects mainly children under five years of age (WHO, 2012b). This disease can be prevented by vaccination; however, there is no specific treatment available (Bonnet and Dutta, 2008). In addition, the World Health Organization estimates that failure to eradicate polio in countries like Afghanistan, Nigeria, and Pakistan could make the disease spread all over the world within 10 years (WHO, 2012b). Experiments performed using extracts containing violacein and deoxyviolacein showed that these compounds can prevent human cell infection by the poliomyelitis virus (May et al., 1991). These extracts presented also activity against Herpes simplex virus cell infection (May et al., 1991).

Violacein is also active against *Leishmania amazonensis* (Leon et al., 2001) and *Trypanosoma cruzi* (Durán et al., 1994) the causative agents of Leishmaniasis and Chagas diseases, respectively. These diseases are members of the group of neglected diseases (Trouiller et al., 2002) or more specifically, diseases for which no investments are made in research due to low profitability of the market formed by the low-income people that are affected by them.

Leukemia is a type of cancer which affects the blood and the bone marrow. In the year 2000, it was estimated that this disease affected 255,932 people causing 209,328 deaths world-wide (Mathers et al., 2001). Violacein obtained from *C. violaceum* presented potential as a drug for leukemia treatment (da Silva Melo et al., 2000). It was effective against HL60 leukemic cells (Ferreira et al., 2004) an established model for studying myeloid leukemia. The mechanism by which violacein induced apoptosis in HL60 cells is related to the activation of the tumor necrosis factor (TNF) receptor signaling (Ferreira et al., 2004). In order to improve the efficiency of violacein against HL60 cells, the use of nanoparticles was tested. The fact that tumor cells have a higher ascorbic acid uptake rate motivated the use of violacein-loaded nanoparticles capped with ascorbic acid as a way to improve

the efficiency against tumor cells. This system was 2-fold more effective than free violacein as antitumoral drug (Martins et al., 2010). In another study (Gimenez et al., 2005), violacein complexed by cyclodextrin-thiol-protected gold nanoparticles presented improved water solubility as compared to free violacein. These nanoparticles presented reduced toxicity activity against normal V79 cells while maintaining the activity against myeloid leukemia HL60 cells. These results show that nanoparticles are an important tool for the targeted delivery of antitumoral compounds, such as violacein and deoxyviolacein, to cancer cells in order to reduce the side effects of chemotherapy.

Colorectal cancer is the fourth most common cancer type (Boyle and Langman, 2000) and the third cause of cancer death (Parkin, 2001). It is estimated that colorectal cancer is responsible for 394,000 deaths annually affecting mainly Europe, North America, and Australasia. In the European Union it is the second cause of men death among the cancer types (Boyle and Langman, 2000). The chemotherapy employed for the treatment of colorectal cancer is done using 5-fluorouracil (Heidelberger et al., 1957), which is the most widely used drug for this type of cancer (Gill et al., 2003), in combination with other compounds such as leucovorin (Machover, 1997). In a phase III study, it was demonstrated that patients treated with either a combination of 5-fluorouracil and leucovorin or 5-fluorouracil, leucovorin and oxaliplatin presented 16 and 53% objective response, respectively (Giacchetti et al., 2000). The objective response was determined by extramural reviews of computed tomography scans. It has been demonstrated that violacein is an effective cytotoxic compound against colorectal cancer cells (Kodach et al., 2006). Violacein could induce apoptosis in colorectal cancer cells by blocking the phosphatidylinositol-3-kinase/Akt (Vivanco and Sawyers, 2002) activation and could increase the chemosensitivity of the cells to 5-fluorouracil when used in combination with this compound. The mechanism by which violacein induces death in the Caco-2 cell line, which is a model for colorectal cancer studies, involves the formation of reactive oxygen species that ultimately culminate in tumor apoptosis (De Carvalho et al., 2006). These results demonstrate the potential application of violacein as chemotherapeutic agent for colorectal cancer treatment. Moreover, violacein and deoxyviolacein were also able to inhibit hepatocellular carcinoma cell proliferation (Jiang et al., 2012).

In addition to *in vitro* studies on the antitumoral properties of violacein, *in vivo* studies were also performed using Ehrlich ascites tumor cells (EAT) as model (Bromberg et al., 2010). Experiments demonstrated that EAT cells were two times more sensitive to violacein than the normal cells. The experiments conducted using mice injected with EAT cells intraperitoneally showed that violacein doses ranging from 0.1 to 1 $\mu\text{g kg}^{-1}$ significantly reduced tumor growth. Moreover, daily violacein doses of 1000 $\mu\text{g kg}^{-1}$ did not cause toxicity to kidneys and liver when injected intraperitoneally.

Antiulcerogenic activity of violacein (Durán et al., 2003) has been demonstrated in experiments using mice as model. Orally administered violacein significantly reduced gastric lesions. Further improvements of the protective effect of violacein were possible by using violacein beta-cyclodextrin (betaCD) inclusion complexes. In this case, reduction of gastric damage of about 85% was possible using violacein loaded betaCD inclusion complexes with 1:2 ratio.

1.2. *E. coli* as industrial production host

E. coli is one of the most used hosts for production of recombinant compounds in industry, due to its well known physiology, availability of tools for genetic manipulation, ease of scale-up, low-cost media and rapid growth (Huang et al., 2012). Specifically, the strain K-12 has been established as standard and received guidelines for safety regarding therapeutics production. One third of the recombinant therapeutics approved by the US Food and Drug Administration and the European Medicines Agency are produced in *E. coli* (Huang et al., 2012). Some examples of approved recombinant therapeutics produced in *E. coli* are Ranibizumab (Lucentis), Somatropin (Accretropin), Certolizumab pegol (Cimzia), PEG interferon alfa-2b (PegIntron), Romiplostim (Nplate), and Interferon beta 1b (Extavia) Pegloticase (Krystexxa). Important advancements have been made in recent years towards the production of complex molecules that require disulfide bond formation and glycosylation. The functional expression of the N-linked glycosylation pathway of *Campylobacter jejuni* in *E. coli* opened up the possibility to generate compounds that require this important type of modification, frequently necessary in drugs for treatment of diseases and for research (Wacker et al.,

2002). In addition to therapeutics production, *E. coli* is also an import host for production of a diverse group of chemicals for different purposes.

Currently, an increasing tendency is observed regarding the use renewable resources for production of commodities and fine chemicals (Bozell and Petersen, 2010). Due to concerns about negative environmental impacts of fossil based resources, as well as limitations in the availability or political instability in the producing countries, biotechnological based production appeared as a potential alternative to overcome these issues. Advancements in research along the years are making the economical feasibility of many biotechnological processes approach a state in which competition with the petrochemical industry can be considered. An indication of this trend is the growing global value of biotechnology industry, which increased from 54 billion dollars in 1999 to about 500 billion dollars in 2011 (Bruschi et al., 2011). An example of chemical produced in industrial scale by *E. coli* is 1,3-propanediol (Laffend et al., 1997), produced since 2006 with a 45,000 tonne/year capacity (Burk, 2010). Another promising compounds, but not limited to, are fuels (1-propanol and 1-butanol), amino acids (L-threonine, L-valine, L-phenylalanine, L-tryptophan, and L-tyrosine), succinic acid, xylitol, and 1,4-butanediol (Burk, 2010; Chen et al., 2013).

1.3. Physiology and metabolism of *E. coli*

In this section, a brief overview of the main pathways of the metabolism of *E. coli* will be given. Relevant aspects of the metabolism, e.g., transport and catabolism of glucose, glycerol, and L-arabinose, as well as the mechanisms of control of gene expression, will be presented. Finally, the L-tryptophan pathway will be covered concerning the relevant factors related to the improvement of the metabolic fluxes for biosynthesis of this fundamental amino acid for violacein and deoxyviolacein production. If not stated otherwise, the information presented in this section was based on the comprehensive works of (Keseler et al., 2005; Neidhardt et al., 1996). A simplified schematic presenting the transport systems of substrates, the central metabolism and biosynthesis of L-tryptophan is presented in Figure 1.

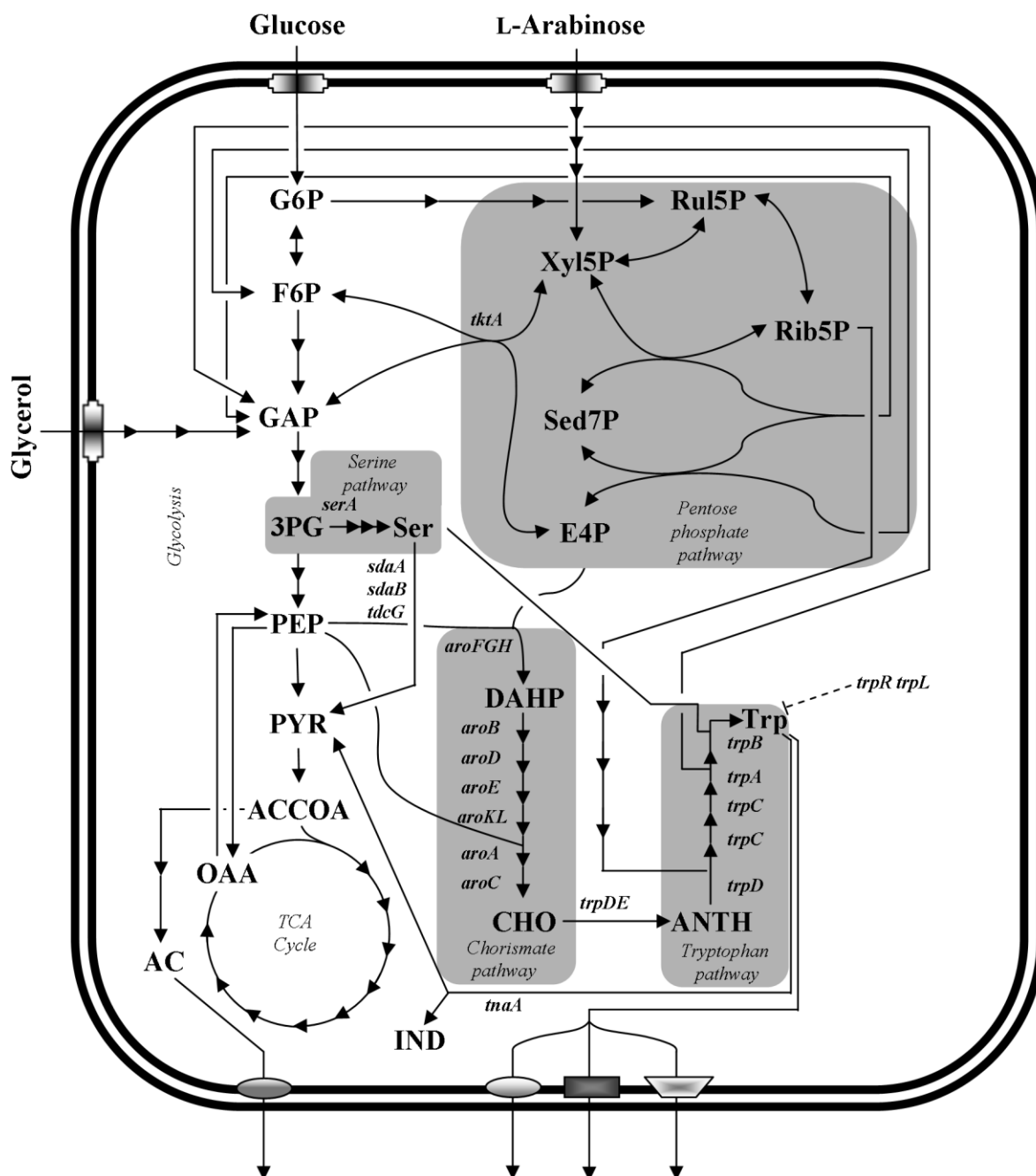


Figure 1. Central metabolism of *E. coli* and L-tryptophan pathway. Compound names: G6P (glucose 6-phosphate), F6P (fructose 6-phosphate), GAP (glyceraldehyde 3-phosphate), 3PG (3-phosphoglycerate), PEP (phosphoenolpyruvate), PYR (pyruvate), ACCOA (acetyl-CoA), OAA (oxaloacetate), IND (indole), Ru5P (ribulose 5-phosphate), Xyl5P (xylulose 5-phosphate), Rib5P (ribose 5-phosphate), Sed7P (sedoheptulose 7-phosphate), E4P (erythrose 4-phosphate), Ser (L-serine), DAHP (3-deoxy-D-arabino-heptulosonate-7-phosphate), CHO (chorismate), ANTH (anthranilate), Trp (L-tryptophan), IPA (indole-3-pyruvic acid imine), PDVA (protodeoxyviolaceinic acid), and AC (acetate).

1.3.1. Transport and metabolism of glucose, L-arabinose and glycerol

Glucose is one of the main carbon sources utilized by *E. coli*. This microorganism is able to metabolize glucose, in addition to some salts, as energy and carbon source to synthesize the other compounds required for growth. Similarly, L-arabinose and glycerol can also serve this purpose. The catabolism of glucose initiates with its transport into the cell. The most used glucose transporter in *E. coli* is the phosphoenolpyruvate phosphotransferase system (PTS). In addition to glucose, the PTS is responsible for the transport of different compounds into the cell, such as mannitol and mannose. Some components of the PTS have a general purpose, while other proteins involved exhibit specificity for the target compound to be transported. The driving force required for this type of transport to take place is derived from phosphoenolpyruvate (PEP). The phosphate of this molecule is ultimately transferred to the respective sugar, during transport from the periplasm into the cytoplasm, releasing pyruvate as byproduct. The PTS responsible for the uptake of glucose is composed of free and membrane-bounded proteins. Enzyme I (EI) and the histidine protein (HPr) encoded by the genes *ptsI* and *ptsH*, respectively; are the free cytoplasmic general-use component part of the system. The sugar specific EII component has also a free and a membrane-bounded part. In the case of the glucose transport, these components are called IIA^{Glc} or Crr and IICB^{Glc} or PtsG encoded by the genes *crr* and *ptsG*, respectively. The transfer of the phosphate group of PEP to glucose occurs in following order: PEP → P-EI → P-HPr → P-EIIA^{Glc} → P-EIICB^{Glc} → glucose-6-P. The general proteins encoded by the genes *ptsH*, *ptsI*, and *crr* of the glucose PTS are clustered in an operon. This operon is constitutively expressed at a basal level, but the level of gene expression is increased upon growth on PTS substrates. The *ptsG* gene is inducible by glucose in *E. coli* K-12. One of the possible explanations for the fact that the *crr* gene is expressed together with the general components EI and HPr can be the role that this protein plays on the transport of other compounds, such as trehalose and sucrose. In addition to glucose transport, the PTS has other important functions in *E. coli*. In a process called inducer exclusion, the EIIA^{Glc} component interacts with proteins related to the metabolism of other carbon sources, e.g., glycerol and lactose,

inhibiting their activity and, consequently, the use of these compounds for growth. This process takes place when the cell is using a PTS carbohydrate as carbon source. Only if some of the above mentioned carbon sources is present that the EIIA^{Glc} protein acts as inhibitor. This occurs because the non-phosphorylated form of EIIA^{Glc} is able to bind and inhibit the activity of different proteins related to the catabolism of alternative carbon sources that are available during the metabolism of glucose. For instance, in the presence of glucose and glycerol, *E. coli* will first transport glucose using the PTS. During the glucose transport, the predominant form of the EIIA^{Glc} protein will be non-phosphorylated, as the phosphates are now being transferred to the transported glucose. As glycerol is also present, the EIIA^{Glc} protein is able to bind to the enzyme glycerol kinase, thereby inhibiting the phosphorylation of glycerol to glycerol-3-phosphate, which is the first intermediate metabolite of the glycerol catabolism. Another important role played by the PTS is the regulation of the adenylate cyclase activity. This enzyme is responsible for the biosynthesis of cyclic AMP (cAMP), an important signaling molecule. The interaction of cAMP with the transcriptional dual regulator CRP (cAMP receptor protein) yields the cAMP-CRP complex which acts globally in the control of transcription initiation in *E. coli*. The phosphorylated form of the EIIA^{Glc} protein stimulates the hydrolysis of ATP by the adenylate cyclase for cAMP production. Therefore, as the concentration of phosphorylated EIIA^{Glc} is low during glucose catabolism, adenylate cyclase activity will also be reduced; on the other hand, it is increased during catabolism of non-PTS compounds. This is the basis of the regulation mechanism known as catabolite repression. An example of carbon source subject to catabolite repression regulation is L-arabinose, as further discussed below. After glucose is transported into the cell with concomitant phosphorylation to glucose-6-phosphate, this metabolite can be promptly catabolized as carbon and energy source by the pathways of the central metabolism.

The transport of L-arabinose, contrary to glucose, does not rely directly on PTS. There are two transport systems for L-arabinose in *E. coli*, a system with high-affinity and another with low-affinity, which are encoded by the *araFGH* and *araE* genes, respectively. L-Arabinose transport through the *araFGH* system is driven by ATP hydrolysis, while the *araE* system consists of a symporter that relies on the electrochemical gradient of protons for the transport of L-arabinose through

the cell membrane. The *araF* gene is responsible for the production of a periplasmic binding protein. The *araG* and *araH* genes encode proteins responsible for the ATP binding and the membrane attachment, respectively. The regulation of gene expression in both systems is controlled by L-arabinose, AraC protein, CRP, and cAMP. When L-arabinose is present, the AraC protein changes its conformation to act as inducer of gene expression. This form of AraC interacts with the cAMP-CRP complex and the RNA polymerase, thereby inducing the expression of the *araFGH* and *araE* genes. Conversely, in absence of L-arabinose, the AraC protein acts as repressor of gene expression. This is a useful characteristic, as it allows the genes under control to be tight repressed or induced, fact that can play a major role regarding stability of heterologous gene expression in *E. coli*. As mentioned above, availability of the cAMP-CRP complex is required for induction of gene expression by the AraC protein. Here is where the catabolism of L-arabinose is affected by catabolic repression. If *E. coli* is metabolizing a PTS compound, the phosphorylation level of the protein EIIA^{Glc} will be low, as the level of the EI protein will also be reduced due to the phosphate demand required by the substrate being transported. Due to the reversibility in the phosphorylation reactions in the PTS, the concentration of the P-EIIA^{Glc} will decrease, thus reducing the activity of adenylate cyclase and, consequently, the intracellular concentration of cAMP. At this moment, the PTS can indirectly affect, provided that a PTS substrate is available, the transport of L-arabinose by repressing *araFGH* and *araE* expression. After transport into the cell, L-arabinose undergoes a series of modifications before it can be catabolized by the central metabolism of *E. coli*. Once L-arabinose is available in cytoplasm, it is metabolized by the enzymes L-arabinose isomerase, L-ribulokinase, and L-ribulose 5-phosphate 4-epimerase of the *araBAD* operon. Similarly, the regulation of gene expression in this operon is subject to control by the AraC protein (Figure 2). In the first reaction, catalyzed by the enzyme L-arabinose isomerase, L-arabinose is converted to L-ribulose. This compound is phosphorylated by L-ribulokinase to yield L-ribulose 5-phosphate, which is finally converted to D-xylulose 5-phosphate and metabolized in central metabolism.

Glycerol transport in *E. coli* occurs through a protein channel encoded by the *glpF* gene. This transport is mediated by facilitated diffusion, so that this carbohydrate can be moved in each direction through the cell membrane. Once

inside the cell, glycerol is phosphorylated by the enzyme glycerol kinase to generate glycerol-3-phosphate, using ATP as phosphoryl donor. The *gplK* gene is responsible for the biosynthesis of glycerol kinase. This enzyme is allosterically inhibited by fructose-1,6-bisphosphate and the non-phosphorylated form of enzyme IIA^{Glc}. Therefore, when *E. coli* is cultivated on glucose as carbon source,

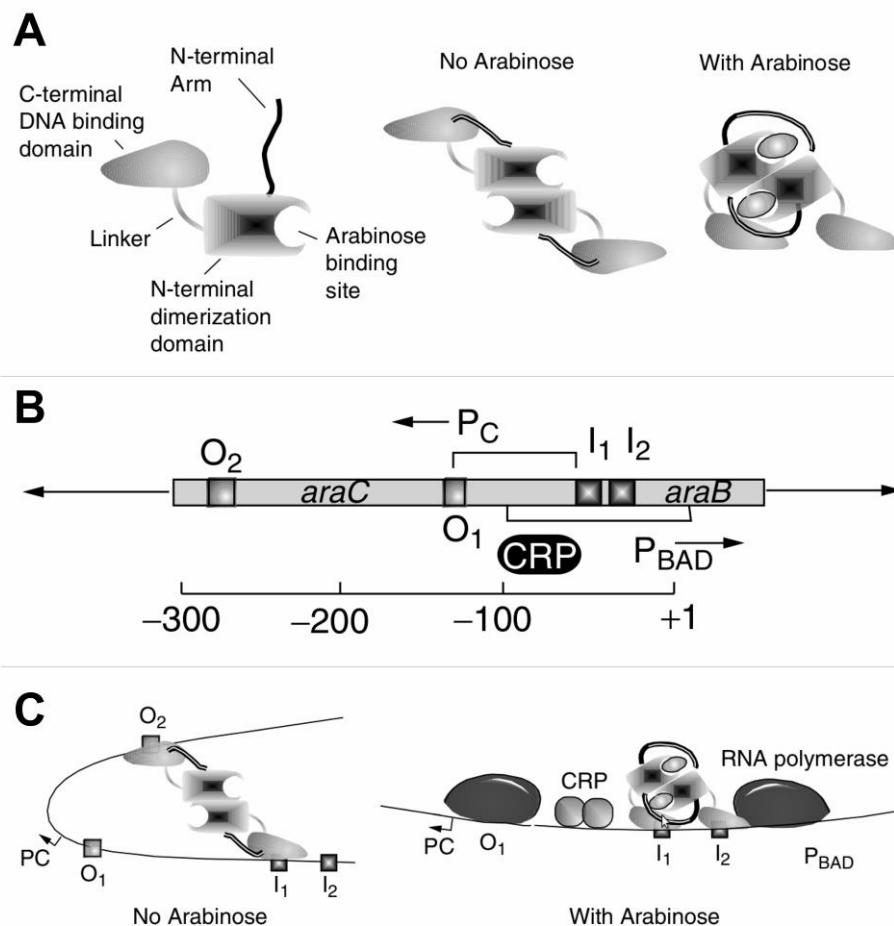


Figure 2. Structure of the AraC protein and mechanism of activation and repression of the *araBAD* promoter. A) Domains of the AraC monomer and the activator and repressor forms of the AraC dimer. B) Organization of the P_{BAD} and P_C promoters. C) Mechanism of repression and activation of the *araBAD* promoter in the presence and absence of L-arabinose and the CRP protein. This figure was modified from (Moat et al., 2003).

the catabolism of glycerol is inhibited. Once glycerol-3-phosphate is produced, it can be further metabolized in different ways, depending on the growth conditions. In aerobically growing cells, glycerol-3-phosphate is converted to dihydroxyacetone phosphate by the glycerol-3-phosphate dehydrogenase (GlpD), which is produced by the *glpD* gene. GlpD is associated with the cell membrane

and uses non-covalently bound FAD as cofactor to perform this oxidation reaction. In addition to dihydroxyacetone phosphate, two protons are released in the cytoplasm and ubiquinone is reduced in this reaction. During anaerobic cultivation, another version of the glycerol-3-phosphate dehydrogenase is expressed by the genes of the *glpACB* operon, and the electrons generated are transferred to either fumarate or nitrate. It has been demonstrated that *E. coli* lacking glycerol-3-phosphate dehydrogenase, could recover its ability to grow on glycerol after selective pressure using this substrate. It was found that the *glpA* gene produced a glycerol dehydrogenase enzyme able to convert glycerol to dihydroxyacetone, which by activity of dihydroxyacetone kinase generated dihydroxyacetone phosphate, thus restoring growth capability on glycerol. Finally, dihydroxyacetone phosphate can be metabolized in the central metabolism.

1.3.2. Metabolic pathways of the central metabolism

The central metabolism comprises the set of pathways responsible for the generation of the metabolic precursors, energy, and reducing power to support biosynthetic reactions required for growth. From the intermediates of these pathways, the other components of the cell can be synthesized. In *E. coli*, these pathways are the Embden-Meyerhof-Parnas pathway (EMF or glycolysis), pentose phosphate pathway (PPP), and tricarboxylic acid cycle (TCA cycle). In cultivations of *E. coli* using glucose as carbon and energy source, about 50% of this sugar is oxidized to generate ATP/reducing power and the other 50% is converted into cell material. As discussed in the previous section, glucose is transported into the cell in the form of glucose-6-phosphate, which will be either metabolized through the PPP or the EMP pathway.

The first reaction of the glucose-6-phosphate metabolism in the EMP pathway starts with its isomerization to fructose-6-phosphate. This reversible reaction is catalyzed by the enzyme phosphoglucose isomerase encoded by the *pgi* gene. Fructose-6-phosphate is subsequently phosphorylated to fructose-1,6-biphosphate in an irreversible reaction in which ATP is used as the phosphoryl donor. The two variants of the enzyme fructose-6-phosphate kinase (PfkI and PfkII), responsible for this reaction, are encoded by the *pfkA* and *pfkB* genes in *E. coli*, respectively. About 90% of the enzyme activity of this reaction is performed by PfkI. This reaction is an important regulatory step of the EMP pathway.

Fructose-6-phosphate kinase activity is stimulated by ADP and is allosterically inhibited by phosphoenolpyruvate. As the sum of the ATP, ADP, and AMP pools is almost constant in the cytoplasm of *E. coli*, an increased concentration of ADP is indication that the level of ATP was reduced, as many reactions involve the hydrolysis of ATP to ADP. One of the functions of the EMP pathway is the regeneration of ATP, thus explaining why this pathway is activated in the presence of ADP. On the other hand, if phosphoenolpyruvate accumulates, this indicates that the pathway must be inhibited, since this metabolite is one of the last intermediates produced in the EMP pathway. Due to the fact that the fructose-6-phosphate kinase reaction is physiologically irreversible, another route to the biosynthesis of the precursor metabolite fructose-6-phosphate must exist to enable growth using other carbon sources, such as glycerol, that enter the central metabolism after the fructose-6-phosphate kinase reaction. This reverse reaction is catalyzed the enzyme fructose-1,6-biphosphate phosphatase, which is inhibited by AMP, thereby avoiding the generation of a futile cycle with fructose-6-phosphate kinase. It was reported that strains of *E. coli* lacking the *fbp* gene encoding fructose-1,6-biphosphate phosphatase are unable to grow on glycerol as single carbon source, although other enzymes able to perform this reaction are present in the chromosome, e.g., GlpX. Once fructose-1,6-biphosphate is produced, it is cleaved to 3-phosphoglyceraldehyde and dihydroxyacetone phosphate. This splitting is catalyzed by the main fructose-1,6-biphosphate aldolase (FbaA) encoded by the gene *fbaA*. Dihydroxyacetone phosphate produced is also converted to 3-phosphoglyceraldehyde by the triosephosphate isomerase (*tpiA* gene). The next reaction of the EMP pathway is an oxidation, where NADH is generated. In this step, catalyzed by triosephosphate dehydrogenase (*gapA* gene), 3-phosphoglyceraldehyde is converted to 1,3-biphosphoglycerate. This is the only reaction of the EMP pathway that regenerates NADH. In the next reaction, 1,3-biphosphoglycerate and ADP are the substrates used for a substrate level phosphorylation carried out by phosphoglycerate kinase (*pgk* gene) that yields ATP and 3-phosphoglycerate. The latter is converted to 2-phosphoglycerate by phosphoglycerate mutase. This enzyme can be produced by the expression of the *gpmA* and *gpmM* genes generating non-homologous isofunctional enzymes. The enzyme produced by *gpmA* is 2,3-bisphosphoglycerate-dependent and presents higher specific activity. The enzyme enolase (*eno* gene)

dehydrates the 2-phosphoglycerate to phosphoenolpyruvate, which is finally used in the second substrate level phosphorylation to produce pyruvate and ATP by the activity of the pyruvate kinase. In *E. coli*, pyruvate kinase I and pyruvate kinase II are encoded by genes *pykF* and *pykA*, respectively. This reaction is also physiologically irreversible and is positively regulated by the presence of fructose-6-phosphate. Overall, the EMP pathway generates two pyruvate molecules, two ATP, two NADH, and two H⁺ for each glucose molecule catabolized and the respective ADPs, P_is, and NAD⁺s processed.

Another important pathway of the central metabolism of *E. coli* is the PPP. This pathway plays an important role in the regeneration of NADPH and the supply of metabolic precursors to the cell. In order to better comprehend how PPP works, it is convenient to divide the whole pathway in three parts. The first part involves the oxidation of glucose-6-phosphate through three biochemical reactions. Initially, glucose-6-phosphate is converted to 6-phosphogluconolactone, which is subsequently metabolized to 6-phosphogluconate. In the final step of the first part, ribulose-5-phosphate is formed from the latter metabolite. The enzymes catalyzing these reactions are glucose-6-phosphate dehydrogenase (*zwf* gene), 6-phosphogluconolactonase (*pgl* gene), and 6-phosphogluconate dehydrogenase (*gnd* gene); respectively. In the *Zwf* and *Gnd* reactions, NADPH is regenerated from NADP⁺. The *Gnd* reaction produces also CO₂ by the decarboxylation of the C₁ of glucose-6-phosphate. The *Pgl* reaction is physiologically irreversible and there are no alternative enzymes able to perform this reaction backwards directly in *E. coli*. However, carbon flowing through these metabolic steps can be recycled back to glucose-6-phosphate using an alternative route, as explained below. The second part of the PPP is the reversible isomerization of ribulose-5-phosphate to either xylulose-5-phosphate or ribose-5-phosphate, catalyzed by the enzymes ribulose-5-phosphate epimerase (*rpe* gene) and ribose-5-phosphate isomerase (*rpiA* and *rpiB* genes), respectively. The ribose-5-phosphate isomerase A of *E. coli* is constitutively expressed and performs about 99% of the isomerization, while ribose-5-phosphate isomerase B can replace the *RpiA* only if it is induced. The part three of the PPP involves a series of reversible carbon transfers between ribose-5-phosphate and xylulose-5-phosphate to generate exclusive PPP intermediates, as well as metabolites shared with the EMP pathway. It starts with the transfer of two carbons from xylulose-5-phosphate to ribose-5-phosphate

generating sedoheptulose-7-phosphate and glyceraldehyde-3-phosphate. This reaction is performed by the enzyme transketolase, which has two variants in *E. coli*, TktI and TktII. Transketolase I (*tktA* gene) has most of the enzyme activity. In the next reaction of the third part of PPP, three carbons of sedoheptulose-7-phosphate are transferred to glyceraldehyde-3-phosphate to form erythrose-4-phosphate and fructose-6-phosphate. This reaction is catalyzed by both transaldolase A (*talA* gene) and B (*talB* gene). The final step is the transketolase mediated transfer of two carbons of xylulose-5-phosphate, which was produced in the second part of PPP, to the erythrose-4-phosphate to produce fructose-6-phosphate and glyceraldehyde-3-phosphate. Due to the reversibility of the phosphoglucose isomerase reaction of the EMP pathway, fructose-6-phosphate produced in the PPP can be converted back to glucose-6-phosphate. Therefore, if the oxidative part of the PPP is necessary, e.g., high NADPH demand, fructose-6-phosphate can be redirected to meet this requirement. Similarly to fructose-6-phosphate, glyceraldehyde-3-phosphate produced in the PPP can also be metabolized through the EMP pathway. Taking into account the above mentioned reversibility of the phosphoglucose isomerase, the overall stoichiometry of the PPP is the production of 3 CO₂, 1 glyceraldehyde-3-phosphate, 6 H⁺ and the regeneration of 6 NADPH for each glucose-6-phosphate molecule processed. As can be seen, the EMP pathway and the PPP are interconnected in such a way that the cell has flexibility to control biosynthesis of precursors and NADPH regeneration. In continuation of the analysis of the central metabolism, the fate of the pyruvate produced in the EMP pathway is addressed.

Different pathways are able to metabolize pyruvate depending on the growth conditions. In anaerobiosis, pyruvate reacts with coenzyme A (CoA) to form acetyl-CoA and formate by the activity of the pyruvate-formate lyase (PflB). During aerobic growth, the pyruvate dehydrogenase complex is responsible for the conversion of pyruvate to acetyl-CoA and CO₂, converting NAD⁺ to NADH. This complex is inhibited by NADH and acetyl-CoA, and is stimulated by PEP and AMP. A third metabolic fate of pyruvate is its conversion to acetate through the activity of the pyruvate oxidase (*poxB* gene) to acetate and CO₂. The acetate is released into the culture medium, but can later be metabolized to acetyl-CoA by two routes. Acetyl-CoA synthetase (*acs* gene) converts acetate to acetyl-CoA using ATP and CoA; releasing AMP and diphosphate. The other route is the *ack*-

pta pathway. The enzymes involved, acetate kinase A (*ackA* gene) and phosphate acetyltransferase (*pta* gene), are constitutively expressed in an operon that enables the reversible conversion of acetate to acetyl-CoA. In this pathway, acetate is first converted to acetyl phosphate (AckA activity) with ATP as the phosphoryl donor; and the latter product reacts with CoA (Pta activity) to form acetyl-CoA. In aerobic conditions the acetyl-CoA formed is subsequently metabolized in the TCA cycle.

The TCA cycle starts with the irreversible condensation of acetyl-CoA and oxaloacetate forming citrate. The enzyme citrate synthase (*gltA* gene) that catalyzes this reaction is allosterically inhibited by NADH and α -ketoglutarate. The citrate formed is converted to isocitrate, with *cis*-aconitate as intermediate. Two enzymes can perform this step, the aconitate hydratase 1 and 2, which are encoded by the genes *acnA* and *acnB*, respectively. Isocitrate is then oxidized to α -ketoglutarate generating CO_2 and NADPH from NADP^+ . The enzyme isocitrate dehydrogenase (*icd*) that performs this reaction is regulated by phosphorylation/dephosphorylation, enabling the fast shift between the TCA cycle and the glyoxalate bypass, as discussed in the next section. Subsequently, succinyl-CoA is formed from α -ketoglutarate, releasing CO_2 and NADH. The reaction is carried out by the α -ketoglutarate dehydrogenase complex (*sucA*, *sucB*, *lpd* genes). As can be seen, two carbons were released as CO_2 up to this point of the TCA cycle. In order to function as a cycle, the carbons of the succinyl-CoA are conserved until the formation of oxaloacetate, which will be used to restart the cycle. The unique substrate level phosphorylation of the TCA cycle is catalyzed by the succinyl-CoA synthetase (*sucD* and *sucC* genes), where succinyl-CoA is converted to succinate, having CoA and ATP as products. In this reaction, inorganic phosphate is used to phosphorylate ADP to form ATP. Succinate is oxidized to fumarate, which is hydrated to L-malate. Finally, oxaloacetate is formed by the oxidation of L-malate. The first of the last three reactions is performed by the enzyme succinate dehydrogenase (*sdhABCD* genes), which yields FADH_2 from FAD, while conversion of fumarate to L-malate is done by the fumarases A, B, and C (*fumA*, *fumB*, *fumC* genes). The fumarases A and B are sensitive to oxidative agents. In conditions of oxidative stress, the fumarase C catalyzes the formation of L-malate. Formation of oxaloacetate can be performed independently by the enzymes malate:quinone oxidoreductase (*mgo* gene) or malate

dehydrogenase (*mdh* gene), releasing a quinol and NADH, respectively. The carbon balance of the TCA cycle demonstrates that, for each acetyl-CoA processed through, two molecules of CO₂ are formed, and the oxaloacetate used in the beginning is cycled back to be used in the next round.

Another metabolic important pathway connected to glycolysis and PPP is the Entner-Doudoroff pathway (ED pathway). This pathway plays an important role during growth on substrates, such as gluconate, glucuronate, or galacturonate. It is connected to the PPP at the level of 6-phosphogluconate. In the ED pathway, this metabolite is firstly converted to 2-dehydro-3-deoxy-D-gluconate 6-phosphate, and then is split to pyruvate and 3-phosphoglyceraldehyde. These products are metabolized in the other pathways of the central metabolism. The two reactions described above are catalyzed by the enzymes phosphogluconate dehydratase (*edd* gene) and 2-keto-3-deoxygluconate 6-phosphate aldolase (*eda* gene), respectively.

The glycolysis, PPP, and the TCA cycle provide the twelve precursor metabolites required to the biosynthesis of the building blocks (Table 1). From these building blocks, all the major components of the cell, e.g., proteins, nucleotides, lipids, polysaccharides; are produced. Another important category of biochemical reactions is required to ensure that the precursor metabolite availability meets the cell requirements. These metabolic steps, known as anapleurotic reactions, are discussed in more detail in the next section.

Table 1. Precursor metabolites required for the biosynthesis of the building blocks.

Precursor metabolites	Building blocks
glucose-6-phosphate	Glycogen, lipopolysaccharides
fructose-6-phosphate	Cell wall
ribose-5-phosphate	Histidine, phenylalanine, tryptophan, nucleotides
erythrose-4-phosphate	Phenylalanine, tryptophan, tyrosine
glyceraldehyde-3-phosphate	Lipids
3-phosphoglycerate	Cysteine, glycine, serine
phosphoenolpyruvate	Tyrosine, tryptophan
pyruvate	Alanine, isoleucine, lysine, leucine, valine
acetyl-CoA	Leucine, lipids
α-ketoglutarate	Glutamate, glutamine, arginine, proline
succinyl-CoA	Methionine, lysine, tetrapyrroles (e.g., heme)
oxaloacetate	Asparagine, aspartate, isoleucine, lysine, methionine, threonine, nucleotides

1.3.3. Anapleurotic reactions

In order to be able to grow, *E. coli* drains precursor metabolites from the central metabolism to produce the required building blocks. Depending on the substrate used as carbon source and the growth conditions, e.g., aerobic or anaerobic, limitations may occur in the pathways of the central metabolism due to this demand. For instance, intermediates of the TCA cycle are used for biosynthesis of building blocks. In cells growing on a substrate like glucose, the TCA cycle would run out of precursor metabolites, as there is not net synthesis of these compounds in the cycle. In order to overcome this limitation, special types of reactions, known as anapleurotic reactions, accomplish the task of replenishing these intermediates.

In aerobic growth on glucose, about 30% of glucose-6-phosphate is metabolized through the PPP and 70% in the glycolysis. Therefore, the precursor metabolites of these pathways are constantly produced. To replenish the TCA cycle intermediates, the enzyme phosphoenolpyruvate carboxylase (*ppc* gene) performs the carboxylation of phosphoenolpyruvate producing oxaloacetate and inorganic phosphate. The activity of this enzyme is also required when the cell is growing on glycerol or L-arabinose. During aerobic growth on glucose, *E. coli* secretes acetate into the culture medium. After glucose is consumed, the accumulated acetate starts to be metabolized as carbon source. Acetate is converted to acetyl-CoA, as described in the previous section, which can be used as single carbon source. Initially, acetyl-CoA is processed in the TCA cycle. As explained above, the TCA cycle loses carbon as CO₂. In this case, as acetyl-CoA is the only carbon source, the cycle would stop, as the oxaloacetate pool would be completely drained for production of building blocks. To circumvent this limitation, the cell utilizes the glyoxylate bypass (also called glyoxylate cycle). Initially, acetyl-CoA is converted to isocitrate through the TCA cycle. The glyoxylate bypass starts from this intermediate, by converting it to succinate and glyoxylate. The latter is subsequently fused to another acetyl-CoA molecule to generate malate and CoA. The two enzymes that perform these reactions are the isocitrate lyase (*aceA* gene) and malate synthase (*aceB* gene), respectively. Malate is then converted to oxaloacetate in the TCA cycle, which is used to produce phosphoenolpyruvate by the ATP-dependent activity of the phosphoenolpyruvate carboxykinase (*pck* gene). Phosphoenolpyruvate is then metabolized in the gluconeogenesis, which is

essentially the reverse form of the glycolysis where the irreversible step of converting fructose-1,6-biphosphate to fructose-6-biphosphate is overcome through the activity of fructose-1,6-biphosphate phosphatase, as explained in the previous section. *E. coli* is also able to grow using pyruvate as carbon source. This carbon source can be converted to acetyl-CoA by the pyruvate dehydrogenase complex. Interestingly, this metabolite is not processed to enable growth the same way that acetate is processed. From pyruvate, phosphoenolpyruvate can be produced by the activity of the ATP-driven phosphoenolpyruvate synthetase (*ppsA* gene). The intermediates of the TCA cycle are replenished through phosphoenolpyruvate carboxylase activity, the same way that occurs during growth using glucose as carbon source. In continuation of the description of the metabolism of *E. coli*, the important pathway of L-tryptophan biosynthesis, the violacein and deoxyviolacein precursor, will be addressed in more detail in the next section.

1.3.4. L-Tryptophan biosynthesis

L-Tryptophan is one of the three aromatic amino acids produced by *E. coli*. The biosynthesis of these amino acids has the chorismate pathway in common. From this metabolite, production of L-tryptophan proceeds independently, while L-tyrosine and L-phenylalanine share the chorismate-derived prephenate as the last common intermediate.

The chorismate pathway starts with the condensation of erythrose-4-phosphate and phosphoenolpyruvate, producing 3-deoxy-D-arabino-heptulosonate-7-phosphate and inorganic phosphate. Three different 2-dehydro-3-deoxyphosphoheptonate (DAHP) aldolase isozymes, also known as DAHP synthases, conduct this reaction in *E. coli*. These enzymes, encoded by the genes *aroF*, *aroG*, and *aroH*, are feedback inhibited by L-tyrosine, phenylalanine, and L-tryptophan, respectively. The DAHP is then converted to 3-dehydroquinate by dehydroquinate synthase (*aroB* gene), which is subsequently used to produce 3-dehydroshikimate through the activity of the 3-dehydroquinate dehydratase (*aroD* gene). Shikimate is produced from 3-dehydroshikimate by two shikimate dehydrogenases, one that utilizes NADPH (*aroE* gene) and another able to use either NADPH or NADH (*ydiB* gene). ATP-driven phosphorylation of shikimate by

shikimate kinase yields shikimate-3-phosphate. Two variants of this enzyme are present in *E. coli*, shikimate kinase I (*aroK* gene) and II (*aroL* gene). Shikimate kinase II is the dominant enzyme in this conversion and its expression is controlled by the TyrR and TrpR repressors. Next, 5-enolpyruvyl-shikimate 3-phosphate is formed by the fusion of shikimate-3-phosphate and phosphoenolpyruvate, releasing inorganic phosphate. This condensation is catalyzed by 3-phosphoshikimate-1-carboxyvinyltransferase (*aroA* gene). The final step of the pathway is the chorismate synthase (*aroC* gene) catalyzed removal of inorganic phosphate from 5-enolpyruvyl-shikimate 3-phosphate to produce chorismate, the first intermediate of L-tryptophan biosynthesis.

All the genes required for the production of L-tryptophan are encoded in the operon *trpEDCBA* in *E. coli*. The transcription of this operon is repressed by the TrpR repressor (*trpR* gene) and also by attenuation involving the *trpL* gene that encodes the leader peptide. The enzyme anthranilate synthase catalyzes the first reaction, where chorismate is converted to anthranilate. The genes *trpED* encode the two components of anthranilate synthase responsible for the transfer of the amino group of glutamine to chorismate, releasing glutamate. In this reaction, a part of the chorismate molecule is released in the form of pyruvate to conclude anthranilate production. Anthranilate synthase is feedback-inhibited by L-tryptophan. Once anthranilate is produced, it is fused with 5-phospho- α -D-ribose 1-diphosphate to generate N-(5-phosphoribosyl)-anthranilate. This reaction is interesting because it is performed by an enzyme, the anthranilate phosphoribosyl transferase, which is also encoded by the *trpD* gene. Therefore, the TrpD enzyme plays two roles in the L-tryptophan biosynthesis. In combination with TrpE, it is involved in the first reaction of the L-tryptophan biosynthesis, while alone it is responsible for the second reaction. Similarly, the next two reactions of the pathway are catalyzed by another bifunctional enzyme encoded by the *trpC* gene. First, TrpC acts as phosphoribosylanthranilate isomerase and later as indole-3-glycerol phosphate synthase to produce 1-(o-carboxyphenylamino)-1'-deoxyribulose 5'-phosphate and indole-3-glycerol-phosphate (in addition to CO₂), respectively. The final two steps of the L-tryptophan biosynthesis are conducted by the L-tryptophan synthase. This bifunctional enzyme converts the indole-3-glycerol-phosphate to indole and glyceraldehyde-3-phosphate. The former is then fused to L-serine to yield L-tryptophan. L-Tryptophan synthase contains two dimers

of α (*trpA* gene) and β (*trpB* gene) subunits. By analyzing the biosynthesis of L-tryptophan since the metabolic precursors, it can be determined that for each molecule of this amino acid one erythrose-4-phosphate, two phosphoenolpyruvates, one L-glutamine, one phosphoribosyl-5-pyrophosphate, and one L-serine molecules are necessary.

The L-tryptophan pathway has been extensively studied along the last decades. In these studies, the important points of metabolic regulation related to the production of L-tryptophan were precisely identified in *E. coli*. This knowledge has enabled the rational engineering of strains able to accumulate this amino acid at high titers, thereby allowing its widespread use for different purposes, such as a feed additive and in the pharmaceutical industry (Shen et al., 2012). Basically, metabolic engineering strategies used develop L-tryptophan producing strains of *E. coli* rely on i) elimination of repressors of the pathways involved, ii) elimination of attenuators, iii) removal of feedback-inhibition of the enzymes involved, iv) overexpression of target pathways, and v) removal of competing pathways (Ikeda, 2006; Sprenger, 2007). Starting from a well known *E. coli* strain, e.g., MG1655, deletion of the repressor of the *trpEDCBA* operon, *trpR* gene, permits the L-tryptophan genes to be expressed to a higher level. The next beneficial genetic modification to allow high level expression of this operon is the removal of leader peptide encoded by the *trpL* gene. At this point, the obtained strain would be able to accumulate a higher level of L-tryptophan in the cytoplasm. However, high L-tryptophan pools trigger the expression of the tryptophanase (*tnaA* gene), which degrades L-tryptophan to indole, pyruvate and NH_4^+ . To avoid this, the *tnaA* gene also needs to be removed. Next, the feedback inhibition of anthranilate synthase should be addressed, by inserting the necessary mutations that enable the enzyme to become insensitive to L-tryptophan inhibition. At this point, the limitations in the availability of the other precursors required for production can also be tackled. For each L-tryptophan produced, one L-serine molecule is required. If the production of this amino acid can not cope with the demand required for L-tryptophan production, the necessary modifications to improve of the L-serine pathway have to be made. The same strategy used for the L-tryptophan pathway can be used here; specifically, overexpression of the L-serine pathway genes, and removal of feedback-inhibition of the first reaction of L-serine production catalyzed by the enzyme D-3-phosphoglycerate dehydrogenase (*serA*

gene). By streaming up the L-tryptophan pathway, the next component required for tryptophan biosynthesis is N-(5-phosphoribosyl)-anthranilate. Production of this molecule can also be improved by modifications of the phosphoribosyl anthranilate transferase expression and removal of L-tryptophan sensitivity (Aiba et al., 1982). At this point, the availability of chorismate must be addressed, as its production is tightly regulated in *E. coli*. Supply of this intermediate is limited at the DAHP synthase level. A general strategy to overcome this limitation is the overexpression of feedback-resistant variants of the *aroF*, *aroG*, and *aroH* genes. Finally, genetic modifications can be done to increase the pool of the precursors of the central metabolism erythrose-4-phosphate and phosphoenolpyruvate. In the case of erythrose-4-phosphate, overexpression of the *tktA* gene, or phosphoglucose isomerase deletion were reported as beneficial, whereas phosphoenolpyruvate availability can be improved by employing different strategies, such as deletion of phosphoenolpyruvate carboxylase or the pyruvate kinases, overproduction of the phosphoenolpyruvate carboxykinase or phosphoenolpyruvate synthetase. Another important aspect relevant to the availability of phosphoenolpyruvate is the type of substrate used during the production. For instance, glucose is transported into the cell by the PTS, which is phosphoenolpyruvate dependent. For each glucose molecule transported, one phosphoenolpyruvate molecule is converted to pyruvate, thereby limiting phosphoenolpyruvate supply for L-tryptophan production. This problem can be overcome by modifying the glucose transport system or using a non-PTS substrate, e.g., glycerol.

1.4. Escherichia coli as host for violacein and deoxyviolacein production

Escherichia coli is one of the most studied microorganisms. Due to the basic research carried out by different groups, a comprehensive systemic understanding of the metabolism in the genomic, transcriptomic, proteomic and fluxomic levels permits the systems-wide engineering of *E. coli* for different purposes. In this section, a brief overview of tools available for optimization of this microorganism for production of metabolites, such violacein and deoxyviolacein, and the heterologous production of these drugs, will be given.

1.4.1. Tools for genetic engineering

Many methods have been developed for the manipulation of genetic material of *E. coli*, each one presenting its peculiarities. For the sake of metabolic engineering studies, methods of molecular biology that allow cloning, insertion, deletion and modification of genes in chromosome or in plasmids are mandatory. One of the techniques that allow these types of genetic modification is known as recombineering. Recombineering stands for *recombination mediated genetic engineering* (Ellis et al., 2001). The advantage of this method is the fact that homologous recombination of single or double-stranded DNA molecules bearing homologous regions as short as 30 bp is possible (H0 and H1 in Figure 3). The necessary homologous DNA sequences can be inserted in other DNA molecules by polymerase chain reaction (PCR) using primers designed to include these regions (Figure 3A). This facilitates the efforts to obtain the linear DNA that will be used for the recombination. After obtaining the desired linear DNA molecule, the next step is its introduction into *E. coli* cells for subsequent recombination (Figure 3B, C, and D). Normal *E. coli* cells have the RecBCD and SbcCD nucleases that degrade linear DNA once it is inserted into the cells. In order to avoid this and permit the recombination event to take place, the recombineering method uses the Red proteins Exo, Beta, and Gam from phage λ . After inserting the linear DNA into *E. coli* expressing the λ Red proteins, Gam inhibits RecBCD and SbcCD activities, thereby allowing homologous recombination to take place by action of Exo and Beta. The function of Exo is the degradation of dsDNA to release ssDNA that will be used for recombination. In case the cell is transformed with ssDNA instead of dsDNA, the activity of Exo is not necessary. Finally, Beta can bind to the ssDNA for recognition of the homologous sequences and subsequent recombination event. Beta also prevents ssDNA degradation by the action nucleases. Expression of Red proteins in *E. coli* can be done using the plasmid pKD46 (Datsenko and Wanner, 2000) (Figure 3B and C). By using the recombineering technology, desired modifications of the *E. coli* genome can be performed. In order to select the clone containing the desired modification, a selection marker is usually employed (Figure 3A). This maker can be a gene conferring antibiotic resistance or another phenotype that permits the desired clone to be differentiated from the other cells. For instance, the inactivation of genes related to production of amino

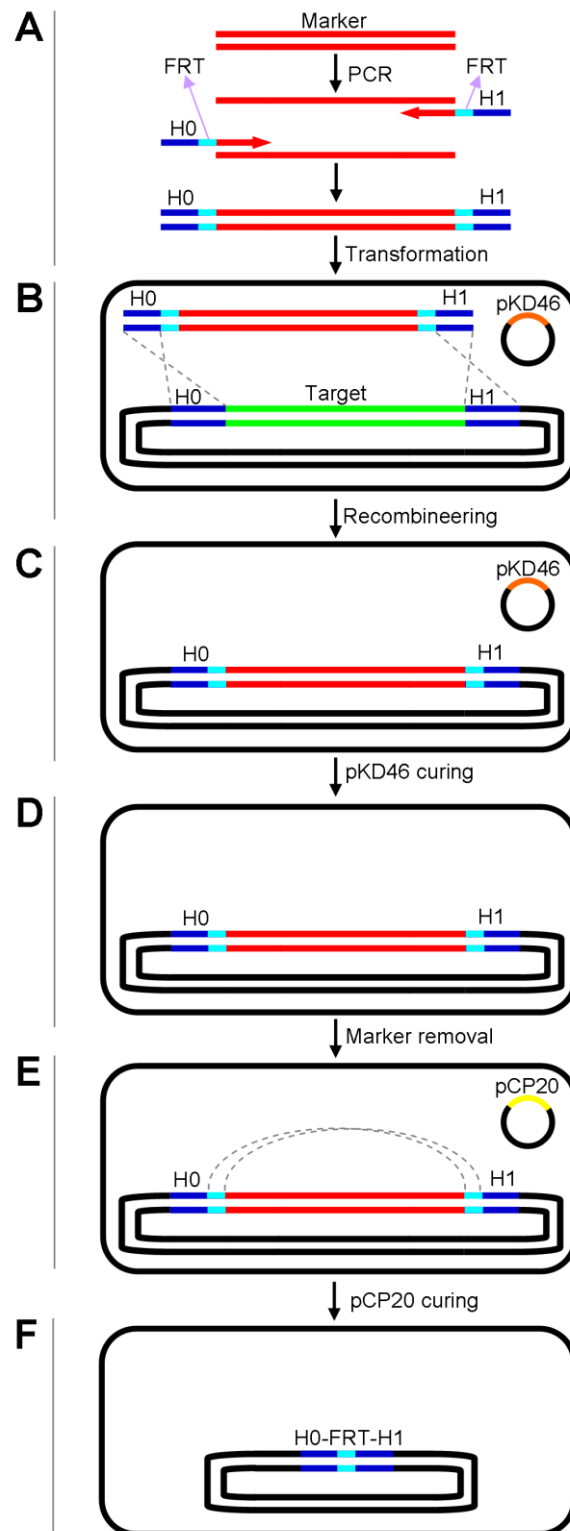


Figure 3. Overview of genetic modification using the recombineering methodology followed by marker removal.

acids produces auxotrophic mutants. Studies in which the objective is the isolation of strains that present enzymes with feedback resistance take advantage of the auxotrophic mutants to select feedback resistant strains. Provided that a feedback

resistant variant of the target genes is available, this can be done by restoring this gene variant to the auxotrophic mutants by recombineering. Afterwards, by cultivating the recombinants in medium containing a suicide inhibitor for the respective enzyme, clones containing the desired variant of the genes can be selected. The advantage of this strategy is that no extra DNA sequences are left in the chromosome after the modification. Alternatively, removal of markers can be performed by flanking them with short direct repeats (FRT sites) sequences that can be later used to remove the DNA between the FRTs by the yeast Flp recombinase (Figure 3E and F) of the pCP20 plasmid (Cherepanov and Wackernagel, 1995).

1.4.2. Heterologous production of violacein and deoxyviolacein

The violacein and deoxyviolacein biosynthetic routes are encoded by the *vioABCDE* operon. In a series of studies, the intermediates of the pathways and the function of the enzymes have been identified (Asamizu et al., 2007; Pemberton et al., 1991; Sánchez et al., 2006; Shinoda et al., 2007). Shortly, the biosynthesis starts from L-tryptophan, which is converted by VioA into indole-3-pyruvic acid imine (Figure 4). Two of these intermediates are fused by concomitant action of VioB and VioE, to yield protodeoxyviolaceinic acid, which is then further processed into violacein by the enzymes VioD and VioC. In contrast, deoxyviolacein biosynthesis only requires VioC activity in the final step so that this derivate can be obtained in pure form via inactivation of the *vioD* gene, resulting in a shortened operon that contains only *vioABCE* (August et al., 2000).

Due to the therapeutic potential of violacein and deoxyviolacein, their production in different natural strains has been thoroughly investigated (Ahmetagic and Pemberton, 2010; August et al., 2000; Jiang et al., 2012; Jiang et al., 2010; Mendes et al., 2001; Yang et al., 2007), but was found limited by low productivity (Yang et al., 2011) of the natural producers. Particularly in the case of deoxyviolacein, the levels in natural producers are low, comprising only 10% of the overall pigment produced (Hoshino, 2011). Isolates of the best-studied natural producers *Chromobacterium violaceum* and *Janthinobacterium lividum* cause rare but highly deadly infections in humans (Patjanasoonorn et al., 1992; Ti et al., 1993), which obviates their use in pharmaceutical biotechnology. This strongly

drives the overexpression of the *vioABCDE* operon in suitable recombinant hosts that exhibit fast growth on simple media, straightforward genetic accessibility, well-understood physiology and that are particularly accepted as safe drug producers. A study have indeed demonstrated recombinant violacein production in *Citrobacter freundii* and *Enterobacter aerogenes* (Yang et al., 2011). Pioneering studies

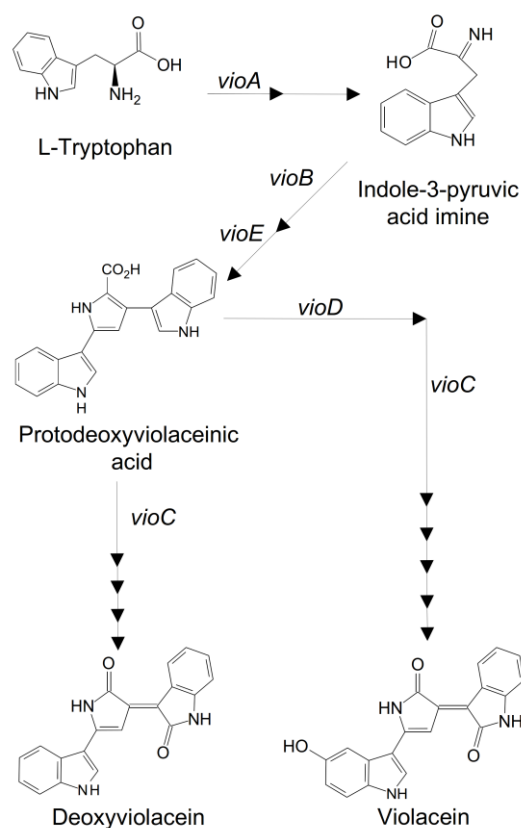


Figure 4. Biosynthetic pathways for violacein and deoxyviolacein.

reported successful heterologous expression of the *vioABCDE* pathway also in *Escherichia coli* (August et al., 2000; Pemberton et al., 1991). This was an early milestone for safe production, as *E. coli* K-12 is widely accepted in industrial biotechnology (Huang et al., 2012) and employed for production of compounds used for human treatment (Ferrer-Miralles et al., 2009). In addition, *E. coli* K-12 strains are efficient in synthesizing L-tryptophan (Azuma et al., 1993; Berry, 1996), the precursor of violacein and deoxyviolacein. The product titers of these recombinant violacein and deoxyviolacein producers are still limited, probably due to the rather local pathway engineering, restricted to exclusive expression of the heterologous biosynthetic chain. At this stage, a next level of production strains with improved performance might be expected from systems metabolic

engineering on a global scale (Becker and Wittmann, 2012), which explores and recruits the complex metabolic and regulatory networks for systems wide re-direction of pathway flux to support production. This seems particularly important for violacein and deoxyviolacein biosynthesis, embedded into the interconnected network of carbon core metabolism and tightly constrained by different layers of metabolic (Zhang et al., 2010) and transcriptional regulation (Landick et al., 1985; McClean et al., 1997).

In this regard, the present work describes systems metabolic engineering of *E. coli* for production of violacein and deoxyviolacein. Initially, an analytical method to quantify the content of violacein and deoxyviolacein with high precision in a single analysis was developed. Afterwards, *E. coli* was recruited due to its high capability to produce L-tryptophan (Balderas-Hernández et al., 2009; Ikeda, 2006), the building block for the desired pigments. Starting from a basic producer that expressed the *vioABCE* genes from *Chromobacterium violaceum*, *E. coli* was stepwise improved for overproduction of deoxyviolacein. Based on careful analysis, the central metabolism of *E. coli* was globally optimized, which involved engineering of (i) the pentose phosphate pathway, (ii) the entire biosynthesis up to the level of the chorismate and (iii) the tryptophan route, (iv) enhanced supply of serine, (v) elimination of tryptophan repression/attenuation and (vi) degradation (tryptophanase). The deoxyviolacein producer *E. coli* dVio-6 comprised these genomic traits together with plasmid-based expression of *vioABCE* under control of the *araBAD* promoter system, inducible by L-arabinose. The mutant accumulated 320 mg L⁻¹ deoxyviolacein, whereby the *araBAD* system mediated a precisely controllable induction of *vioABCE*. The titer was markedly higher than that achieved in previous approaches, but still left space for further improvement. Particularly, L-arabinose had to be used as source of carbon, as *E. coli* is able to metabolize this sugar (Desai and Rao, 2010; Englesberg et al., 1965), which enabled only slow growth and resulted in unfavorable long process times. Moreover, L-arabinose was required in large amounts, limiting economic success due to high price of L-arabinose, about hundred-fold higher than that of traditional biotechnology sugars. Accordingly, the next-generation strain able to use alternative raw materials was constructed. Strain engineering involved elimination of L-arabinose catabolism, while L-arabinose uptake encoded by *araE* and *araFGH* was retained. Isotope experiments with ¹³C L-arabinose verified that L-arabinose

was still taken up and served as inducer of *vioABCE* expression, but was no longer metabolized by the created mutant. Out of different raw materials tested, glycerol was identified as promising carbon source for production. In a glycerol-based fed-batch process the novel mutant produced 1.6 g L^{-1} of deoxyviolacein, which is five-fold higher than previously achieved and provides an attractive option to derive this valuable drug from cheap raw materials. Afterwards, by integration of the *vioD* gene into the chromosome, the *E. coli* with optimized metabolism for high tryptophan production was additionally modified into a violacein producer. In all cases, the desired compound could be obtained as exclusive product using L-arabinose as carbon source. Subsequently, the performance of the engineered overproducer was assessed in a fed-batch process, yielding about 700 mg L^{-1} of pure violacein.

2 Materials and Methods

2.1. Development of methods for separation and quantification of violacein and deoxyviolacein

2.1.1. Organisms and growth conditions

Recombinant *Escherichia coli* TOP10 (Invitrogen), harboring the violacein operon from *Chromobacterium violaceum* on pBvioABCDE (Rodrigues et al., 2013), on pJP1000 or on pPSX-Vio+ (Sarovich and Pemberton, 2007) and the natural producer *Janthinobacterium lividum* DSM 1522 (Pantanella et al., 2007), obtained from the DSMZ (Braunschweig, Germany), were used for production. Liquid cultures were performed in shake flasks at 25 °C on LB medium with 10 g L⁻¹ L-arabinose (*E. coli*) or with 10 g L⁻¹ glycerol (*J. lividum*). In addition, plate cultures were grown on LB agar at 20 °C until pigmented colonies were obtained. For pigment extraction, cells were collected by centrifugation (4650×g, 15 min, 4 °C, Multifuge 4KR, Heraeus, Hanau, Germany) either from the broth of a liquid culture or from a colony suspension of a plate culture in deionized water. Subsequently, violacein and deoxyviolacein were extracted from the cells with ethanol (Mendes et al., 2001).

2.1.2. Preparation of pure violacein and deoxyviolacein

Pure deoxyviolacein was prepared from ethanol extracts of *E. coli* TOP10 pBvioABCDE. The obtained ethanol extract was separated from the cells by centrifugation and then concentrated at reduced pressure (Laborota 4000, Schwabach, Germany). The concentrated extract was purified by flash-chromatography using silica gel 60 (0.040-0.063 mm, Merck, Darmstadt, Germany) and 70% (v v⁻¹) ethanol as mobile phase. The violet fraction containing deoxyviolacein was collected, concentrated under reduced pressure and dried. Analysis by ¹H and ¹³C NMR spectroscopy (Wille and Steglich, 2001) and HR-ESI-MS ([M+H]⁺: calc. 328.10805, found 328.10782) confirmed the identity and purity of deoxyviolacein without any detectable amounts of violacein (This analysis was performed at the Institute of Organic Chemistry, Technische Universität

Braunschweig by the work group of Prof. Dickschat). Similarly, a violacein standard from cultures of *E. coli* TOP10 pPSX-Vio+ was obtained.

2.1.3. Quantification of violacein and deoxyviolacein

Samples were analyzed by HPLC (LaChrom Elite, Hitachi High-Technologies Corporation, Mannheim, Germany) with a C18 column (Thermo Scientific, Hypersil ODS, 5 μm , 250x4.6 mm) at 30 °C. Different concentrations of methanol and ethanol were tested as mobile phase at a flow rate of 0.5 mL min⁻¹. The injection volume was 10 μl . The detection was based on a diode array detector with signal monitoring between 200-700 nm. Violacein and deoxyviolacein were quantified on basis of external standards.

2.1.4. Estimation of extinction coefficients

A spectrophotometer Libra S11 (Biochrom, Cambridge, UK) was used for determination of the extinction coefficients of violacein and deoxyviolacein dissolved in ethanol solutions at different ratios.

2.2. Systems metabolic engineering of *Escherichia coli* for production of violacein and deoxyviolacein from L-arabinose

2.2.1. Strains and plasmids

Escherichia coli K-12 MG1655 (Jensen, 1993) (CGSC 6300) was used as host for heterologous production. Its derivative, *E. coli* BW25113 (Datsenko and Wanner, 2000) was used for chromosomal integration cloning, as given in the Supplementary Information. *E. coli* DH10B (Life GmbH, Darmstadt, Germany) was used for standard cloning and plasmid maintenance. The *vioABCDE* operon that encoded the violacein biosynthetic pathway was derived from genomic DNA of *Chromobacterium violaceum* ATCC 12472 (American Type and Culture Collection, Manassas, USA). The *vioD* gene was cloned from *Janthinobacterium lividum* DSM 1522 (Leibniz Institute DSMZ - German Collection of Microorganisms and Cell Cultures, Braunschweig, Germany). The plasmid pBADMyHisB was used for heterologous expression of the *vio* operon in *E. coli* (Life GmbH, Darmstadt,

Germany). This plasmid contains the *bla* gene for ampicillin resistance and the L-arabinose inducible P_{BAD} promoter upstream of the multiple cloning site. The plasmids pKD3, pKD4, pKD46 (Datsenko and Wanner, 2000), pClik5a (Krömer et al., 2006) and pCP20 (Cherepanov and Wackernagel, 1995) were used to perform genetic modifications in *E. coli* K-12 MG1655. Chaperone expressing plasmids pGro7, pG-KJE8, pKJE7, pG-Tf2, and pTf16 were purchased from Takara Bio, Inc., Japan. The plasmid pJNNmod (see Appendix) was used for cloning of the *vioD* gene from *J. lividum*. All plasmids and strains used are listed in Table 2. Generally, molecular biology procedures followed standard protocols (Sambrook and Russell, 2001). Gene deletion and genomic modification of *E. coli* was performed by recombineering (Datsenko and Wanner, 2000) using specific primer pairs as indicated (Table 3). All strains were maintained as glycerol stocks at -80 °C.

2.2.2. Construction of the violacein production plasmid

First, the *vioABCD* genes of *C. violaceum* ATCC 12472 were amplified from genomic DNA by nested PCR (Mastercycler Gradient Thermal Cycler, Eppendorf, Hamburg, Germany) with external (1, 2) and internal primers (3, 4) as given in Table 3. The plasmid pBvioABCD was then constructed by insertion of the *vioABCD* genes into the multiple cloning site. The *vioE* gene was amplified from genomic DNA of *C. violaceum* ATCC 12472 using the primers 5 and 6 (Table 3). The plasmid pBvioABCDE was obtained by subsequent insertion of the *vioE* gene downstream of *vioD* into the plasmid pBvioABCD. The correct insertion of the heterologous *vio* genes was verified by sequencing (Macrogen, Korea).

Table 2. Strains and plasmids.

Strains and plasmids	Relevant genotype	Reference
Strains		
<i>E. coli</i>		
DH10B	$\Delta(ara,leu)7697$ <i>araD139</i>	(Life GmbH, Darmstadt, Germany)
BW25113 (CGSC#:	MG1655 <i>lacI^f</i> <i>rrnB_{T14}</i> $\Delta lacZ_{WJ16}$ <i>hsdR514</i> $\Delta araBAD_{AH33}$ $\Delta rhaBAD_{LD78}$	(Datsenko and Wanner,

Material and Methods

7636)		2000)
MG1655 (CGSC#: 6300)	Wild type <i>E. coli</i> K-12	(Jensen, 1993)
TRP1	BW25113 $\Delta sdaA::FRT-Cm-FRT$	see Appendix.
TRP2	BW25113 $\Delta trpE::FRT-Km-FRT$	see Appendix.
TRP3	BW25113 $\Delta trpL trpE^{fr}$	see Appendix.
TRP4	F52 $\Delta lac::_{PTAC}aroFBL-FRT-Km-FRT$	see Appendix.
TRP5	BW25113 Ara+ $\Delta tktA \Delta gal::_{PTAC}tktA-FRT-Cm-FRT$	see Appendix.
TRP6	BW25113 $\Delta serA \Delta xyl::_{PTAC}serA^{fr}-FRT-Km-FRT$	see Appendix.
TRP7	MG1655 $\Delta trpR::FRT \Delta tnaA::FRT \Delta sdaA::FRT-Cm-FRT$	This study
TRP8	MG1655 $\Delta trpR::FRT \Delta tnaA::FRT \Delta sdaA::FRT-Cm-FRT \Delta trpL trpE^{fr}$	This study
TRP9	MG1655 $\Delta trpR::FRT \Delta tnaA::FRT \Delta sdaA::FRT lac::_{PTAC}aroFBL-FRT \Delta trpL trpE^{fr}$	This study
TRP10	MG1655 $\Delta trpR::FRT \Delta tnaA::FRT \Delta sdaA::FRT \Delta lac::_{PTAC}aroFBL-FRT \Delta trpL trpE^{fr} \Delta gal::_{PTAC}tktA-FRT-Cm-FRT$	This study
TRP11	MG1655 $\Delta trpR::FRT \Delta tnaA::FRT \Delta sdaA::FRT \Delta lac::_{PTAC}aroFBL-FRT \Delta trpL trpE^{fr} \Delta gal::_{PTAC}tktA-FRT \Delta xyl::_{PTAC}serA^{fr}-FRT$	This study
NC	MG1655 pBADMyHisB-Km	This study
dVio-1	MG1655 pBvioABCE-Km	This study
dVio-2	MG1655 $\Delta trpR::FRT \Delta tnaA::FRT \Delta sdaA::FRT-Cm-FRT$ pBvioABCE-Km	This study
dVio-3	MG1655 $\Delta trpR::FRT \Delta tnaA::FRT \Delta sdaA::FRT-Cm-FRT \Delta trpL trpE^{fr}$ pBvioABCE-Km	This study
dVio-4	MG1655 $\Delta trpR::FRT \Delta tnaA::FRT \Delta sdaA::FRT \Delta lac::_{PTAC}aroFBL-FRT \Delta trpL trpE^{fr}$ pBvioABCE-Km	This study
dVio-5	MG1655 $\Delta trpR::FRT \Delta tnaA::FRT \Delta sdaA::FRT \Delta lac::_{PTAC}aroFBL-FRT \Delta trpL trpE^{fr} \Delta gal::_{PTAC}tktA-FRT-Cm-FRT$ pBvioABCE-Km	This study
dVio-6	MG1655 $\Delta trpR::FRT \Delta tnaA::FRT \Delta sdaA::FRT \Delta lac::_{PTAC}aroFBL-FRT \Delta trpL trpE^{fr} \Delta gal::_{PTAC}tktA-FRT$	This study

	$\Delta xyl::_{PTAC} serA^{fr}-FRT$ pBvioABCE-Km	
Vio-1	BW25113 $\Delta fuc::_{PTAC} vioD-FRT-Km-FRT$	This study
	MG1655 $\Delta trpR::FRT \Delta tnaA::FRT \Delta sdaA::FRT$	
Vio-2	$\Delta lac::_{PTAC} aroFBL-FRT \Delta trpL trpE^{fr} \Delta gal::_{PTAC} tktA-FRT$	This study
	$\Delta xyl::_{PTAC} serA^{fr}-FRT \Delta fuc::_{PTAC} vioD-FRT-Km-FRT$	
	MG1655 $\Delta trpR::FRT \Delta tnaA::FRT \Delta sdaA::FRT$	
Vio-3	$\Delta lac::_{PTAC} aroFBL-FRT \Delta trpL trpE^{fr} \Delta gal::_{PTAC} tktA-FRT$	This study
	$\Delta xyl::_{PTAC} serA^{fr}-FRT \Delta fuc::_{PTAC} vioD-FRT$	
	MG1655 $\Delta trpR::FRT \Delta tnaA::FRT \Delta sdaA::FRT$	
Vio-4	$\Delta lac::_{PTAC} aroFBL-FRT \Delta trpL trpE^{fr} \Delta gal::_{PTAC} tktA-FRT$	This study
	$\Delta xyl::_{PTAC} serA^{fr}-FRT \Delta fuc::_{PTAC} vioD-FRT$ pBvioABCE-Km	
<i>Chromobacterium violaceum</i>		
	ATCC 12472 <i>vioABCDE</i>	(de Vasconcelos et al., 2003)
<i>Janthinobacterium lividum</i>		
	DSM 1522 <i>vioD</i>	(Kimmel and Maier, 1969)
Plasmids		
pG-KJE8	<i>dnaK-dnaJ-grpE-groES-groEL, araB, Pzt-I</i>	Takara Bio Inc., Japan
pGro7	<i>groES-groEL, araB</i>	Takara Bio Inc., Japan
pKJE7	<i>dnaK-dnaJ-grpE, araB</i>	Takara Bio Inc., Japan
pG-Tf2	<i>groES-groEL-tig, Pzt-I</i>	Takara Bio Inc., Japan
pTf16	<i>tig, araB</i>	Takara Bio Inc., Japan
pBADMycHis B	$P_{BAD} bla$	(Life GmbH, Darmstadt, Germany)
pBADMycHis B-Km	$P_{BAD} bla Km$	This study
pKD3	<i>Cm</i>	(Datsenko and Wanner, 2000)

pKD4	<i>Km</i>	(Datsenko and Wanner, 2000)
pKD46	P_{BAD} <i>gam-bet-exo</i>	(Datsenko and Wanner, 2000)
pCP20	<i>FLP</i>	(Cherepanov and Wackernagel, 1995)
pClik5a	<i>Km</i>	(Krömer et al., 2006)
pBvioABCD	<i>vioABCD</i>	This study
pBvioABCDE	<i>vioABCDE</i>	This study
pBvioABCDE-Km	<i>vioABCDE Km</i>	This study
pBvioABCE-Km	<i>vioABCE Km</i>	This study
pJNNmod	P_{TAC} , <i>lacI^l</i> , ColE1 origin of replication	see Appendix.
pJNNmod+ <i>vioD</i>	P_{TAC} <i>vioD</i>	This study
pJNNmod+ <i>vioD-Km</i>	P_{TAC} <i>vioD-FRT-Km-FRT</i>	This study

The *aphA* gene for kanamycin resistance (*Km*) was amplified from plasmid pKD4 using the primers 7 and 8 for insertion into the plasmid pBvioABCDE. The obtained PCR product was digested with DpnI to degrade the template DNA. The amplicon containing the *Km* (*aphA* gene) was isolated and purified by agarose gel electrophoresis and was then cloned into pBvioABCDE yielding the plasmid pBvioABCDE-Km. The obtained plasmid was then transformed in *E. coli* using standard protocols (Sambrook and Russell, 2001).

2.2.3. Construction of the deoxyviolacein production plasmid

In order to remove the *vioD* gene from pBvioABCDE-Km, the upstream and downstream regions of this gene were amplified by PCR using the primer pairs 9, 10 and 11, 12, respectively (Table 3). The PCR products were isolated by agarose gel electrophoresis and applied to overlapping extension PCR using primers 9 and

12 (Table 3). The PCR product was used to replace the *vioD* gene by the shortened fragment yielding the plasmid pBvioABCE-Km. The construct was validated by PCR.

2.2.4. Genomic integration of the *vioD* gene

The *vioD* gene was amplified from *J. lividum* DSM 1522 using primers 23 and 24 (Table 3). The amplicon containing the *vioD* ORF was isolated by agarose gel electrophoresis, digested with NdeI and HindIII and cloned into pJNNmod previously digested with the same restriction enzymes. The construct was sequenced (GATC Biotech AG, Konstanz, Germany) to ensure proper replacement of the native promoter of the *vioD* gene by the P_{TAC} promoter. The *Km* from pKD4 was subsequently inserted as resistance marker. Finally, the P_{TAC}*vioD-FRT-Km-FRT* construct was inserted into the *fucPIK* locus of *E. coli* BW25113 using primers 25 and 26 (Albermann et al., 2010) (Table 3).

2.2.5. Transduction of target constructs

The strains TRP1 through TRP3, TRP5, TRP6 (Table 2 and Supplementary Information), and Vio-1 (Table 2) are derivatives of strain BW25113 and were used as sources of the following gene constructs: $\Delta sdaA::FRT-Cm-FRT$; $\Delta trpE::Km$;

Table 3. Primers used for genetic construction work.

Primer ID	Primers (5'→3')	Target
1	acgaaaggcagcatcccgattcc	Amplification of <i>vioABCD</i> in <i>C. violaceum</i> ATCC 12472
2	gcgctcgtagtcgaaccagcagtag	
3	aggacattctcgaggaagcattctccgatatctg	
4	actccggtaccacacataggcgctgctc	
5	gcgctgtacctgcaacgctgaggag	Amplification of <i>vioE</i> in <i>C. violaceum</i> ATCC 12472
6	cgaaaggtaccccgttttctgcccgat	
7	gtggccagtccaagcttgcacgc	Amplification of <i>Km</i> in pKD4 for eventual insertion into pBvioABCDE, pBADMycHisB, and pJNNmod+ <i>vioD</i>
8	ggcaagcttaacggctgacatgggaattag	

Material and Methods

9	ggcgcgcgccaactacgacgtgctca	
10	gcggtgcagcgcgtagcgcacagaatcttcatcagttgac	Deletion of <i>vioD</i> in
11	gtcaactgatgaagattctgtgcgctacgcgctgcaacgc	pBvioABCDE-Km
12	cgtagtcgaaccagcagtagccggacgtca	
13	tttatgatatgctatcgctactctttagcaggtacaaccggggagggaag	Amplification of <i>Km</i> in
14	ttcctatacttctagagaataggaactccacgcgcatatgactagtt	pClik5a for <i>trpR</i> deletion
14	tcggtgcacgatgcctgatgcgccacgtcttatcaggcctacaaaaga	in <i>E. coli</i> K-12 MG1655
14	agttcctattctctagaaagtataggaactccagcagtcagtgagcg	
14	agg	
15	tttatgatatgctatcgctactctttagcaggtacaaccggggagggtgta	Amplification of <i>Cm</i> in pKD3
15	ggctggagctgcttc	for <i>Km</i> deletion in <i>E. coli</i>
16	tcggtgcacgatgcctgatgcgccacgtcttatcaggcctacaaaatg	K-12 MG1655 $\Delta trpR$ -FRT-
16	ggaattagccatggtcc	<i>Km</i> -FRT
17	caattgctggatccggaacgaatatcaac	Amplification of <i>trpR</i> of <i>E.</i>
18	cgctgagtcggttcataatgccgtgat	<i>coli</i>
18		K-12 MG1655 to check for
18		<i>trpR</i> deletion
19	gcatatatactggcgaattaatcggtatagcagatgtaatattcacagg	Amplification of <i>Cm</i> in pKD3
19	gtgtaggctggagctgcttc	for <i>tnaA</i> deletion in <i>E. coli</i>
20	tgtagggtaaagagagtggctaacatccttatagccactctgtagtattaa	K-12 MG1655 $\Delta trpR$ -FRT
20	atgggaattagccatggtcc	
21	catcaccagagccaaaccgattagattcaa	Amplification of <i>tnaA</i> in <i>E.</i>
22	cgctgataatgttccaggtgttaccgat	<i>coli</i>
22		K-12 MG1655 $\Delta trpR$ -FRT to
22		check
22		for <i>tnaA</i> deletion
23	taaacatatgaaaattctcgatcggcgcagg	Amplification of <i>vioD</i> in <i>J.</i>
24	ggtaaagcttttagcggccagcgcgta	<i>lividum</i> DSM 1522 for
24		insertion into pJNNmod
25	tgctgtgctcactgttttcttggcggtagccaataacctaacgacatt	Amplification of P_{TAC} <i>vioD</i> -
25	tattatcaaggcgcactcccgttctgg	FRT- <i>Km</i> -FRT in
26	cagcatggaggcgagagtgataaagtctgcgccaacgtggccgatg	pJNNmod+ <i>vioD</i> - <i>Km</i> for
26	gtcagaacccccagggttattgtctcatgagcg	insertion into
26		<i>E. coli</i> BW25113

$\Delta trpL$, $trpE^{fr}$; $\Delta gal::_{PTAC} tktA-FRT-Cm-FRT$; $\Delta xyl::_{PTAC} serA^{fr}-FRT-Km-FRT$; and $\Delta fuc::_{PTAC} vioD-FRT-Km-FRT$, respectively. Strain TRP4, a W3110 derivative (Supplementary Information), was the ultimate source of the construct $\Delta lac::_{PTAC} aroFBL-FRT-Km-FRT$. Recombinant *E. coli* strains were obtained by transferring these genes among the strains by transduction using phage P1 *vir*, following a previously described method (Thomason et al., 2007).

2.2.6. Growth media

LB medium was composed of 10 g L⁻¹ NaCl, 5 g L⁻¹ yeast extract (Difco, Detroit, USA), and 10 g L⁻¹ tryptone (Difco, Detroit, USA) at pH 7. For strains harboring plasmids that had been derived from pBADMyHisB, the medium was additionally amended with 100 µg mL⁻¹ ampicillin, except for strains containing pBvioABCE-Km that received either 100 µg mL⁻¹ ampicillin or 50 µg mL⁻¹ kanamycin. In case of strains that contained chaperone-expression plasmids, the medium was supplemented with 20 µg mL⁻¹ chloramphenicol. Tetracycline (5 ng mL⁻¹) was used for induction of gene expression in plasmids pG-Tf2 and pG-KJE8. For evaluation of production performance on plates, the LB medium was supplemented with 1 g L⁻¹ L-arabinose for induction and solidified by addition of 15 g L⁻¹ agar. Medium sterilization was carried out by autoclaving. L-Arabinose and antibiotic stock solutions were filter-sterilized (0.22 µm, Sartorius Stedim Biotech, Germany) and added to the medium at room temperature. The mineral medium used for production was modified from (Al Zaid Siddiquee et al., 2004) and contained per liter of deionized water: 0.58 g NaCl, 5.29 g (NH₄)₂SO₄, 17.41 g K₂HPO₄, 13.61 g KH₂PO₄, 0.25 g MgSO₄ 7H₂O, 1 µg thiamin HCl, 3 mg vitamin B₃, 1 mg vitamin B₂, 5.51 mg CaCl₂, 16.66 mg FeCl₃ 6H₂O, 1 mg MnCl₂ 4H₂O, 1.7 mg ZnCl₂, 340 µg CuCl₂, 470 µg CoCl₂ and 600 µg Na₂MoO₄ 2H₂O. The pH was adjusted to 7.8 with 4 M NaOH. The vitamin solutions were filter-sterilized (0.22 µm, Sartorius Stedim Biotech, Germany). The remaining components were sterilized by autoclaving, cooled to room temperature and mixed together before use. For pre-cultivation and production of the pigments, 10 g L⁻¹ glucose and 10 g L⁻¹ L-arabinose were used as carbon source, respectively. Hereby the glucose stock solution (10x) used was sterilized by autoclaving, whereas the L-arabinose stock (20x) solution was sterilized by filtration (Minisart, 0.2 µm, 28 mm, Sartorius, Göttingen, Germany). The medium used for pre-cultivation in shake-flasks and for

the batch-phase of the bioreactor cultivations was a modification of the mineral medium described above, in which the concentration of K_2HPO_4 and KH_2PO_4 were changed to 12.542 g L^{-1} and 2.313 g L^{-1} , respectively. In addition, 12 g L^{-1} tryptone (Difco, Detroit, USA) and 24 g L^{-1} yeast extract (Difco, Detroit, USA) were added. For pre-cultivation and production of the pigments in bioreactor, 10 g L^{-1} glucose and 10 g L^{-1} L-arabinose were added to each medium, respectively. The medium used for the fed-batch phase was composed of 21.4 g L^{-1} $MgSO_4 \cdot 7H_2O$, 50 mg L^{-1} kanamycin and 360 g L^{-1} L-arabinose. The medium was sterilized by filtration (Sartolab-P20 plus, $0.2\ \mu\text{m}$, Sartorius, Göttingen, Germany). Antifoam agent (Ucolub N115, Fragol Industrieschmierstoffe, Germany) was manually added in pulses of $30\ \mu\text{L}$, when necessary.

2.2.7. Cultivation in shake flasks

Glycerol stocks were used as inoculum for pre-cultures in mineral medium, which were incubated for 18 h at $37\text{ }^\circ\text{C}$. Cells obtained from pre-cultures were washed two times by centrifugation (5 min, $9800\times g$, $20\text{ }^\circ\text{C}$, Biofuge Stratos, Heraeus, Hanau, Germany). After re-suspension in 0.85% ($w\ v^{-1}$) NaCl solution, they were used as inoculum for the main cultures. All cultivations were performed in baffled shake flasks with 10% filling volume and incubated on an orbital shaker at 230 rpm. Different incubation temperatures were applied, as specified below. For on-line dissolved oxygen quantification, shake flasks were equipped with non-invasive oxygen sensors (PreSens, Regensburg, Germany) and connected to a 4-channel fiber optic oxygen transmitter (OXY-4, PreSens, Regensburg, Germany) as described previously (Wittmann et al., 2003).

2.2.8. Fed-batch production in bioreactor

Exponentially growing cells from pre-cultures were collected by centrifugation (5 min, $10016\times g$, $20\text{ }^\circ\text{C}$, Biofuge Stratos, Heraeus, Hanau, Germany), washed with culture medium and used as inoculum. A lab scale (700 mL) DASGIP bioreactor system (Jülich, Germany) was used for production of violacein by the recombinant *E. coli* Vio-4. The initial settings of the process included a temperature of $20\text{ }^\circ\text{C}$, aeration rate of 6.0 sL h^{-1} , and stirrer speed of 400 rpm. Dissolved oxygen was measured by an optic sensor (Hamilton, Höchst, Germany) which was set to 30% by controlling the stirring speed. The pH was

maintained at 7.8 by addition of 1 M HCl or 25% NH₄OH. During later stages of the process, exponential feeding was applied as given by Equation 1.

$$F = \frac{\mu X_0 V_0 e^{\mu t}}{S_0 Y_{x/s}} \quad (1)$$

Hereby, F , μ , X_0 , V_0 , t , S_0 and $Y_{x/s}$ denote the feed rate, specific growth rate, initial cell concentration, initial medium volume, time, substrate concentration in the feed medium and the biomass yield on substrate, respectively (Yee and Blanch, 1992). The parameters ($\mu_{\max} = 0.0182 \text{ h}^{-1}$, $Y_{x/s} = 0.235 \text{ g g}^{-1}$) were determined based on the results obtained from the cultivations of strain dVio-6 in mineral medium with L-arabinose. The addition of the feed medium was controlled by a REGLO *Digital* MS-2/12 pump (Ismatec, Glattbrugg, Switzerland).

2.2.9. Quantification of cell concentration

Cell dry weight (CDW) was determined gravimetrically. Culture broth was filtered on pre-dried and pre-weighted filters (cellulose acetate, 0.2 μm , 25 mm, Sartorius, Göttingen, Germany). The filters were dried until constant weight, cooled in a desiccator to room temperature and then used for gravimetric biomass quantification (Analytical balance BP 210D, Sartorius, Göttingen, Germany). In addition, the cell concentration was also quantified via measurement of the optical density at 600 nm. This yielded a correlation factor of $1 \text{ OD}_{600} = 0.221 \text{ (g CDW) L}^{-1}$.

2.2.10. Quantification of violacein and deoxyviolacein

For extraction of the products, 600 μL culture broth was mixed thoroughly with 1.2 mL ethyl acetate and 175 mg glass beads (0.5 mm diameter). The cells were separated by centrifugation (3 min, 9800 $\times g$, 20 °C, Biofuge Stratos, Heraeus, Hanau, Germany) and subjected to repeated extraction until no more pigment color accumulated in the organic phase. All ethyl acetate extracts were pooled and dried at 20 °C. The obtained pigments were re-dissolved in ethanol. Violacein and deoxyviolacein were then quantified in these solutions by HPLC as described previously (Rodrigues et al., 2012).

2.2.11. Quantification of sugars and organic acids

Culture samples were centrifuged (3 min, 9800×g, 20 °C, Biofuge Stratos, Heraeus, Hanau, Germany), filtered (cellulose acetate, 0.2 µm, 25 mm, Sartorius, Göttingen, Germany) and analyzed for organic acids (Becker et al., 2009a) and sugars (Buschke et al., 2011) by HPLC (LaChromElite, Hitachi, VWR, Darmstadt, Germany). Separation of organic acids was performed on a reversed phase column (Aminex HPX 87H, 300×78 mm, Bio-Rad, Hercules, California) with 12.5 mM H₂SO₄ as mobile phase at a flow rate of 0.5 mL min⁻¹ and 45 °C. Quantification was carried out via external calibration and UV detection at 210 nm. Glucose and L-arabinose were separated on a Metacarb 87C column (300 × 78 mm, Varian Inc., Palo Alto, USA) at 85 °C with purified water (Milli-Q Gradient A10 Water Purification System, Millipore, Schwalbach am Taunus, Germany) as mobile phase, flow rate of 0.6 mL min⁻¹ and quantified via the refraction index after external calibration.

2.2.12. Intracellular amino acids

Sampling was performed using fast filtration and washing with isotonic NaCl solution, a method that had been validated for accurate quantification of intracellular metabolites in *E. coli* (Bolten et al., 2007). Samples of exponentially growing cultures were harvested by fast filtration (cellulose acetate filter, 0.2 µm, 25 mm, Sartorius, Göttingen, Germany) and washed with 31.4 g L⁻¹ NaCl solution that equaled the ionic strength of the mineral medium. In order to extract the intracellular amino acids, the filters were incubated for 15 min at 100 °C in 2 mL boiling water, which contained the internal standard 200 µM α-aminobutyrate, and then cooled on ice. Extracts were recovered after centrifugation (3 min, 9800×g, 4 °C, Biofuge Stratos, Heraeus, Hanau, Germany) and used for quantification by HPLC (Agilent 1200, Agilent, Waldbronn, Germany) with a reverse phase column (Gemini 5 µm C18 110 Å, 150×4.6 mm, Phenomenex, Aschaffenburg, Germany) (Krömer et al., 2005). Before injection, the amino acids were derivatized with o-phthaldialdehyde and detected by fluorescence with excitation at 340 nm and emission at 540 nm (Agilent, Waldbronn, Germany).

2.2.13. Extraction and crystallization of violacein

Cells were collected by centrifugation (5 min, $10016 \times g$, 20 °C, Biofuge Stratos, Heraeus, Hanau, Germany). Violacein was then extracted by mixing the cells with ethanol followed by separation of the violacein extract (5 min, $10016 \times g$, 20 °C, Biofuge Stratos, Heraeus, Hanau, Germany). This procedure was repeated until violacein was completely extracted from the cells. The obtained extract was filtered (Rapid 250, 0.22 μm PES membrane, TPP Techno Plastic Products AG, Trasadingen, Switzerland), dried at reduced pressure (Laborota 4000, Schwabach, Germany) and solubilized in boiling acetone (Wrede and Rothhaas, 1933). One volume of purified water (Milli-Q Gradient A10 Water Purification System, Millipore, Schwalbach am Taunus, Germany) at 100 °C was added to the boiling acetone-violacein extract. Subsequently, crystallization of violacein was carried out by incubation at 20 °C for 24 h. Crystal formation was evaluated by microscopy (EVOS xl, Advanced Microscopy Group, Bothell, USA). Finally, the crystals were recovered by filtration (0.2 μm regenerated cellulose membrane, Sartorius Stedim Biotech, Germany), washed with purified water, dried at 80 °C until constant weight and stored at 0 °C. The purity of violacein crystals was evaluated by HPLC as described above. Violacein crystals were solubilized in ethanol prior to analysis.

2.3. Systems metabolic engineering of *Escherichia coli* for production of deoxyviolacein from glycerol

2.3.1. Strains and plasmids

The *araBAD* operon, encoding enzymes of L-arabinose catabolism, was deleted in *E. coli* K-12 MG1655 (Jensen, 1993) (CGSC 6300) for later transduction of the obtained $\Delta\text{araBAD}::\text{FRT-Cm-FRT}$ construct into deoxyviolacein producing strains. *E. coli* dVio-6 and *E. coli* TRP11 were taken from previous work (Rodrigues et al., 2013). The pBvioABCE-Km plasmid (Rodrigues et al., 2013), encoding the biosynthetic pathway of deoxyviolacein, was employed for production of deoxyviolacein with L-arabinose as inducer of gene expression. Plasmids pKD3 and pKD46 (Datsenko and Wanner, 2000) were used to perform genetic

Material and Methods

modifications in *E. coli* K-12 MG1655. All strains were maintained as glycerol stocks at -80 °C. All strains and plasmids, used in the present work, are summarized in Table 4.

Table 4. Strains and plasmids used in the present work.

	Relevant genotype	Reference
Strains		
<i>E. coli</i>		
MG1655 (CGSC#: 6300)	Wild type <i>E. coli</i> K-12	(Jensen, 1993)
Δ araBAD	MG1655 Δ araBAD::FRT-Cm-FRT	This study
TRP11	MG1655 Δ trpR::FRT Δ tnaA::FRT Δ sdaA::FRT Δ lac::P _{TAC} aroFBL-FRT Δ trpL trpE ^{fr} Δ gal::P _{TAC} tktA-FRT Δ xyl::P _{TAC} serA ^{fr} -FRT	(Rodrigues et al., 2013)
dVio-6	MG1655 Δ trpR::FRT Δ tnaA::FRT Δ sdaA::FRT Δ lac::P _{TAC} aroFBL-FRT Δ trpL trpE ^{fr} Δ gal::P _{TAC} tktA-FRT Δ xyl::P _{TAC} serA ^{fr} -FRT pBvioABCE-Km	(Rodrigues et al., 2013)
dVio-7	MG1655 Δ trpR::FRT Δ tnaA::FRT Δ sdaA::FRT Δ lac::P _{TAC} aroFBL-FRT Δ trpL trpE ^{fr} Δ gal::P _{TAC} tktA-FRT Δ xyl::P _{TAC} serA ^{fr} -FRT Δ araBAD::FRT-Cm-FRT	This study
dVio-8	MG1655 Δ trpR::FRT Δ tnaA::FRT Δ sdaA::FRT Δ lac::P _{TAC} aroFBL-FRT Δ trpL trpE ^{fr} Δ gal::P _{TAC} tktA-FRT Δ xyl::P _{TAC} serA ^{fr} -FRT Δ araBAD::FRT-Cm-FRT pBvioABCE-Km	This study
Plasmids		
pKD3	Cm	(Datsenko and Wanner, 2000)
pKD46	P _{BAD} gam-bet-exo	(Datsenko and Wanner, 2000)
pBvioABCE-Km	vioABCE Km Amp	(Rodrigues et al., 2013)

2.3.2. Genetic engineering

The recombineering method (Datsenko and Wanner, 2000) was used to delete genes in *E. coli*. The chloramphenicol resistance gene of pKD3 plasmid was taken as selection marker. Specific primers for implementation and validation of genetic modifications are listed in Table 5. Transfer of genetic constructs among strains was performed with transduction (Thomason et al., 2007), using the phage

P1 *vir*. For heterologous production of deoxyviolacein, plasmid pBvioABCE-Km was transferred into *E. coli* (Sambrook and Russell, 2001).

Table 5. Primers used for deletion of *araBAD* in *E. coli*.

No.	Primers (5'→3')	Target
1	atggcgattgcaattggcctcgatttggcagtgattctgtgagcgtttgtgta ggctggagctgcttc	<i>Cm</i> of pKD3
2	gcttgagtatagcctggttcgtttgattggctgtggtttatacagtcaatggga attagccatggctc	
3	atatcaccggctcggcagacaaattctcgt	validating deletion of
4	aatatgctgagcgcggggaacctga	<i>araBAD</i> in <i>E. coli</i> K-12 MG1655 Δ <i>araBAD</i>
5	caattgctggatccggaacgaatatcaac	
6	cgctgagtccttcataatgccgtgtat	validating deletion of <i>trpR</i>

2.3.3. Growth media

Complex LB medium (pH 7) contained 10 g L⁻¹ NaCl, 5 g L⁻¹ yeast extract (Difco, Detroit, MI, USA), and 10 g L⁻¹ tryptone (Difco, Detroit, MI, USA). For strains, that harbored the deoxyviolacein plasmid (pBvioABCE-Km), it was additionally amended with either 100 µg mL⁻¹ carbenicillin or with 50 µg mL⁻¹ kanamycin, respectively. For evaluation of production performance on plates, LB medium was further supplemented with 1 g L⁻¹ L-arabinose for induction and solidified by addition of 15 g L⁻¹ agar. Mineral medium (Rodrigues et al., 2013) contained per liter of deionized water: 0.58 g NaCl, 5.29 g (NH₄)₂SO₄, 12.542 g K₂HPO₄, 2.313 g KH₂PO₄, 0.25 g MgSO₄ × 7H₂O, 1 µg thiamin HCl, 3 mg vitamin B3, 1 mg vitamin B2, 5.51 mg CaCl₂, 16.66 mg FeCl₃ × 6H₂O, 1 mg MnCl₂ × 4H₂O, 1.7 mg ZnCl₂, 340 µg CuCl₂, 470 µg CoCl₂ and 600 µg Na₂MoO₄ × 2H₂O at pH 7. For strains, that harbored the deoxyviolacein plasmid (pBvioABCE-Km), the medium was additionally amended with either 100 µg mL⁻¹ carbenicillin or with 50 µg mL⁻¹ kanamycin. Media for cultivation of strains, harboring the construct

$\Delta araBAD::FRT-Cm-FRT$, were supplemented with $20 \mu\text{g mL}^{-1}$ chloramphenicol, except for bioreactor cultivations. Cultivation in microplates was conducted in mineral medium (see above), which was additionally amended with 3 g L^{-1} tryptone (Difco, Detroit, MI, USA), 6 g L^{-1} yeast extract (Difco, Detroit, MI, USA), and $100 \mu\text{g mL}^{-1}$ carbenicillin. Either 10 g L^{-1} glycerol or 10 g L^{-1} fructose were added as extra carbon source. L-Arabinose concentrations between 10 and 500 mg L^{-1} were tested for induction of gene expression. L-Arabinose-based medium and feed solution, used for fed-batch production with *E. coli* dVio-6, were as described previously (Rodrigues et al., 2013). Additionally, novel media were developed for fed-batch production with alternative carbon sources in this work. For the initial batch phase, mineral medium, as described above, was supplemented with 10 g L^{-1} glucose and with $100 \mu\text{g mL}^{-1}$ carbenicillin. Subsequently, a variant of this medium was added, in which glucose was replaced by 10 g L^{-1} glycerol and additionally 6 g L^{-1} tryptone (Difco, Detroit, MI, USA), 12 g L^{-1} yeast extract (Difco, Detroit, MI, USA), 6 g L^{-1} L-arabinose, and $100 \mu\text{g mL}^{-1}$ carbenicillin. The feed-solution contained 21.4 g L^{-1} $\text{MgSO}_4 \times 7\text{H}_2\text{O}$ and 756.6 g L^{-1} glycerol. Antifoam agent (Ucolub N115, Fragol Industrieschmierstoffe, Germany) was manually added to bioreactor cultivations, when necessary.

2.3.4. Microplate cultivation

Glycerol stocks were used as inoculum for pre-cultivation in mineral medium with glucose. Baffled flasks (500 mL) with 50 mL medium were incubated for 17 h at $37 \text{ }^\circ\text{C}$ and 230 rpm on an orbital shaker (Multitron, Infors AG, Bottmingen, Switzerland). Cells were collected by centrifugation (5 min, $9800 \times g$, $20 \text{ }^\circ\text{C}$). After re-suspension in mineral medium, cells were used as inoculum for the microplate cultivations. Parallel cultivation in 48-well microtiter flower-plates was conducted with the BioLector system (DASGIP, Jülich, Germany). Cultivations were performed at $20 \text{ }^\circ\text{C}$, 95% humidity, and 1000 rpm. Each well was filled with 1 mL medium. Cell growth was determined by online monitoring of optical density at 620 nm.

2.3.5. Shake flask cultivation

Pre-cultivations were done as described above. Dissolved oxygen level in shake-flask cultures was quantified with the shake-flask reader SFR (PreSens Precision Sensing GmbH, Regensburg, Germany). Cultures (500 mL flasks with 50 mL medium) were incubated at 37 °C and 230 rpm on an orbital shaker (Multitron, Infors AG, Bottmingen, Switzerland).

2.3.6. Fed-batch cultivation

A lab scale bioreactor system (DASGIP, Jülich, Germany) was used for production of deoxyviolacein. Initial settings of the fed-batch experiment with strain dVio-6 were as described previously (Rodrigues et al., 2013). Initial settings of the fed-batch with strain dVio-8, developed in this work, were 37 °C, an aeration rate of 6.0 sL h⁻¹, a cell concentration of OD₆₀₀ of 1, a stirrer speed of 400 rpm, and a filling volume of 300 mL medium. Dissolved oxygen was measured by an optical sensor (Hamilton, Höchst, Germany) and kept above 30% by automatic adjustment of stirrer speed. The pH was maintained at 7 by addition of 3 M HCl and 25% NH₄OH, respectively. After initial glucose was consumed, modified batch medium was added and the reactor was cooled down to 20 °C. When the dissolved oxygen level had reached 60%, the feed was started. Medium addition was then performed in pulses of 5 g L⁻¹ glycerol, each time the dissolved oxygen level increased to values above 60%. Addition of feed medium was conducted by a REGLO *Digital* MS-2/12 pump (Ismatec, Glattbrugg, Switzerland).

2.3.7. Quantification of cell concentration

A spectrophotometer (Libra S11, Biochrom, Cambridge, UK) was used for determination of cell concentration via measurement of optical density at 600 nm (Rodrigues et al., 2013).

2.3.8. Quantification of sugars, glycerol and acetate

Culture samples were centrifuged (3 min, 9800×g, 20 °C), filtered (cellulose acetate, 0.2 µm, 25 mm, Sartorius, Göttingen, Germany) and analyzed by HPLC (LaChromElite, Hitachi, VWR, Darmstadt, Germany) for acetate (Becker et al., 2009a), sugars, and glycerol (Buschke et al., 2011). Additionally, glucose concentration was measured with a biochemical analyzer (YSI 2700 Select, Kreienbaum, Langenfeld, Germany).

2.3.9. Quantification of deoxyviolacein

For extraction of deoxyviolacein from cells, 50 µL broth was thoroughly mixed for 2 min with 1.8 mL ethanol and 175 mg glass beads (0.106-0.125 mm diameter, Worf Glaskugeln GmbH, Mainz, Germany). Afterwards, cells were separated by centrifugation (3 min, 9800×g, 20 °C) and subjected to repeated extraction cycles until no more pigment accumulated in the supernatant. All ethanol extracts were finally combined and analyzed by HPLC (Rodrigues et al., 2012).

2.3.10. Purification of deoxyviolacein

Cells were harvested by centrifugation (30 min, 5346×g, 4 °C). Deoxyviolacein was extracted by three cycles of cell homogenization with ethanol and extract recovery by centrifugation (30 min, 5346×g, 4 °C). In each cycle, the volume of ethanol used corresponded to the initial volume of broth collected. Purification of combined extract fractions was done by flash-chromatography using silica gel 60 (0.04–0.06 mm diameter, Merck, Darmstadt, Germany) (Rodrigues et al., 2012). Ethanol and ethyl acetate were used as mobile phase.

2.3.11. GC-MS labelling analysis

Mass isotopomer fractions of proteinogenic amino acids were quantified by GC-MS (Wittmann et al., 2004; Wittmann et al., 2007). Biomass samples of 1 mg were hydrolyzed for 12 h in 50 µL 6 M HCl and subsequently filtrated (0.22 µm Ultrafree MC GV Durapore PVDF, EMD Millipore Corporation, Billerica, MA, USA).

Samples were dried at 20 °C under a stream of N₂ and then solubilized in 50 µL dimethylformamide (0.1% pyridine). For derivatization, 50 µL *N*-methyl-*N*-*t*-butyldimethyl-silyl-trifluoroacetamide (MBDSTFA; Macherey-Nagel, Düren, Germany) was added, following incubation at 80 °C for 30 min. After derivatization, samples were centrifuged (1 min, 9800 × *g*, 20 °C) and the supernatant was analyzed by GC-MS (Agilent Technologies, Santa Clara, CA, USA). All measurements were first conducted in scan mode to exclude isobaric overlay with the analytes of interest. Mass isotopomer distributions were then quantified with selective ion monitoring (Wittmann, 2007).

3 Results

3.1. HPLC-based separation and quantification of violacein and deoxyviolacein

3.1.1. Evaluation of photometric measurement of crude violacein

To evaluate the suitability of the widely applied spectrophotometric method for the analysis of the pigment content, the extinction coefficient was determined for different mixtures of the two compounds. This revealed an almost 50% change of the extinction coefficient in mixtures with increasing concentration of violacein

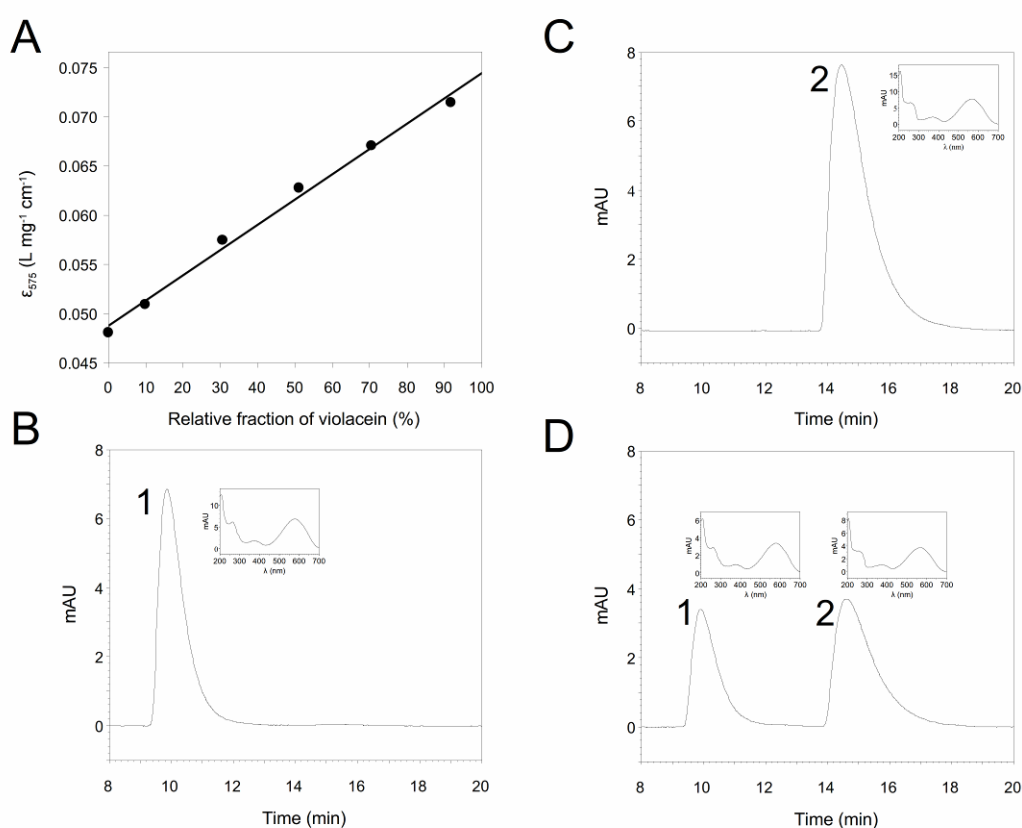


Figure 5. Analysis of violacein and deoxyviolacein: Extinction coefficients for mixtures of violacein and deoxyviolacein (A), HPLC analysis of violacein (B), deoxyviolacein (C) and a mixture (D) on a C18 column with 50% (v v⁻¹) ethanol as mobile phase. The samples reflect standard solutions of 6.0 mg L⁻¹ violacein (B), 19.5 mg L⁻¹ deoxyviolacein (C) and 1:1 (v v⁻¹) mix of both (D). The respective UV-Vis spectrum is presented for each peak. For measurement of extinction coefficients, the pigments were dissolved in ethanol and analyzed at $\lambda = 575$ nm.

from 0 to 100% (Figure 5A), which has not been considered so far. Clearly, this can result in up to a 50% error in the estimated total pigment amount from photometric readouts. Beyond that, the method fails to resolve the two products, information that is highly relevant for screening of novel isolates as well as optimization of strains and processes.

3.1.2. Development of an HPLC method for quantification of violacein and deoxyviolacein

As violacein and deoxyviolacein are soluble in ethanol (Mendes et al., 2001), different concentrations of this alcohol in HPLC-grade water were tested as mobile phase in the HPLC analysis. The use of 50% (v v⁻¹) ethanol resulted in single peaks for violacein and deoxyviolacein for all concentrations tested, i.e. ranging from 5-50 mg L⁻¹ violacein and 0.5-150 mg L⁻¹ deoxyviolacein as given in Figure 5B, C and D. By variation of the concentration of ethanol between 50 and 100 % (v v⁻¹) in the mobile phase, it was possible to influence the retention time for both compounds towards an improved separation. The use of 50% (v v⁻¹) ethanol as mobile phase allowed optimum separation, as shown in the chromatogram of a standard mixture of the pigments (Figure 5D). The values of the concentrations of violacein and deoxyviolacein calculated for this mixture were consistent with that of the pure standard solutions used to make the mixture (Figure 5B and C), demonstrating that the pigments could be totally separated. For both compounds, linear calibration curves were obtained. For the UV signal at 580 nm a correlation coefficient of 0.99 resulted in each case. The slopes of the calibration curves of violacein and deoxyviolacein were 4.57×10^{-6} and 7.06×10^{-6} , respectively. Methanol, previously described as solvent for analysis of violacein (Jiang et al., 2010), was also tested, but did not provide defined peaks for the pigments. With increasing concentrations of the violacein and deoxyviolacein standards, more than two peaks were observed in the chromatogram, which did not yield useful calibration curves. A similar effect was described previously (Rettori and Durán, 1998). Moreover, violacein and deoxyviolacein partly precipitated from solutions in methanol, when the temperature of the auto sampler was set below 20 °C, which is problematic for the processing of bio-analytical samples. This was not the case for solutions in ethanol.

3.1.3. Quantification of violacein and deoxyviolacein in microbial cultures

The developed approach was tested for plate grown cultures of *E. coli* harboring two different plasmids as well as the natural producer *J. lividum*. For all microbial strains the two pigments could be precisely quantified, revealing that the relative fraction of violacein and deoxyviolacein strongly depend on the genetic background of the production strain (Table 6).

Table 6. Production of violacein and deoxyviolacein by different strains cultivated on LB agar for 2 weeks.

Strain	Violacein (mg L ⁻¹)	Deoxyviolacein (mg L ⁻¹)	Relative fraction of violacein (%) ^b	Relative fraction of deoxyviolacein (%)	Crude violacein (mg L ⁻¹)
<i>E. coli</i> TOP 10 pJP1000	23.5 ± 0.0	1.1 ± 0.1	96	4	24.6 ± 0.1
<i>E. coli</i> TOP 10 pPSX-Vio+	6.0 ± 0.0	n.d. ^a	100	0	6.0 ± 0.0
<i>J. lividum</i> DSM 1522	16.3 ± 0.1	4.2 ± 0.0	79	21	20.5 ± 0.1

^a not detectable (the limit of detection was < 0.1 mg L⁻¹).

^b relative to the sum of violacein and deoxyviolacein concentrations.

During the cultivation of *J. lividum* DSM 1522 in liquid medium, both pigments accumulated in the broth, whereby the ratio between violacein and deoxyviolacein remained constant (Figure 6).

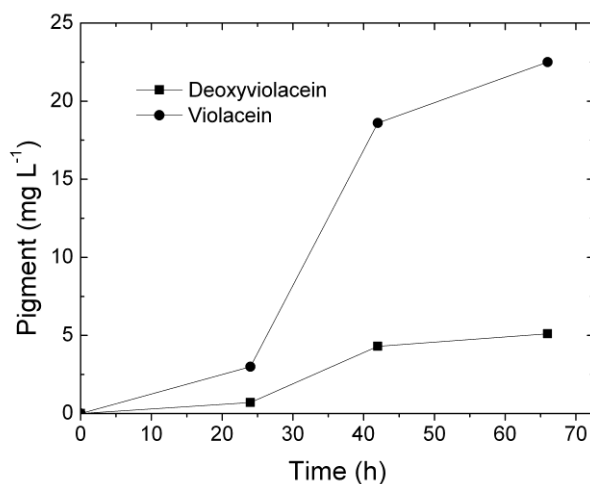


Figure 6. Violacein and deoxyviolacein production profiles of *J. lividum* DSM 1522 cultivated in LB medium with 1% (w v⁻¹) glycerol at 25 °C.

3.2. Systems metabolic engineering of *Escherichia coli* for production of violacein and deoxyviolacein

3.2.1. Construction of a basic strain for deoxyviolacein production

The first step of the present work was the genetic construction of a basic recombinant production strain. For this purpose, *E. coli* K-12 MG1655 was transformed with the plasmid pBvioABCE-Km that contained the deoxyviolacein pathway genes from *C. violaceum* ATCC 12472. The obtained mutant, designated *E. coli* dVIO-1 (Table 2) exhibited violet colonies, when grown on agar plates with L-arabinose, the inducer of the deoxyviolacein genes (Figure 7).

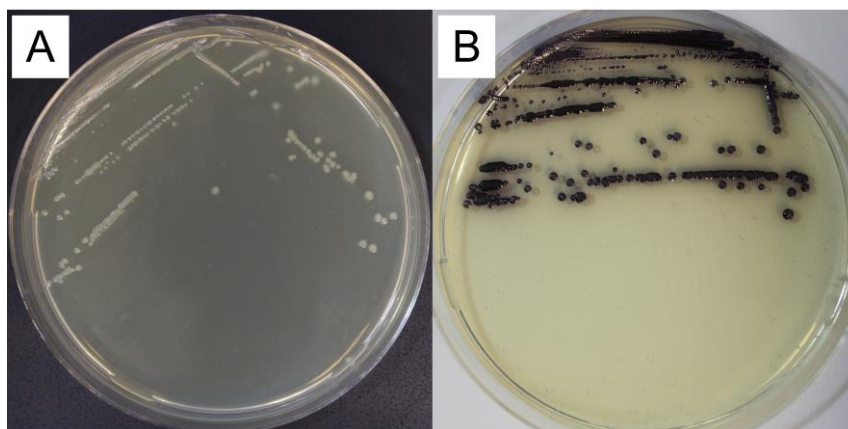


Figure 7. Control of the deoxyviolacein production in *E. coli* dVio-1, using the AraC system and L-arabinose as inducer for *vioABCE* expression: plate-grown cells on complex LB medium with kanamycin (A) and on complex LB medium with kanamycin and L-arabinose (B).

This was a first indication that the pathway was functionally expressed in *E. coli*. In liquid culture with L-arabinose as sole source of carbon (10 g L^{-1}), incubated at $20 \text{ }^\circ\text{C}$, the novel strain was able to produce $176.1 \pm 5.9 \text{ mg L}^{-1}$ of deoxyviolacein (Figure 8A). The desired product was formed from early on, whereby production seemed associated to the growth of the cells. During the cultivation, L-arabinose was completely consumed. The cells accumulated acetate during the first phase, but later re-utilized the by-product together with L-arabinose. Violacein was not detected, indicating desired formation of the pure deoxyviolacein (Figure 9B).

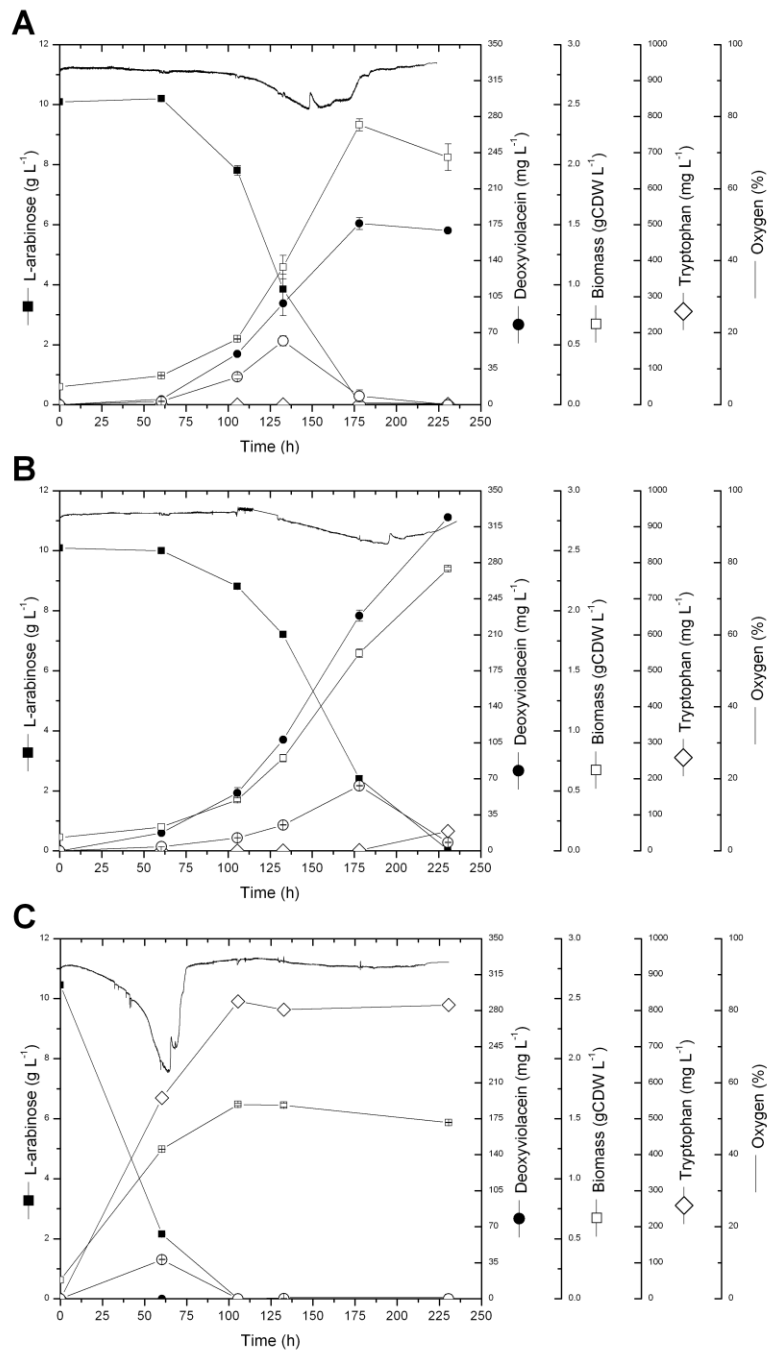


Figure 8. Growth and production profile of recombinant *E. coli* dVio-1 (A), dVio-6 (B), and TRP11 (C) in mineral medium containing 10 g L⁻¹ L-arabinose as carbon and energy source. n=3.

During the whole process, the dissolved oxygen level remained above 80% of saturation (Figure 8A). This showed that the cells were sufficiently supplied with oxygen, which obviously did not limit the production, and could be excluded as triggering agent for acetate overflow. This was in line with an unaffected growth and production behavior at reduced shaking rates of 100 and 50 rpm (data not shown).

3.2.2. Evaluation of deoxyviolacein and violacein analytics

As shown, the recombinant strain accumulated about 180 mg L^{-1} of deoxyviolacein (Figure 8A). In contrast to HPLC based quantification of the product, performed here, deoxyviolacein and violacein are typically monitored via photometric analysis of extracts that contain the pigment. Depending on the wavelength applied, different extinction coefficients are reported to estimate the concentration. The parallel analysis of deoxyviolacein extracts and solutions with the purified compound revealed that photometric measurement strongly over estimates the level of deoxyviolacein by up to 320% (Table 7). In the case of violacein this amounts up to about 680% (Table 8). Accordingly, all further analytics relied on HPLC measurement to ensure accurate data.

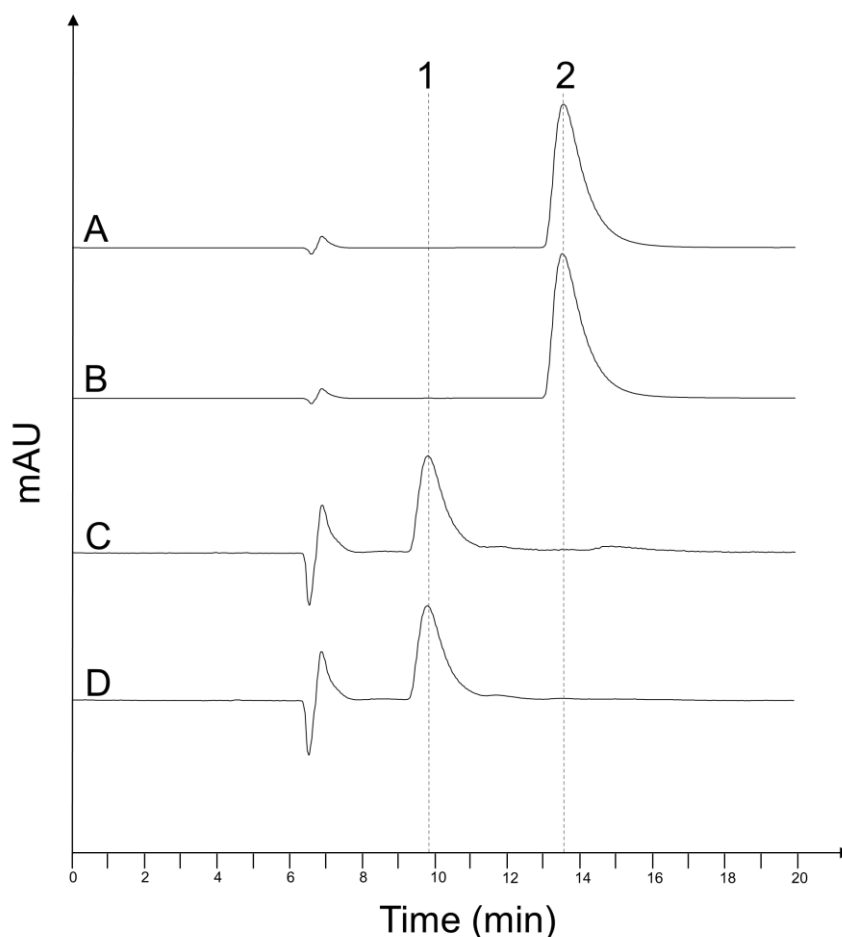


Figure 9. HPLC based analysis of violacein and deoxyviolacein. The chromatograms display a purified deoxyviolacein standard (A), an extract from the culture broth of *E. coli* dVio-1 (B), a purified violacein standard (C), and an extract from the culture broth of *E. coli* Vio-4 (D). The eluting compounds represent violacein (1) and deoxyviolacein (2).

Results

Table 7. Revision of analytical approaches for the quantification of deoxyviolacein. The evaluation investigated pure standard solutions of the analyte with absolute concentrations of 3.7 mg L⁻¹ (standard 1), 7.7 mg L⁻¹ (standard 2) and 38.3 mg L⁻¹ of deoxyviolacein and one extract from the cultivation broth of the recombinant producer *E. coli* dVio-6, which were analyzed in parallel by HPLC (Rodrigues et al., 2012) and photometrical measurement at a wavelength of 560 nm (Jiang et al., 2012). The latter recruited the reported extinction coefficient of $\epsilon_{560} = 15.955 \text{ L (g cm)}^{-1}$ to estimate the deoxyviolacein content. Concentrations given are mean values and deviations from three replicates.

Sample	HPLC (mg L ⁻¹)	Photometry at 560 nm (mg L ⁻¹)	Correlation factor
Standard 1	3.7 ±0.0	11.8 ±0.0	3.2
Standard 2	7.7 ±0.1	24.8 ±0.2	3.2
Standard 3	38.3 ±0.0	122.7 ±0.1	3.2
Broth extract of dVio-6	21.1 ±0.0	64.6 ±0.0	3.1

Table 8. Revision of analytical approaches for the quantification of violacein. The evaluation investigated pure standard solutions of the analyte with absolute concentrations of 3.2 mg L⁻¹ (standard 1), 6.4 mg L⁻¹ (standard 2) and 12.8 mg L⁻¹ of violacein and one extract from the cultivation broth of the recombinant producer *E. coli* Vio-4. These were analyzed in parallel by HPLC (Rodrigues et al., 2012) and by photometry at 570 nm with $\epsilon_{570} = 10.955 \text{ L (g cm)}^{-1}$ (photometry 1, (Wang et al., 2009)), at 575 nm with $\epsilon_{575} = 56.010 \text{ L (g cm)}^{-1}$ (photometry 2, (Mendes et al., 2001)), and at 575 nm with $\epsilon_{575} = 29.700 \text{ L (g cm)}^{-1}$ (photometry 3, (Durán et al., 2007)). Concentrations given are mean values and deviations from three replicates. The correlation factors (from left to right) relate HPLC to the different photometrical assays.

Sample	HPLC (mg L ⁻¹)	Photometry 1 (mg L ⁻¹)	Photometry 2 (mg L ⁻¹)	Photometry 3 (mg L ⁻¹)	Correlation factors
Standard 1	3.2 ±0.0	21.8 ±0.0	4.3 ±0.0	8.1 ±0.0	6.8 / 1.3 / 2.5
Standard 2	6.4 ±0.0	43.1 ±0.1	8.5 ±0.0	16.0 ±0.0	6.7 / 1.3 / 2.5
Standard 3	12.8 ±0.1	86.4 ±0.1	17.0 ±0.1	32.1 ±0.1	6.7 / 1.3 / 2.5
Broth extract of Vio-4	25.6 ±0.0	172.4 ±0.2	34.0 ±0.0	64.2 ±0.0	6.7 / 1.3 / 2.5

3.2.3. Impact of temperature and chaperone co-expression on deoxyviolacein production by recombinant *E. coli*

It was interesting to note that the temperature had a pronounced effect on deoxyviolacein production. At 20 °C, the production was highest. Elevated temperatures improved the overall growth of the recombinant strain, but significantly reduced the product level to 14.5% at 30 °C and even 0.2% at 37 °C. This behavior, at least potentially, indicated stability or folding problems of the heterologous proteins introduced into the host. Different chaperones were therefore co-expressed in the producing strain. However, none of the candidates tested, i.e. DnaK, DnaJ, GrpE, GroES, GroEL, and Tig, improved the deoxyviolacein titer beyond the optimum at 20 °C. At 30 °C, the chaperones showed a positive effect, which pointed towards folding problems of the heterologous enzymes at higher temperature (Figure 10). However, the maximum product level corresponded to only 43% of the highest value observed at 20 °C.

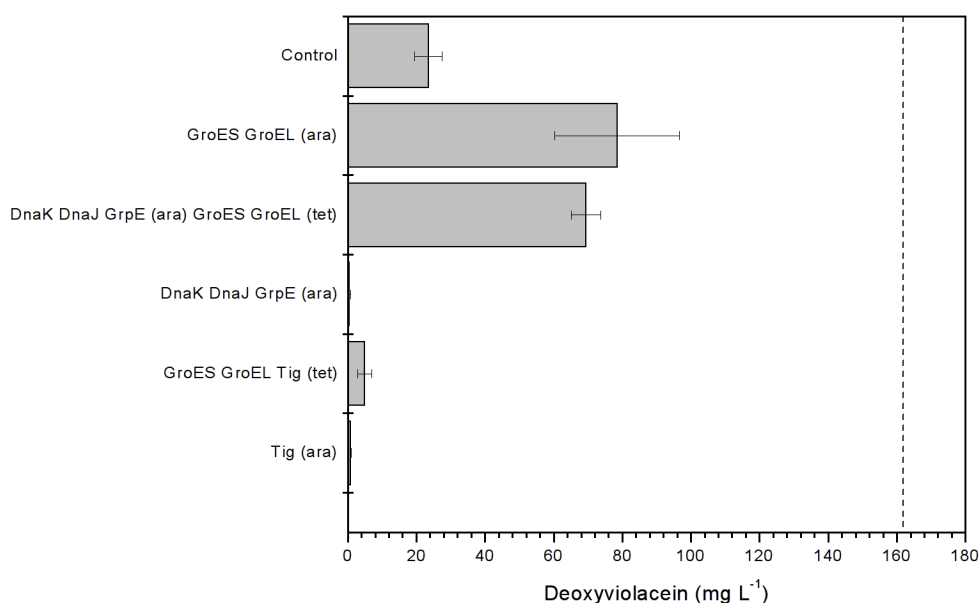


Figure 10. Effect of chaperone co-expression on deoxyviolacein production by recombinant *E. coli* dVio-1 at 30 °C. The expressed chaperones correspond to the different plasmids (Table 2) used, i.e. pGro7 (*groES groEL*). Their expression was induced by addition of tetracycline (tet) and/or L-arabinose (ara). The dashed line marks the level of the basic producer at 20 °C. n=3.

3.2.4. Quantification of intracellular precursor availability by targeted metabolite analysis

L-Tryptophan, the building block for deoxyviolacein, typically occurs in low amounts inside *E. coli*. It thus appeared relevant in a next step, to investigate the impact of its demand for deoxyviolacein production on the intracellular availability. For this purpose, the free intracellular pool of L-tryptophan was compared between the strain dVio-1 and the control strain (NC) that harbored the empty plasmid (Table 2). The analysis involved sampling by fast filtration and subsequent extraction in boiling water, a technique that has been previously validated for intracellular amino acid analysis in *E. coli* (Bolten et al., 2007). Whereas the control strain did not accumulate any pigment, the producer accumulated almost 180 mg deoxyviolacein L⁻¹ (Figure 11A). It turned out, that the level of intracellular tryptophan was decreased by 63% as response to deoxyviolacein production (Figure 11B). Obviously, L-tryptophan could not be efficiently replenished to account for the withdrawal into the implemented pathway. Due to the fact, that the enzyme VioA exhibit a rather low (K_M of $31 \pm 11 \mu\text{M}$) affinity for L-tryptophan (Balibar and Walsh, 2006), this likely limited the performance of the producer and displayed a promising target for the improvement of deoxyviolacein production in *E. coli*. L-Serine, as up-stream intermediate, is also involved in the supply of L-tryptophan. The L-serine level also decreased in response to deoxyviolacein production (Figure 11C). Due to this, next rounds of strain engineering focused on increasing the intracellular availability of L-tryptophan and L-serine in supporting pathways of the carbon core metabolism of *E. coli*, upstream of the novel heterologous pathway.

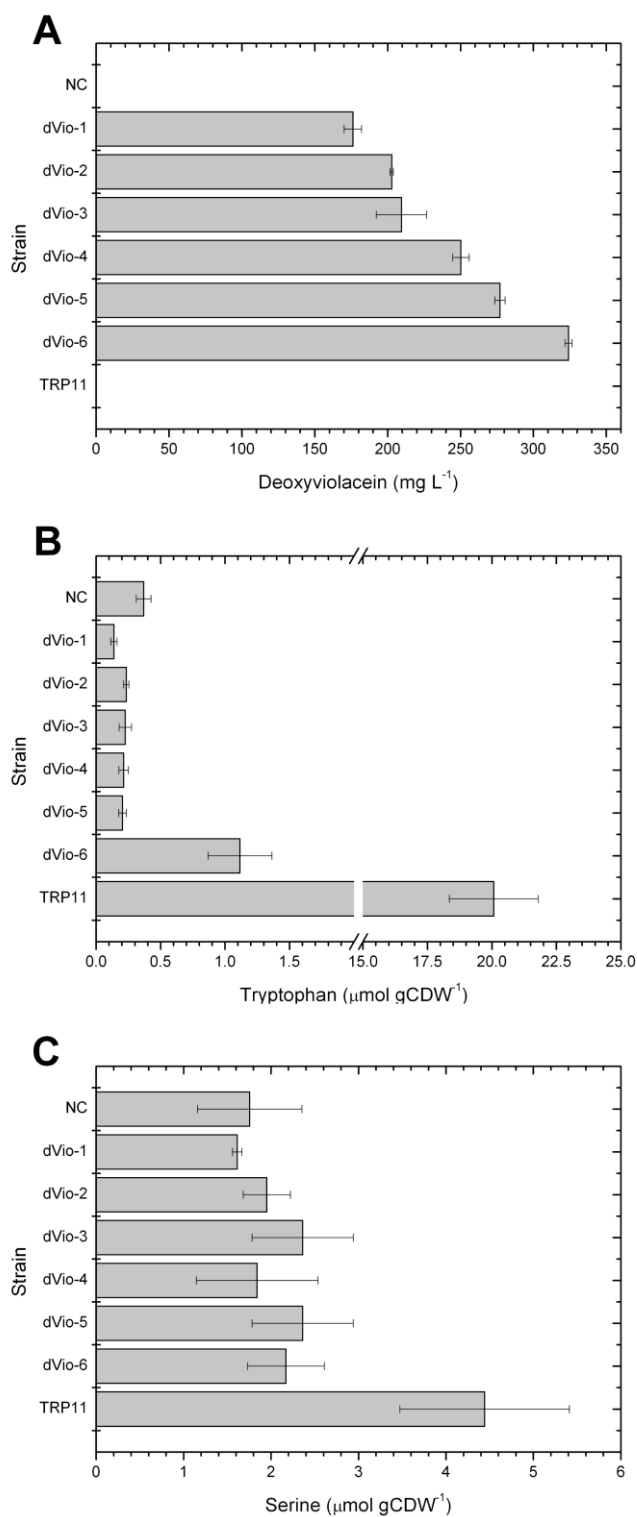


Figure 11. Deoxyviolacein titer (A) and intracellular levels of tryptophan (B) and serine (C) in the parent strain *E. coli* NC (control), the recombinant producers dVio-1 through dVio-6, and the tryptophan producer TRP11 (Table 2) in L-arabinose mineral medium. n=3.

3.2.1. Design of feedback-resistant enzymes in supporting pathways

Tryptophan synthesis in *E. coli* is controlled by several layers of regulation, i.e. by repression (*trpR*), attenuation (*trpL*), and feedback-inhibition of enzymes (Sprenger, 2007). Elimination of the corresponding genomic elements appeared straightforward to remove the undesired transcriptional control mechanisms, as shown below. However, full pathway de-regulation of pathway flux required the release from feed-back control. Anthranilate synthase, encoded by the *trpE* gene, is regulated via feedback-inhibition by L-tryptophan. Therefore, a feedback-resistant form was designed and constructed by site-directed mutagenesis (see Appendix) to yield a *trpE^{fr}* allele. The obtained feedback resistant enzyme variant comprised four amino acid exchanges, i.e. Asn168Asp, Cys237Arg, Met293Thr and Ala478Thr, respectively. As production of L-serine, which contributes to tryptophan synthesis, is also regulated by feedback inhibition exerted upon 3-phosphoglycerate dehydrogenase by L-serine, a feedback-resistant form (*serA^{fr}*) was also constructed by site-directed mutagenesis, based on experimental evidence (Maier and Flinspach). The superior variant exhibited the amino acid exchange Thr372Asp.

3.2.2. Metabolic engineering of tryptophan supply

The complex network of tryptophan biosynthesis and degradation pathways in *E. coli* suggested a multi-target approach to increase pathway flux. In order to improve the intracellular availability of tryptophan, a set of three genetic modifications was therefore implemented into the basic producer *E. coli* dVio-1 (Table 2, Figure 12). First, the gene for the repressor of the tryptophan operon (*trpR*) was deleted. Moreover, pathways involved in degradation of tryptophan and serine were eliminated to enable increased pool sizes. For this purpose, the gene *tnaA* that encodes tryptophanase, responsible for L-tryptophan degradation, and the *sdaA* gene, involved in serine degradation, were deleted. The novel strain *E. coli* dVio-2, comprising (i) the heterologous plasmid, (ii) the de-repressed tryptophan pathway and (iii) eliminated degradation routes for the precursors, tryptophan and L-serine, respectively, was tested for production (Figure 11A). Most strikingly, it exhibited an elevated product titer of $202.8 \pm 1.2 \text{ mg L}^{-1}$. The success

In order to exploit this effect, additional modifications were implemented into the tryptophan pathway. As first target, *trpL*, involved in the attenuation of the *trp* operon (Gu et al., 2012; Henkin and Yanofsky, 2002), was deleted. Subsequently, the L-tryptophan pathway was decoupled from feedback control via replacement of the native *trpE* gene by the variant *trpE^{fr}* ((Caligiuri and Bauerle, 1991), see Appendix for details). TrpE catalyzes the first step of the L- tryptophan pathway and forms anthranilate from chorismate. Interestingly, these additional modifications did not have any further impact on the deoxyviolacein titer and on the intracellular tryptophan pool (Figure 11A and B), both of which remained almost unchanged in the dVio-3 ($209.5 \pm 17.3 \text{ mg L}^{-1}$ deoxyviolacein, $1.6 \pm 0.7 \text{ } \mu\text{mol gCDW}^{-1}$ L-tryptophan) as compared to the parent strain ($202.8 \pm 1.2 \text{ mg L}^{-1}$ deoxyviolacein, $1.5 \pm 0.4 \text{ } \mu\text{mol gCDW}^{-1}$ L-tryptophan). These results suggested the preceding chorismate pathway as relevant next target.

3.2.3. Metabolic engineering of the chorismate supply

To improve chorismate biosynthesis, the corresponding pathway was substantially engineered (Figure 11). First, an extra copy of the *aroFBL* genes (Rüffer et al., 2004) was integrated as an artificial operon into the chromosome of *E. coli* replacing the resident *lacZYA* genes to generate strain TRP4 (Table 2). The three genes are placed under control of the P_{TAC} promoter (see Suppl. Figure 3 and Appendix). The construct $\Delta lac::P_{TAC}aroFBL-FRT-Km-FRT$ was transferred into strain *E. coli* dVio-3 (Table 2). The created strain, designated *E. coli* dVio-4, exhibited a 19.5% increased deoxyviolacein titer of $250.3 \pm 5.7 \text{ mg L}^{-1}$ (Figure 11A). It was interesting to note that the tryptophan level of this strain remained at a similar level, as compared to the parental producer (Figure 11B), whereby no tryptophan accumulated in the broth during the cultivation. Obviously, the extra tryptophan produced was fully directed to deoxyviolacein production, suggesting an extra capacity of the terminal pathway to receive a further enhanced carbon flux. As the modification of the chorismate pathway successfully increased the product level, the next genetic modification aimed at improving the availability of the chorismate precursor, erythrose 4-phosphate.

3.2.4. Metabolic engineering of erythrose 4-phosphate supply

In arabinose-grown *E. coli*, erythrose-4-phosphate is provided by the enzyme transketolase in the non-oxidative part of the pentose phosphate pathway (Sprenger, 1995). It therefore appeared straightforward to amplify the gene for the major transketolase, *tktA* (Sprenger et al., 1995), in order to increase the flux. This was realized by inserting the *tktA* gene, controlled by the P_{TAC} promoter, into the genome of *E. coli*, i.e. the *gal* locus of strain dVio-4 (Table 2). The resulting over-producer *E. coli* dVio-5 (Table 2) achieved an increased deoxyviolacein titer of 277.0 ±3.5 mg L⁻¹. The tryptophan level inside the cell did not change as compared to dVio-4.

3.2.5. Metabolic engineering of serine supply

Along the strain genealogy, the intracellular L-serine pool responded in rather complex manner to the genetic changes. The overall level in the non-producing wild type and the best producer *E. coli* dVio-6 was always the same at about 2 μmol (g CDW)⁻¹ (Figure 11C). However, a closer inspection showed that the L-serine pool always decreased, when the corresponding genetic modification resulted in a strong production increase, i.e. from the control strain to dVio-1, and from dVio-3 to dVio-4. This suggested a benefit, if the availability of L-serine could be further enhanced. Due to this, the feedback-resistant variant *serA*^{fr} of the *serA* gene was additionally inserted into the *xyl* locus (Table 2 and Appendix). The gene encodes 3-phosphoglycerate dehydrogenase, responsible for the first step in the serine pathway that converts 3-phosphoglycerate into 3-phosphohydroxypyruvate. The created mutant *E. coli* dVio-6 accumulated 324.1 ±2.4 mg L⁻¹ of deoxyviolacein (Figure 11A). Upon the increased serine supply, the intracellular tryptophan pool raised about fivefold (Figure 11B). No accumulation of L-tryptophan in the supernatant was observed, as long as L-arabinose was available to induce gene expression (Figure 8B). Towards the very end of the process, when arabinose had been depleted and the cells switched to re-use acetate, tryptophan (55 mg L⁻¹) accumulated in the broth (Figure 8B). In addition, minor amounts of L-serine (6 mg L⁻¹) were secreted, together with about 3 mg L⁻¹ of glycine.

3.2.6. Evaluation of the capacity of carbon core metabolism and the heterologous deoxyviolacein pathway

The appropriate balancing of pathway modules along a biosynthetic chain is one of the crucial tasks of successful strain engineering. To investigate the underlying characteristics in the designed over-producer, a specific reporter strain was generated. This strain, designated *E. coli* TRP11, corresponded to the genotype of the best deoxyviolacein producer, dVio-6, except for the presence of the heterologous plasmid pBvioABCE-Km. This strain grew much faster than the corresponding producer dVio-6 (Figure 8C). It consumed arabinose within only about 75 h, as indicated by the rise in the dissolved oxygen level, and the strain secreted about 800 mg L⁻¹ tryptophan. Tryptophan could not be re-utilized due to the introduced block of the catabolic pathway. The intracellular levels of tryptophan and serine increased twentyfold and twofold, respectively (Figure 11B and C) indicating the effectiveness of the strategy employed to improve the intracellular levels of these deoxyviolacein and violacein precursors.

3.2.7. Fed-batch production of deoxyviolacein in *E. coli* dVio-6 from L-arabinose as carbon source

In a first experiment, the previously derived strain *E. coli* dVio-6 (Table 4) was evaluated for deoxyviolacein production. L-Arabinose simultaneously served as carbon source for growth and as inducer for expression of the plasmid encoded deoxyviolacein pathway, whereby the entire process was operated at 20 °C. During the initial batch phase, *E. coli* dVio-6 produced 100 mg L⁻¹ deoxyviolacein (Figure 13). When L-arabinose was completely consumed, the feed was started and the process was continued. However, the concentration of deoxyviolacein increased only slightly further. After about 125 h, L-arabinose began to accumulate in the medium, followed by accumulation of acetate. At this time, cell concentration decreased. At 210 h of cultivation, the deoxyviolacein titer reached a maximum value of 250 mg L⁻¹ (Figure 13). At this point, L-arabinose and acetate had strongly accumulated, indicating inhibiting cultivation conditions. *E. coli* dVio-6 successfully produced deoxyviolacein. However, the obtained titer was low. It was even lower than that previously obtained in shake-flasks cultivations (Rodrigues et al., 2013).

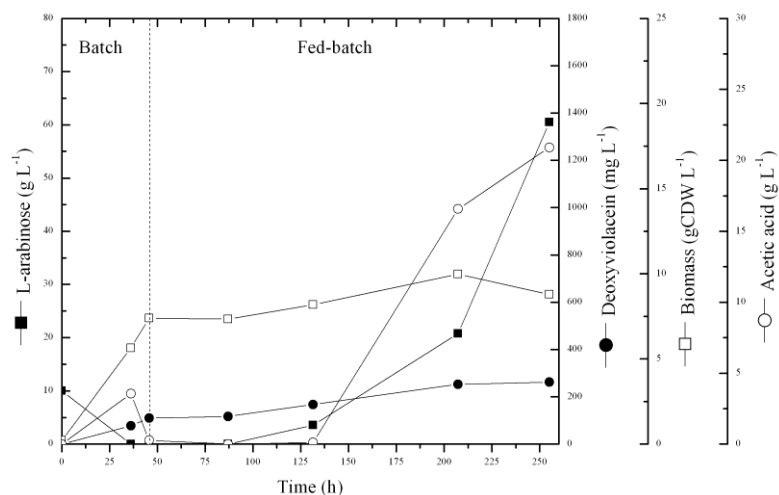


Figure 13. Fed-batch production of deoxyviolacein in *E. coli* dVio-6. The dashed line marks the beginning of the feed phase. The feed rate was adjusted to a constant growth rate of 0.011 h^{-1} , based on growth parameters ($\mu_{\max} = 0.018 \text{ h}^{-1}$, $Y_{x/s} = 0.235 \text{ g g}^{-1}$) previously obtained (Rodrigues et al., 2013).

Moreover, growth of *E. coli* on L-arabinose was slow, so that the total process took more than one week. Taken together, production of deoxyviolacein from L-arabinose was suboptimal, leaving space and need for improvement.

3.2.8. Elimination of L-arabinose metabolism in producing *E. coli*

It appeared important to eliminate the breakdown of L-arabinose in producing *E. coli* to allow its exclusive use as inducer for gene expression of the heterologous pathway and to hopefully reduce the need for this expensive sugar to lower amounts. For this purpose, the following strategy was chosen. First, the *araBAD* genes of *E. coli* K-12 MG1655 were inactivated by replacement of the genomic sequence of *araBAD* with the chloramphenicol marker. In this procedure, the target DNA region between the homology extensions, present in the primers, was totally removed. Chloramphenicol resistant clones, obtained from *E. coli* K-12 MG1655 after deletion, were analyzed by fragment size PCR. On basis of the used primer pairs, the expected fragment size of the PCR product was 1875 bp for the deletion strain, and 4986 bp for wild type, respectively. Electrophoretic analysis

of the PCR products of wild-type and one of the chloramphenicol resistant clones indeed revealed the expected sizes (Figure 14).

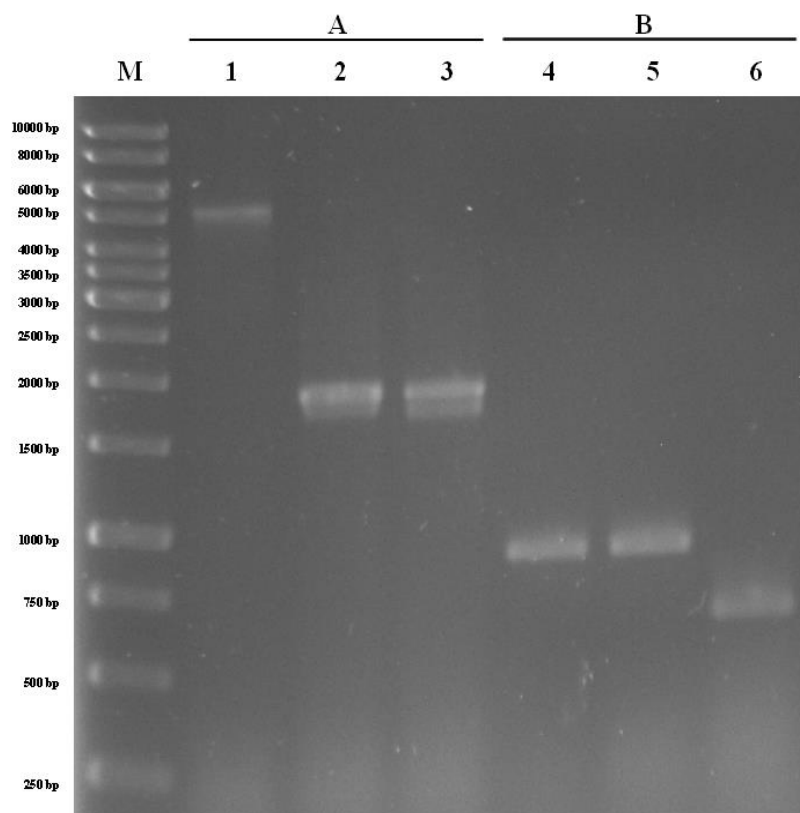


Figure 14. Validation of genetic modifications in deoxyviolacein producing *E. coli* dVio-8: deletion of *araBAD* (A) and of *trpR* (B). Lanes 1-3 show PCR products for validation of *araBAD* deletion in strains MG1655 (1), Δ *araBAD* (2), and dVio-8 (3). Lanes 4-6 show PCR products for validation of *trpR* deletion in strains MG1655 (4), Δ *araBAD* (5), and dVio-8 (6).

The clone, in which *araBAD* was removed was then used to obtain a P1 *vir* lysate. The latter was applied to integrate the construct Δ *araBAD*::*FRT-Cm-FRT* into *E. coli* TRP11. The created strain was designated *E. coli* dVio-7 (Table 4). *E. coli* dVio-7 was transformed with the biosynthetic deoxyviolacein pathway plasmid (pBvioABCE-Km). This yielded the desired producer *E. coli* dVio-8. *E. coli* dVio-8 showed the shortened PCR product that corresponded to successful deletion of *araBAD* (Figure 14). Additionally, the mutant was no more able to grow in mineral medium with L-arabinose as sole carbon and energy source (Figure 15B), as opposed to its parent *E. coli* dVio-6 (Figure 15A). Cultivation in complex medium with L-arabinose as inducer served to evaluate the metabolic engineering strategy with regard to production of the antitumor drug.

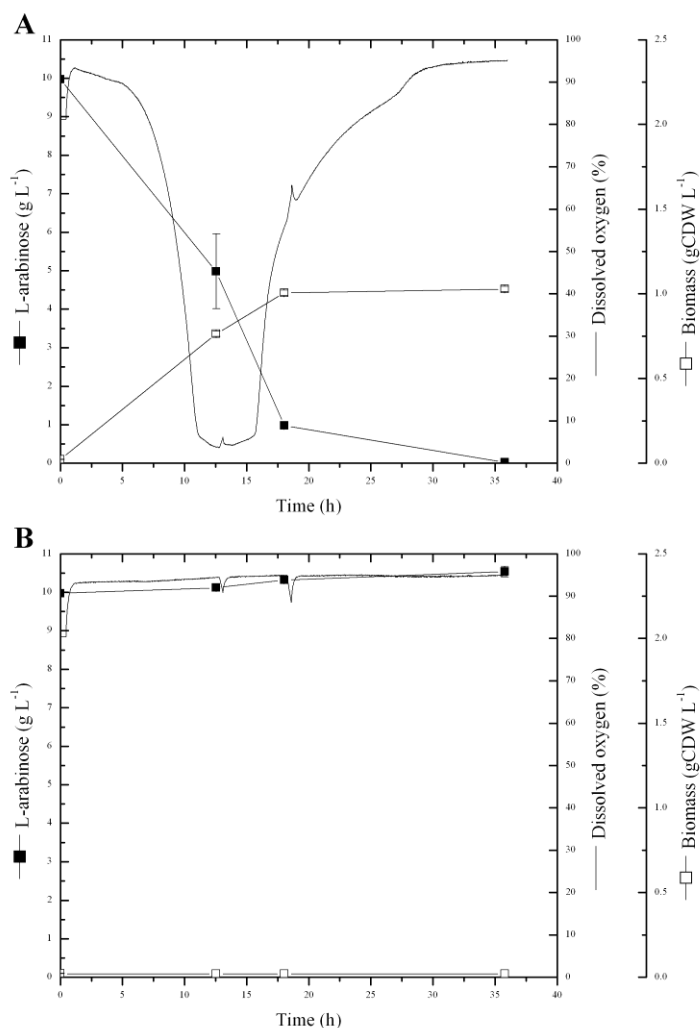


Figure 15. Growth of *E. coli* strains dVio-6 (A) and dVio-8 (B) in mineral medium with L-arabinose as single carbon source. Cultivations were performed in shaken flasks (n=3).

E. coli dVio-8, grown on LB plates containing L-arabinose, formed violet pigmented colonies (Figure 16). This proved that L-arabinose was obviously taken up by the cells and induced gene expression for deoxyviolacein production.



Figure 16. *E. coli* dVio-8 is grown on LB agar plates with L-arabinose as inducer of gene expression of the biosynthetic deoxyviolacein pathway. Pigmentation of the colonies verifies successful induction of the heterologous operon.

3.2.9. Verification of deletion of the gene of the tryptophan repressor, TrpR

Transduction with the phage P1 *vir* system can potentially transfer up to 100 kbp (Thomason et al., 2007). As the distance between the deleted *araBAD* locus and the $\Delta trpR$ mutation, implemented in *E. coli* dVio-8 to de-bottleneck the tryptophan pathway, was only about 80 kbp, it could not be excluded that the wild-type *trpR* from the donating strain *E. coli* $\Delta araBAD$ (Table 4) was co-transduced undesirably, thereby reducing the ability to produce the deoxyviolacein precursor L-tryptophan. Therefore, deletion of *trpR* in *E. coli* dVio-8 was additionally checked by PCR. In this case, an amplicon with either 638 bp or 897 bp should be observed for deletion of *trpR* or wild-type, respectively. The PCR results demonstrate that *E. coli* dVio-8 still carried the $\Delta trpR$ modification, as compared to the negative control *E. coli* MG1655 (Figure 14).

3.2.10. Evaluation of deoxyviolacein production on different carbon sources

In order to evaluate production of deoxyviolacein in *E. coli* dVio-8, microplate cultivations were performed. Either 10 g L⁻¹ fructose or glycerol replaced L-arabinose as carbon source. Hereby, different concentrations of L-arabinose were tested for induction of gene expression. Glucose was not considered, because it inhibits expression of the *araBAD* promoter by catabolite repression (Desai and Rao, 2010). Both, fructose and glycerol enabled efficient growth of the recombinant *E. coli* strain. Using fructose as carbon source, maximum cell concentration was reached after 23-30 h of cultivation time, depending on the L-arabinose level (Figure 17A). It was interesting to note that higher levels of L-arabinose seemed to suppress growth. A similar trend was also observed for glycerol. The time required to reach maximal cell concentration on glycerol correlated with L-arabinose concentration (Figure 17B). Samples for determination of deoxyviolacein were collected, when cultures had reached stationary phase. On fructose, the deoxyviolacein titer increased up to 250 mg L⁻¹ with increasing initial L-arabinose level (Figure 17C). In case of glycerol, a

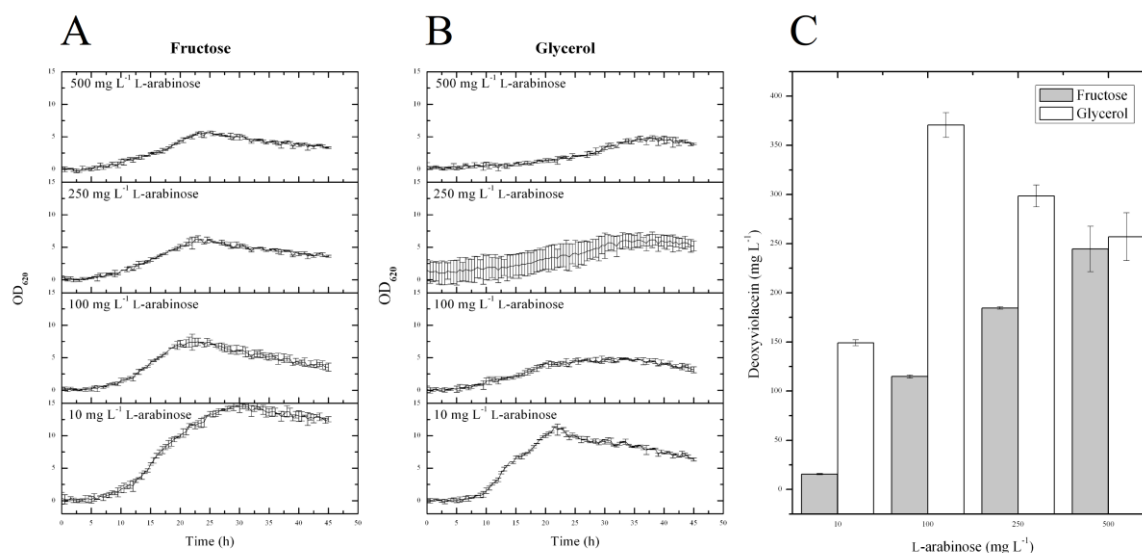


Figure 17. Impact of fructose (A) and glycerol (B) as carbon source on growth and deoxyviolacein production in *E. coli* dVio-8. Different levels of L-arabinose (10-500 mg L⁻¹) were tested to identify optimum inducing conditions for deoxyviolacein production (C). Cultivations were performed in microplates (n=3).

maximum deoxyviolacein concentration of even 370 mg L⁻¹ was reached. Here, already 100 mg L⁻¹ L-arabinose were found sufficient for induction. As use of glycerol clearly permitted a higher titer, this compound was selected as preferred carbon source for further production.

3.2.11. Investigation of remaining L-arabinose turnover in *E. coli* Δ *araBAD* using ¹³C labeling experiments

As sole source of carbon, L-arabinose did not support growth of the producer *E. coli* dVio-8, which lacked the *araBAD* operon. However, it appeared possible that L-arabinose was still co-metabolized by the recombinant cells in presence of a second fully functional carbon source, such as glycerol. In such a case, one would expect L-arabinose carbon in other metabolic intermediates and, consequently, in amino acids derived therefrom. Based on this hypothesis, the following isotope experiment was done to clarify the metabolic fate of L-arabinose in *E. coli* lacking *araBAD*. *E. coli* dVio-6 and dVio-8 were independently cultivated with glycerol as primary carbon source, together with either L-[1-¹³C] arabinose or naturally labeled L-arabinose. The labeling pattern of proteinogenic amino acids of

E. coli dVio-6, which carried a functional *araBAD* pathway, was significantly enriched in ^{13}C , when L-[1- ^{13}C] arabinose was used, as compared to the non-labeled control (Figure 18A).

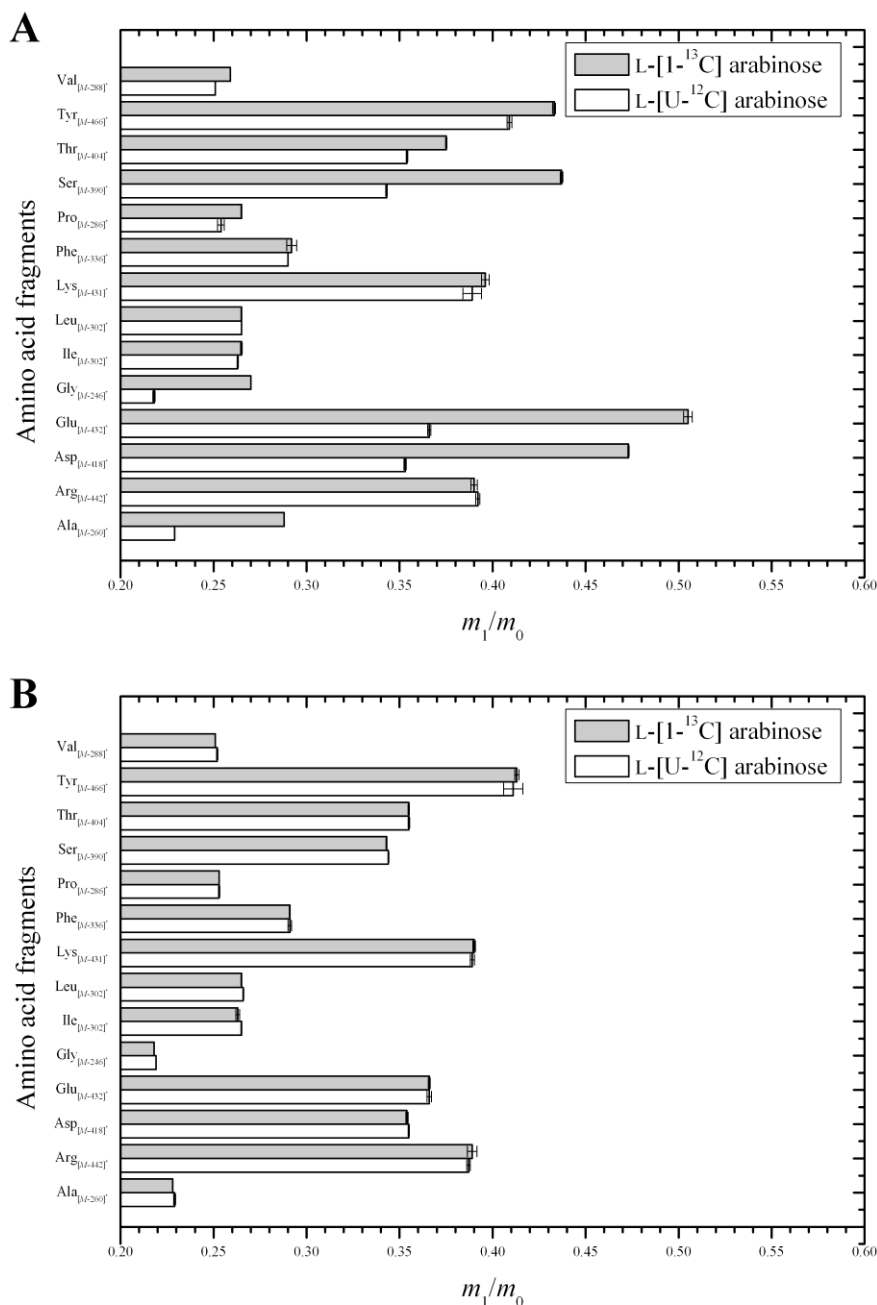


Figure 18. Elucidation of L-arabinose catabolism in *E. coli* dVio-6 (A) and dVio-8 (B). Strains were cultured in media containing non-labeled or 99% L-[1- ^{13}C] arabinose, respectively. Metabolization of L-arabinose was assessed by ^{13}C labeling analysis of amino acids from the cell protein.

Obviously, the strain catabolized L-arabinose in presence of other medium ingredients so that its carbon skeleton entered central metabolism and

biosynthetic pathways of amino acids. In contrast, *E. coli* dVio-8, which lacked the *araBAD* metabolic route, did not show any ^{13}C enrichment, when cultivated on ^{13}C -labelled L-arabinose (Figure 18B). For all amino acids analyzed, the labeling pattern was identical to that of the non-labeled control. This demonstrated the inability of strain *E. coli* dVio-8 to convert L-arabinose, even in presence of other nutrients.

3.2.12. Glycerol-based fed-batch production of deoxyviolacein by *E. coli* dVio-8

For production of deoxyviolacein, *E. coli* dVio-8 was transferred into a fed-batch set-up. The process design comprised two phases: an initial growth phase at 37 °C and a second production phase at 20 °C (Figure 19).

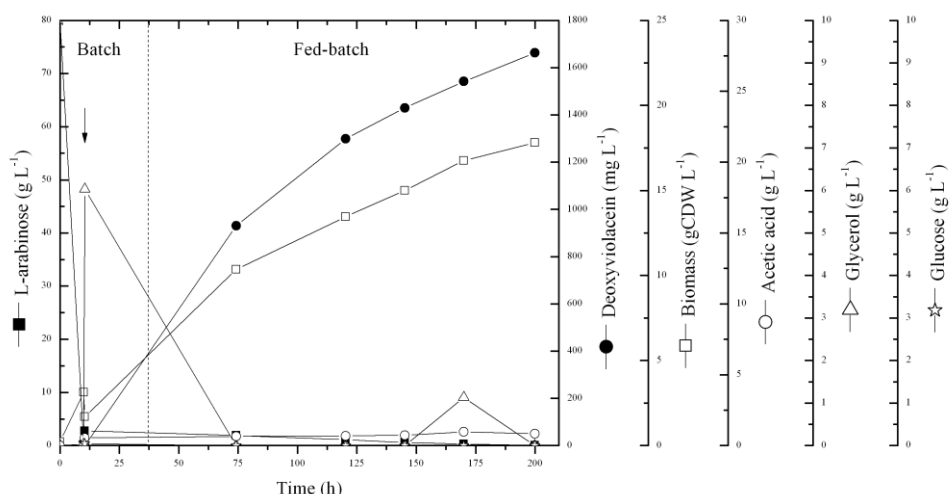


Figure 19. Fed-batch production of deoxyviolacein in *E. coli* dVio-8. The arrow indicates the time point of glucose depletion, at which the reactor was cooled from 37°C to 20°C and the carbon source was switched to glycerol. The dashed line marks the beginning of the feed phase.

During the initial phase at 37 °C, production of deoxyviolacein was completely shut off, because glucose was used as carbon source (Desai and Rao, 2010). After 10 h, glucose was completely consumed. Temperature was then shifted to 20 °C (Rodrigues et al., 2013). When the reactor had reached 20 °C, glycerol-based medium was added and cells switched to use this as carbon source and started to produce deoxyviolacein. Upon depletion of the batched glycerol, pulse-wise feeding of glycerol started. After about 200 h, a deoxyviolacein titer of 1.6 g L⁻¹

was reached; alongside with a maximal cell concentration of 17.7 (g dry biomass) L⁻¹. L-Arabinose was available throughout the whole process. At the end of cultivation, 150 mg L⁻¹ L-arabinose was still left, as determined by HPLC. The acetate level remained below 1 g L⁻¹ during the process and no accumulation of glycerol was observed. When the filling volume approached the maximal working volume, the process was stopped. Subsequently, deoxyviolacein was extracted from the recovered cells, concentrated and purified. HPLC analysis demonstrated highly pure deoxyviolacein (> 99.5%, Figure 20). Overall, the yield of deoxyviolacein on glycerol was 20 mg g⁻¹ and the productivity was 8 mg L⁻¹ h⁻¹.

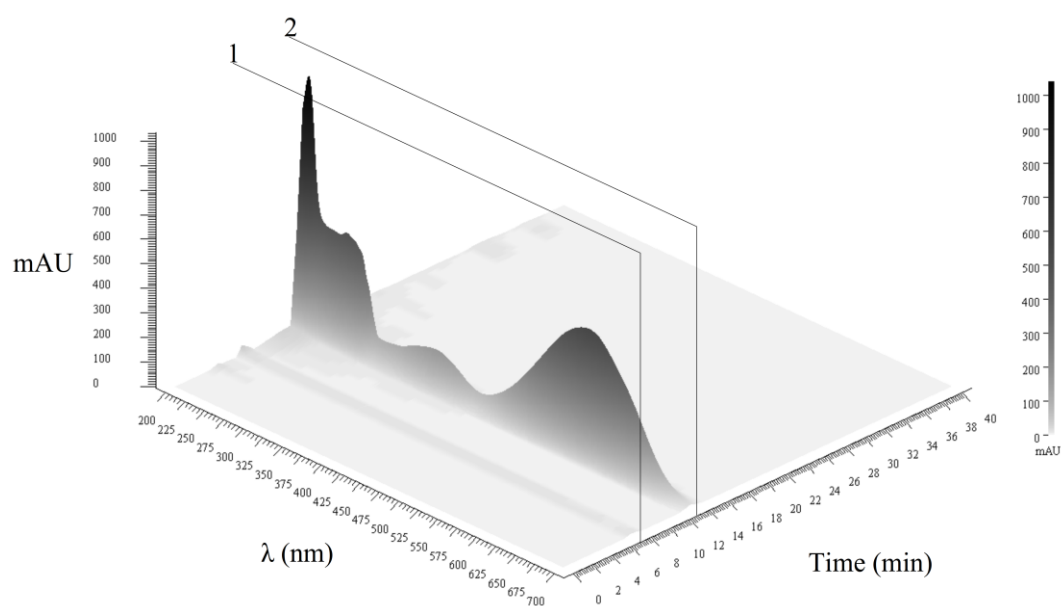


Figure 20. Validation of purity of deoxyviolacein after extraction from culture broth and purification by flash chromatography. The signals of the sample reflect the dead volume of the column (1) and the target compound deoxyviolacein (2). The peak areas reveal a purity of > 99.5%. Analysis was conducted with HPLC and detection with a diode array detector.

3.2.13. Extension of the product spectrum to violacein

In order to engineer a strain of *E. coli* for production of violacein, the biosynthetic cluster was completed by the *vioD* gene using the following strategy. The *vioD* gene of *J. lividum* was cloned under control of the P_{TAC} promoter and inserted into the *fuc* locus of *E. coli* BW25113. The strain obtained (strain Vio-1, Table 2) was used to integrate the construct $\Delta fuc::P_{TAC}vioD-FRT-Km-FRT$ into the genome of the strain TRP11, which already encoded all beneficial modifications of

the supporting pathways. Subsequently, the resistance marker *Km* was removed and the full violacein pathway was restored by transformation with the plasmid pBvioABCE-Km (Table 2). The resulting mutant *E. coli* Vio-4 was evaluated for violacein production. HPLC analysis of the extracted culture broth, harvested at the end of the process, revealed that the product spectrum was successfully switched. Violacein was the only compound, whereas deoxyviolacein was completely eliminated (Figure 9D).

3.2.14. Production performance of the designed violacein mutant in a fed-batch process

The potential of the novel mutant was next evaluated under industrial production conditions. In order to reach higher cell concentration, a fed-batch process was designed. The production medium was enriched with yeast extract and tryptone to avoid eventual nutrient limitations during the process and further support growth. During the initial batch phase, *E. coli* Vio-4 completely consumed arabinose and produced 70 mg L⁻¹ violacein (Figure 21). With the depletion of the carbon source after 48 h, the feed-phase was initiated. Based on the growth performance from preceding shake flask cultivations, the exponential feed was adjusted such that the cells grew at a constant specific growth rate of 0.011 h⁻¹.

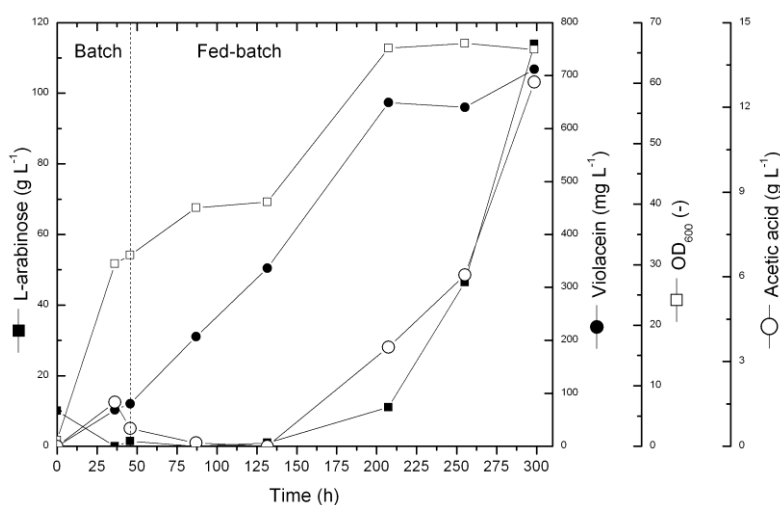


Figure 21. Fed-batch production of violacein by recombinant *E. coli* Vio-4. The values, given for feed-batch phase are normalized by the initial medium volume to account for dilution of the medium.

Within 200 h, the cells reached an optical density of almost 70. Violacein reached a final level of 710 mg L^{-1} (Figure 21). During the later process stages, acetate accumulated in the medium, which probably inhibited further growth and pigment production. Due to the reduced performance at this time point, the externally added L-arabinose was no longer fully utilized, but also increased in the broth, which leaves space for future improvement. Violacein was the exclusive heterologous product, as verified by HPLC analysis (data not shown). The cells were harvested from the bioreactor, followed by extraction into ethanol, drying, and crystallization of the product in a mixture of acetone and water. The product exhibited a purity of 99.8 %, as evaluated by HPLC analysis (Figure 22). No traces of deoxyviolacein were detected.

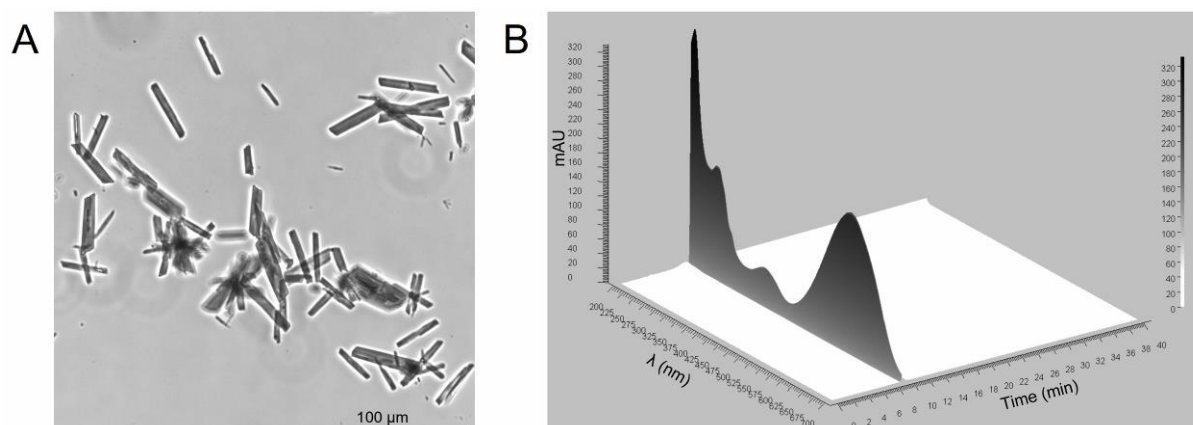


Figure 22. Purification of violacein: crystallized violacein (A) and chromatogram of the violacein crystals, solubilized in ethanol (B).

4 Discussion

4.1.1. HPLC method for quantification of violacein and deoxyviolacein

A method that enables the quantification of the exact content of violacein and deoxyviolacein in ethanol extracts of culture samples was developed. This is an important contribution to future screening of novel isolates, the evaluation of the effects of medium modification, or studies on metabolic engineering or process engineering regarding the production of these relevant pigments. It appears likely, that also other pathway intermediates, not considered so far, might be detected by the developed method, further extending its application range.

4.1.2. The synthetic *E. coli* based producers enable efficient and safe production of violacein and deoxyviolacein

Systems-wide metabolic pathway engineering enabled pure and efficient production of violacein and deoxyviolacein in tailor-made recombinant *E. coli* strains. Both pigments receive high interest due to their biological action against pathogenic bacteria, viruses and various tumor cells, so that the present work is a milestone towards their tailor-made synthesis. However, natural microbial producers of the pigments exhibit low productivity (Yang et al., 2011), spontaneous formation of non-producing variants (Jiang et al., 2010) and have been shown to cause human infections with high mortality (Patjanasontorn et al., 1992; Ti et al., 1993). Safety, well-known genetics, high transformation efficiency, cultivation simplicity, rapidity and inexpensiveness contribute to the preferred selection of *E. coli* as recombinant host for therapeutics (Ajikumar et al., 2010; Saïda et al., 2006). More than 20 years ago, the pioneering expression of the violacein pathway opened the door to obtain violacein and deoxyviolacein in this widely accepted host (Pemberton et al., 1991).

4.1.3. Systems metabolic engineering of supporting pathways drives secondary metabolite production

The design of the novel strains, described here, involved global optimization of supporting biochemical reactions from pentose phosphate pathway, serine, chorismate and tryptophan biosynthesis (Figure 12). This almost doubled the production as compared to the basic producer. In this line, the designed strains display a next level of producers beyond recent attempts that exclusively expressed the heterologous pathway (August et al., 2000). Such strains showed rather weak performance, which underlines the importance to apply systems metabolic engineering for production of high-value pharmaceuticals in recombinant hosts (Korneli et al., 2013). Towards further optimization of the developed strains, increased expression of the serine pathway enhanced the intracellular tryptophan level and the product titer. This points at the genes *sdaB* and *tdcG*, responsible for serine catabolism in *E. coli* as promising targets (Li et al., 2012). The inactivation of these genes, together with deletion of *sdaA*, previously increased the serine concentration from 0.03 to 0.13 mmol gCDW⁻¹ in *E. coli* (Li et al., 2012). Recent examples have impressively demonstrated the power of systems metabolic engineering for microbial overproduction of primary metabolites (Olano et al., 2008; Park et al., 2007; Sawada et al., 2010; Tyo et al., 2010). As shown, this strategy is also valuable for secondary metabolites. Clearly, the synthesis of such heterologous compounds is driven by up-stream metabolic engineering of supporting pathways that supply building blocks, energy and cofactors.

4.1.4. The arabinose-inducible system mediates stable expression of the heterologous pathway

A bio-based process typically comprises several stages of seed cultivation prior to the production itself. Previously, recombinant *E. coli* strains suffered from instable production characteristics, when the cells went through sequential cultivations with actively expressed *vio* genes (August et al., 2000). In the present work, this was overcome by an inducible expression control, so that the cells maintained high productivity throughout the entire production process. Many available inducible expression systems use lac-derived promoters from *E. coli* that

exhibit relatively low level of inducible expression and leaky basal expression (Zhang et al., 2012). In light of the previous findings, this would have been undesired for production of violacein and deoxyviolacein, so that the particularly chosen strategy aimed at a tight control of heterologous expression, using the *araBAD* promoter in combination with arabinose as inducer. The *araC* protein is an efficient repressor in the absence of arabinose, but acts to induce gene expression, when the sugar is present (Lee et al., 1987). This allowed silencing the cluster during all pre-cultivation stages and activating its expression on demand. The beneficial performance of the arabinose-inducible expression system has recently also been described for other microorganisms (Zhang et al., 2012) suggesting a broader use in the future. The removal of the arabinose degradation pathway in *E. coli* seems promising for further engineering, as it would allow using only small amounts of this sugar as inducer in combination with cheaper carbon sources, as well as faster growth. In addition, alternative inducible promoters could be of interest to suppress basal expression at high induction efficiency (Saïda et al., 2006).

4.1.5. The comparative evaluation of deoxyviolacein and violacein production should consider the analytical method used

The method of choice for determination of deoxyviolacein and violacein concentrations is photometrical analysis of broth extracts with organic solvents (Rodrigues et al., 2012). Although such approaches allow fast and simple measurement, one should notice that they can result in over estimation of product titers. The comparison with HPLC-based analysis of the separated products, used here, revealed that optical protocols cause threefold overestimation for deoxyviolacein (Table 7). Violacein titers were up to sevenfold higher, when assessed by photometric measurement (Table 8). This provides guidelines for the evaluation and comparison of violacein and deoxyviolacein producers and processes. Obviously, accurate quantification requires separation of the analyte of interest from the broth, as realized during HPLC analysis, to eliminate matrix effects. In this regard, the obtained correlation factors between the different analytical protocols might be used to correct for overestimation from photometric assays.

4.1.6. Production of deoxyviolacein using glycerol as carbon source

Here, we describe a novel strain of *E. coli* that produces 1.6 g L⁻¹ from glycerol as carbon source in a fed-batch process. The titer is five-fold higher than achievements until now (Rodrigues et al., 2013) and the successful surpassing of the gram scale displays an important benchmark for heterologous production of high-value drugs in *E. coli*. Most relevant, the novel process opens the door to provide deoxyviolacein with high purity and quantity for biological tests, as well as for subsequent chemical modification towards novel biological functions. Such advanced tests require supply in gram scale (Koehn and Carter, 2005). The use of *E. coli* is particularly attractive, because it is safe for production of pharmaceutical compounds intended for human treatment (Ferrer-Miralles et al., 2009).

A central achievement of our study is decoupling of production from L-arabinose as carbon source. The elimination of arabinose catabolism disrupts L-arabinose and carbon core metabolism of *E. coli*. In the novel strain, the expensive pentose is fully available for induction of heterologous gene expression so that its supply can be strongly reduced (Figure 23). The optimized metabolism enables the use of other carbon sources. We demonstrate that glycerol is an excellent carbon source to drive deoxyviolacein production in *E. coli*. From an economic perspective, glycerol is a highly promising raw material (Yang et al., 2012). It is widely available as a side product from biodiesel industry, due to growing demand for renewable transportation fuels. The low price for glycerol has recently opened a range of applications, including bio-based production of bulk chemicals such as lactic acid (Mazumdar et al., 2013) and succinic acid (Blankschien et al., 2010) or aromatic compounds (Martínez-Gómez et al., 2012), such as L-phenylalanine (Weiner et al., 2014). Thus, production of deoxyviolacein from glycerol is promising, particularly, regarding larger scales. From a metabolic viewpoint, glycerol is channeled into central metabolism at the level of dihydroxyacetone phosphate (Figure 23). With only one biochemical reaction (triosephosphate isomerase), this intermediate is converted into glyceraldehyde 3-phosphate, the starting precursor of deoxyviolacein. The tight connection of substrate influx and product formation might explain the excellent performance of glycerol-grown *E. coli* for deoxyviolacein synthesis (Figure 17, Figure 19). Obviously, the

overexpressed transketolase directly acts at the crossroad of substrate entry and production biosynthesis, so that carbon is pushed towards the desired product. The entire flux, channeled into the tryptophan pathway is utilized for deoxyviolacein production, as no tryptophan accumulated as side product (Rodrigues et al., 2013). This reveals high capacity of the engineered production route and underlines the synthetic power of the genomic traits, implemented in *E. coli* dVio-8 (Figure 23).

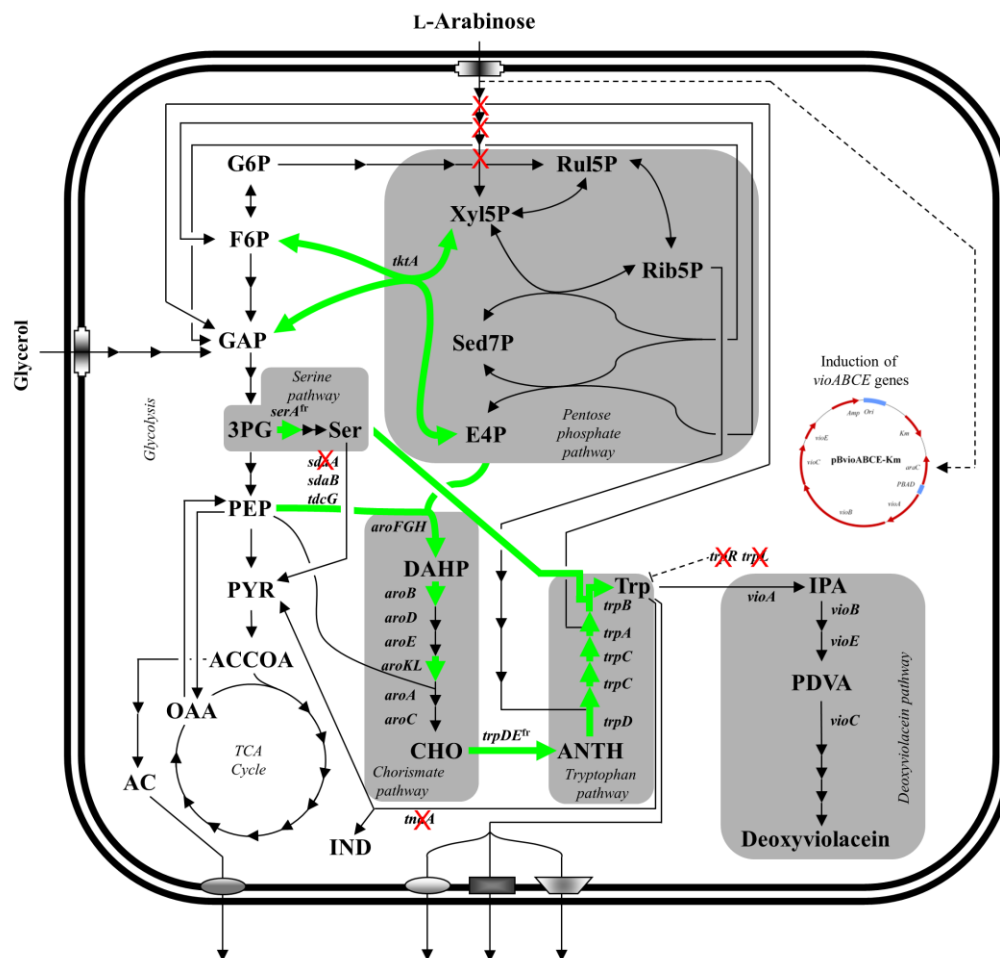


Figure 23. Systems metabolic engineering strategy for deoxyviolacein production in *E. coli* dVio-8, using glycerol as carbon source and L-arabinose as inducer. Compound names: G6P (glucose 6-phosphate), F6P (fructose 6-phosphate), GAP (glyceraldehyde 3-phosphate), 3PG (3-phosphoglycerate), PEP (phosphoenolpyruvate), PYR (pyruvate), ACCOA (acetyl-CoA), OAA (oxaloacetate), IND (indole), Ru5P (ribulose 5-phosphate), Xyl5P (xylulose 5-phosphate), Rib5P (ribose 5-phosphate), Sed7P (sedoheptulose 7-phosphate), E4P (erythrose 4-phosphate), Ser (L-serine), DAHP (3-deoxy-D-arabino-heptulosonate-7-phosphate), CHO (chorismate), ANTH (anthranilate), Trp (L-tryptophan), IPA (indole-3-pyruvic acid imine), PDVA (protodeoxyviolaceinic acid), and AC (acetate).

Studies that focus on overproduction of tryptophan (Shen et al., 2012) and related metabolites (Balderas-Hernández et al., 2009; Patnaik and Liao, 1994; Patnaik et al., 1995) in *E. coli* provide valuable information that can guide further metabolic engineering. As example, production of tryptophan by *E. coli* in a fed-batch process was increased to 40 g L⁻¹ after overexpressing genes, encoding for transketolase (*tktA*) and phosphoenolpyruvate synthase (*ppsA*) (Shen et al., 2012). Joint overexpression of *ppsA*, *aroG* and *tktA* was also beneficial for generation of 3-deoxy-D-arabino-heptulosonate-7-phosphate (DAHP), a common precursor of aromatic amino acids in *E. coli* (Patnaik et al., 1995). *E. coli* dVio-8 has two of the three genes overexpressed: *tktA* and *aroF*, catalyzing the same biochemical reaction as *aroG*. In this line, *ppsA* appears as promising target for further improvement of deoxyviolacein production in *E. coli* dVio-8.

The proven use of different raw materials for efficient production of violacein (Rodrigues et al., 2013) and deoxyviolacein (this work) points at high flexibility and capacity of *E. coli* metabolism. The engineered core machinery of *E. coli* dVio-8 allows to direct different substrates of interest towards the desired products. In this line, the created metabolic chassis is not restricted to production of violacein (Rodrigues et al., 2013) and deoxyviolacein (this work), but at the same time, enables access also to other L-tryptophan derived drugs with benefits already implemented, including rebeccamycin and staurosporine, both important antitumor molecules (Howard-Jones and Walsh, 2006). Such a versatility of producing strains is highly desirable as it provides a higher degree of freedom for process changes and speeds up development by taking full advantage of pre-engineered pathway chassis. The power of this approach has been recently demonstrated by straightforward design of novel producing strains for the monomer building block diaminopentane (Kind et al., 2010) and the chemical chaperone ectoine (Becker et al., 2013), both using a metabolic chassis of *Corynebacterium glutamicum*, previously developed for hyper-production of L-lysine (Becker et al., 2011).

5 Conclusions and Outlook

In the present work, *E. coli* could be successfully engineered for biosynthesis of either deoxyviolacein or violacein. Starting from a basic deoxyviolacein producer, systems metabolic engineering enabled the identification of limitations in the availability of the precursor metabolite L-tryptophan, which was subsequently addressed by modifications in the genome for improvement of the metabolic fluxes towards this amino acid. The improved deoxyviolacein producer was additionally modified to inactivate the catabolism of L-arabinose, so that this sugar could be used exclusively for induction of gene expression. After bioprocess optimization, 1.6 g L⁻¹ deoxyviolacein could be produced in a fed-batch cultivation using glycerol as main carbon source. Subsequent downstream operations allowed deoxyviolacein to be recovered at high purity (>99%). By utilizing the chassis strain with improved metabolism for L-tryptophan biosynthesis, additional integration of the *vioD* of *J. lividum* permitted complete redirection of the pathway fluxes to produce violacein, without any detectable amounts of deoxyviolacein. Similarly, a fed-batch process allowed production of 700 mg L⁻¹ violacein using L-arabinose as main carbon source. The product could be recovered at high purity (>99%) in crystalline form after extraction. A variant of the above mentioned violacein producer with disrupted L-arabinose catabolism was also constructed; however, due to time constraints, this mutant could not be extensively tested and was left out of the present work.

Additional strategies that can be used to improve the production capabilities of the strains constructed should consider all aspects from gene expression, bioprocess optimization, and downstream processes. Usually, optimization of processes for production of heterologous products involves the maximization of the metabolic capabilities of the producing organism towards the desired product. Different approaches are available for this objective. One of these is the stabilization of the mRNA related to the pathway of the desired product. This objective can be achieved by inserting protective elements at the two ends of the mRNA to reduce its degradation speed (Makrides, 1996), thereby allowing reduction in the use of inducers of gene expression, and potentially increase accumulation of the desired product. Although the violacein and deoxyviolacein pathways are functional in *E. coli*, it can not be ruled out that some limitation

regarding codon usage (Makrides, 1996) may be taking place. Analysis of the codon usage in the *vio* genes followed by replacement of rare codons could also be helpful for the improvement of production. Complete integration of the heterologous pathways into the chromosome would permit reduction of the metabolic burden related to plasmid maintenance and the elimination of the use of antibiotics, possibly allowing increases of growth and production rates. Improvements are also possible from the bioprocess point of view. Experimental design can be used to optimize the medium and culturing conditions during batch and fed-batch phases of the production processes (Mandenius and Brundin, 2008). Additionally, as violacein and deoxyviolacein are hydrophobic molecules that accumulate in the cells, two-phase systems (Banik et al., 2003) could be tested to evaluate if extractive cultivations could improve the production and/or the later downstream operations, which accounts to about 60-90% of the cost of most biological processes.

The created violacein and deoxyviolacein producers, which comprise a high-flux tryptophan pathway encoded in their genome, are powerful starting points to derive other high-value tryptophan-based therapeutics. Prominent candidates are rebeccamycin and staurosporine, both important antitumor molecules (Howard-Jones and Walsh, 2006).

6 References

- Ahmetagic, A., Pemberton, J. M., 2010. Stable high level expression of the violacein indolocarbazole anti-tumour gene cluster and the *Streptomyces lividans amyA* gene in *E. coli* K12. *Plasmid*. 63, 79-85.
- Aiba, S., Tsunekawa, H., Imanaka, T., 1982. New approach to tryptophan production by *Escherichia coli*: genetic manipulation of composite plasmids in vitro. *Applied and Environmental Microbiology*. 43, 289-297.
- Ajikumar, P. K., Xiao, W. H., Tyo, K. E. J., Wang, Y., Simeon, F., Leonard, E., Mucha, O., Phon, T. H., Pfeifer, B., Stephanopoulos, G., 2010. Isoprenoid pathway optimization for Taxol precursor overproduction in *Escherichia coli*. *Science*. 330, 70-74.
- Al Zaid Siddiquee, K., Arauzo-Bravo, M. J., Shimizu, K., 2004. Metabolic flux analysis of *pykF* gene knockout *Escherichia coli* based on ¹³C-labeling experiments together with measurements of enzyme activities and intracellular metabolite concentrations. *Applied Microbiology and Biotechnology*. 63, 407-417.
- Albermann, C., Trachtmann, N., Sprenger, G. A., 2010. A simple and reliable method to conduct and monitor expression cassette integration into the *Escherichia coli* chromosome. *Biotechnology Journal*. 5, 32-38.
- Asamizu, S., Kato, Y., Igarashi, Y., Onaka, H., 2007. VioE, a prodeoxyviolacein synthase involved in violacein biosynthesis, is responsible for intramolecular indole rearrangement. *Tetrahedron Letters*. 48, 2923-2926.
- August, P. R., Grossman, T. H., Minor, C., Draper, M. P., MacNeil, I. A., Pemberton, J. M., Call, K. M., Holt, D., Osburne, M. S., 2000. Sequence analysis and functional characterization of the violacein biosynthetic pathway from *Chromobacterium violaceum*. *Journal of Molecular Microbiology and Biotechnology*. 2, 513-519.
- Azuma, S., Tsunekawa, H., Okabe, M., Okamoto, R., Aiba, S., 1993. Hyperproduction of L-tryptophan via fermentation with crystallization. *Applied Microbiology and Biotechnology*. 39, 471-476.

- Balderas-Hernández, V. E., Sabido-Ramos, A., Silva, P., Cabrera-Valladares, N., Hernández-Chávez, G., Báez-Viveros, J. L., Martínez, A., Bolívar, F., Gosset, G., 2009. Metabolic engineering for improving anthranilate synthesis from glucose in *Escherichia coli*. *Microbial Cell Factories*. 8, 19.
- Balibar, C. J., Walsh, C. T., 2006. In vitro biosynthesis of violacein from L-tryptophan by the enzymes VioA-E from *Chromobacterium violaceum*. *Biochemistry*. 45, 15444-15457.
- Banik, R. M., Santhiagu, A., Kanari, B., Sabarinath, C., Upadhyay, S. N., 2003. Technological aspects of extractive fermentation using aqueous two-phase systems. *World Journal of Microbiology and Biotechnology*. 19, 337-348.
- Becker, J., Klopprogge, C., Schröder, H., Wittmann, C., 2009a. Metabolic engineering of the tricarboxylic acid cycle for improved lysine production by *Corynebacterium glutamicum*. *Applied and Environmental Microbiology*. 75, 7866-7869.
- Becker, J., Schäfer, R., Kohlstedt, M., Harder, B. J., Borchert, N. S., Stöveken, N., Bremer, E., Wittmann, C., 2013. Systems metabolic engineering of *Corynebacterium glutamicum* for production of the chemical chaperone ectoine. *Microbial Cell Factories*. 12, 110.
- Becker, J., Wittmann, C., 2012. Systems and synthetic metabolic engineering for amino acid production – the heartbeat of industrial strain development. *Current Opinion in Biotechnology*. 23, 718-726.
- Becker, J., Zelder, O., Häfner, S., Schröder, H., Wittmann, C., 2011. From zero to hero - Design-based systems metabolic engineering of *Corynebacterium glutamicum* for L-lysine production. *Metabolic Engineering*. 13, 159-168.
- Becker, M. H., Brucker, R. M., Schwantes, C. R., Harris, R. N., Minbiole, K. P. C., 2009b. The bacterially produced metabolite violacein is associated with survival of amphibians infected with a lethal fungus. *Applied and Environmental Microbiology*. 75, 6635.
- Berry, A., 1996. Improving production of aromatic compounds in *Escherichia coli* by metabolic engineering. *Trends in Biotechnology*. 14, 250-256.

- Blankschien, M. D., Clomburg, J. M., Gonzalez, R., 2010. Metabolic engineering of *Escherichia coli* for the production of succinate from glycerol. *Metabolic Engineering*. 12, 409-419.
- Boisbaudran, L. D., 1882. Matiere colorante se formant dans la cole de farine. *Compt Rend*. 94, 562-563.
- Bolten, C. J., Kiefer, P., Letisse, F., Portais, J. C., Wittmann, C., 2007. Sampling for metabolome analysis of microorganisms. *Analytical Chemistry*. 79, 3843-3849.
- Bonnet, M. C., Dutta, A., 2008. World wide experience with inactivated poliovirus vaccine. *Vaccine*. 26, 4978-4983.
- Boyle, P., Langman, J. S., 2000. ABC of colorectal cancer: Epidemiology. *BMJ: British Medical Journal*. 321, 805.
- Bozell, J. J., Petersen, G. R., 2010. Technology development for the production of biobased products from biorefinery carbohydrates—the US Department of Energy’s “Top 10” revisited. *Green Chemistry*. 12, 539-554.
- Bromberg, N., Dreyfuss, J. L., Regatieri, C. V., Palladino, M. V., Duran, N., Nader, H. B., Haun, M., Justo, G. Z., 2010. Growth inhibition and pro-apoptotic activity of violacein in Ehrlich ascites tumor. *Chemico-Biological Interactions*. 186, 43-52.
- Bruschi, F., Dundar, M., Gahan, P. B., Gartland, K., Szente, M., Viola-Magni, M. P., Akbarova, Y., 2011. Biotechnology worldwide and the ‘European Biotechnology Thematic Network’ Association (EBTNA). *Current Opinion in Biotechnology*. 22, S7-S14.
- Burk, M. J., 2010. Sustainable production of industrial chemicals from sugars. *International Sugar Journal*. 112, 30-35.
- Buschke, N., Schröder, H., Wittmann, C., 2011. Metabolic engineering of *Corynebacterium glutamicum* for production of 1,5-diaminopentane from hemicellulose. *Biotechnology Journal*. 6, 306–317.
- Caligiuri, M. G., Bauerle, R., 1991. Identification of amino acid residues involved in feedback regulation of the anthranilate synthase complex from *Salmonella*

References

typhimurium. Evidence for an amino-terminal regulatory site. *Journal of Biological Chemistry*. 266, 8328-8335.

Chen, X., Zhou, L., Tian, K., Kumar, A., Singh, S., Prior, B. A., Wang, Z., 2013. Metabolic engineering of *Escherichia coli*: A sustainable industrial platform for bio-based chemical production. *Biotechnology Advances* 31, 1200-1223.

Cherepanov, P. P., Wackernagel, W., 1995. Gene disruption in *Escherichia coli*: TcR and KmR cassettes with the option of Flp-catalyzed excision of the antibiotic-resistance determinant. *Gene*. 158, 9-14.

da Silva Melo, P., Maria, S. S., Vidal, B. d. C., Haun, M., Duran, N., 2000. Violacein cytotoxicity and induction of apoptosis in V79 cells. *In Vitro Cellular & Developmental Biology-Animal*. 36, 539-543.

Datsenko, K. A., Wanner, B. L., 2000. One-step inactivation of chromosomal genes in *Escherichia coli* K-12 using PCR products. *Proceedings of the National Academy of Sciences of the United States of America*. 97, 6640-6645.

De Carvalho, D. D., Costa, F., Duran, N., Haun, M., 2006. Cytotoxic activity of violacein in human colon cancer cells. *Toxicology in Vitro*. 20, 1514-1521.

de Vasconcelos, A. T. R., de Almeida, D. F., Hungria, M., Guimaraes, C. T., Antônio, R. V., Almeida, F. C., de Almeida, L. G. P., de Almeida, R., Alves-Gomes, J. A., Andrade, E. M., 2003. The complete genome sequence of *Chromobacterium violaceum* reveals remarkable and exploitable bacterial adaptability. *Proceedings of the National Academy of Sciences of the United States of America*. 100, 11660-11665.

Desai, T. A., Rao, C. V., 2010. Regulation of arabinose and xylose metabolism in *Escherichia coli*. *Applied and Environmental Microbiology*. 76, 1524-1532.

Durán, N., Antonio, R. V., Haun, M., Pilli, R. A., 1994. Biosynthesis of a trypanocide by *Chromobacterium violaceum*. *World Journal of Microbiology and Biotechnology*. 10, 686-690.

- Durán, N., Justo, G. Z., Ferreira, C. V., Melo, P. S., Cordi, L., Martins, D., 2007. Violacein: properties and biological activities. *Biotechnology and Applied Biochemistry*. 48, 127-134.
- Durán, N., Justo, G. Z., Melo, P. S., De Azevedo, M. B. M., Brito, A. R. M. S., Almeida, A. B. A., Haun, M., 2003. Evaluation of the antiulcerogenic activity of violacein and its modulation by the inclusion complexation with β -cyclodextrin. *Canadian Journal of Physiology and Pharmacology*. 81, 387-396.
- Ellis, H. M., Yu, D., DiTizio, T., 2001. High efficiency mutagenesis, repair, and engineering of chromosomal DNA using single-stranded oligonucleotides. *Proceedings of the National Academy of Sciences*. 98, 6742-6746.
- Englesberg, E., Irr, J., Power, J., Lee, N., 1965. Positive control of enzyme synthesis by gene C in the L-arabinose system. *Journal of Bacteriology*. 90, 946-957.
- Ferreira, C. V., Bos, C. L., Versteeg, H. H., Justo, G. Z., Durán, N., Peppelenbosch, M. P., 2004. Molecular mechanism of violacein-mediated human leukemia cell death. *Blood*. 104, 1459-1464.
- Ferrer-Miralles, N., Domingo-Espín, J., Corchero, J. L., Vázquez, E., Villaverde, A., 2009. Microbial factories for recombinant pharmaceuticals. *Microbial Cell Factories*. 8, 17.
- Fürste, J. P., Pansegrau, W., Frank, R., Blöcker, H., Scholz, P., Bagdasarian, M., Lanka, E., 1986. Molecular cloning of the plasmid RP4 primase region in a multi-host-range *tacP* expression vector. *Gene*. 48, 119-131.
- Giacchetti, S., Perpoint, B., Zidani, R., Le Bail, N., Faggiuolo, R., Focan, C., Chollet, P., Llory, J. F., Letourneau, Y., Coudert, B., 2000. Phase III multicenter randomized trial of oxaliplatin added to chronomodulated fluorouracil-leucovorin as first-line treatment of metastatic colorectal cancer. *Journal of Clinical Oncology*. 18, 136-136.
- Gill, S., Thomas, R. R., Goldberg, R. M., 2003. Colorectal cancer chemotherapy. *Alimentary Pharmacology & Therapeutics*. 18, 683-692.

References

- Gimenez, I. F., Anazetti, M. C., Melo, P. S., Haun, M., De Azevedo, M. M. M., Durán, N., Alves, O. L., 2005. Cytotoxicity on V79 and HL60 cell lines by thiolated-beta-cyclodextrin-Au/violacein nanoparticles. *Journal of Biomedical Nanotechnology*. 1, 352-358.
- Gu, P., Yang, F., Kang, J., Wang, Q., Qi, Q., 2012. One-step of tryptophan attenuator inactivation and promoter swapping to improve the production of L-tryptophan in *Escherichia coli*. *Microbial Cell Factories*. 11, 30.
- Heidelberger, C., Chaudhuri, N. K., Danneberg, P., Mooren, D., Griesbach, L., Duschinsky, R., Schnitzer, R. J., Plevin, E., Scheiner, J., 1957. Fluorinated pyrimidines, a new class of tumour-inhibitory compounds. *Nature*. 30.
- Henkin, T. M., Yanofsky, C., 2002. Regulation by transcription attenuation in bacteria: how RNA provides instructions for transcription termination/antitermination decisions. *Bioessays*. 24, 700-707.
- Hogrefe, H. H., Cline, J., Youngblood, G. L., Allen, R. M., 2002. Creating randomized amino acid libraries with the QuikChange® multi site-directed mutagenesis kit. *BioTechniques*. 33, 1158-1165.
- Hoshino, T., 2011. Violacein and related tryptophan metabolites produced by *Chromobacterium violaceum*: biosynthetic mechanism and pathway for construction of violacein core. *Applied Microbiology and Biotechnology*. 91, 1463-1475.
- Howard-Jones, A. R., Walsh, C. T., 2006. Staurosporine and rebeccamycin aglycones are assembled by the oxidative action of StaP, StaC, and RebC on chromopyrrolic acid. *Journal of the American Chemical Society*. 128, 12289-12298.
- Howe, R. A., Bowker, K. E., Walsh, T. R., Feest, T. G., MacGowan, A. P., 1998. Vancomycin-resistant *Staphylococcus aureus*. *The Lancet*. 351, 602.
- Huang, C. J., Lin, H., Yang, X., 2012. Industrial production of recombinant therapeutics in *Escherichia coli* and its recent advancements. *Journal of Industrial Microbiology & Biotechnology*. 39, 383-399.

- Ikeda, M., 2006. Towards bacterial strains overproducing L-tryptophan and other aromatics by metabolic engineering. *Applied Microbiology and Biotechnology*. 69, 615-626.
- Jensen, K. F., 1993. The *Escherichia coli* K-12 "wild types" W3110 and MG1655 have an *rph* frameshift mutation that leads to pyrimidine starvation due to low *pyrE* expression levels. *Journal of Bacteriology*. 175, 3401-3407.
- Jiang, P., Wang, H., Xiao, S., Fang, M., Zhang, R., He, S., Lou, K., Xing, X. H., 2012. Pathway redesign for deoxyviolacein biosynthesis in *Citrobacter freundii* and characterization of this pigment. *Applied Microbiology and Biotechnology*. 94, 1521-1532.
- Jiang, P., Wang, H., Zhang, C., Lou, K., Xing, X. H., 2010. Reconstruction of the violacein biosynthetic pathway from *Duganella* sp. B2 in different heterologous hosts. *Applied Microbiology and Biotechnology*. 86, 1077-1088.
- Keseler, I. M., Collado-Vides, J., Gama-Castro, S., Ingraham, J., Paley, S., Paulsen, I. T., Peralta-Gil, M., Karp, P. D., 2005. EcoCyc: a comprehensive database resource for *Escherichia coli*. *Nucleic Acids Research*. 33, D334-D337.
- Kimmel, K. E., Maier, S., 1969. Effect of cultural conditions on the synthesis of violacein in mesophilic and psychrophilic strains of *Chromobacterium*. *Canadian Journal of Microbiology*. 15, 111-116.
- Kind, S., Jeong, W. K., Schröder, H., Wittmann, C., 2010. Systems-wide metabolic pathway engineering in *Corynebacterium glutamicum* for bio-based production of diamino-pentane. *Metabolic Engineering*. 12, 341-351.
- Kodach, L. L., Bos, C. L., Durán, N., Peppelenbosch, M. P., Ferreira, C. V., Hardwick, J. C. H., 2006. Violacein synergistically increases 5-fluorouracil cytotoxicity, induces apoptosis and inhibits Akt-mediated signal transduction in human colorectal cancer cells. *Carcinogenesis*. 27, 508-516.
- Koehn, F. E., Carter, G. T., 2005. The evolving role of natural products in drug discovery. *Nature Reviews Drug Discovery*. 4, 206-220.

References

- Korneli, C., David, F., Biedendieck, R., Jahn, D., Wittmann, C., 2013. Getting the big beast to work - systems biotechnology of *Bacillus megaterium* for novel high-value proteins. *Journal of Biotechnology*. 163, 87-96.
- Kovach, M. E., Phillips, R. W., Elzer, P. H., Roop, R. M., 1994. pBBR 1 MCS: a broad-host-range cloning vector. *BioTechniques*. 16, 800-802.
- Krömer, J. O., Fritz, M., Heinzle, E., Wittmann, C., 2005. In vivo quantification of intracellular amino acids and intermediates of the methionine pathway in *Corynebacterium glutamicum*. *Analytical Biochemistry*. 340, 171-173.
- Krömer, J. O., Heinzle, E., Schröder, H., Wittmann, C., 2006. Accumulation of homolanthionine and activation of a novel pathway for isoleucine biosynthesis in *Corynebacterium glutamicum* McbR deletion strains. *Journal of Bacteriology*. 188, 609-618.
- Laffend, L. A., Nagarajan, V., Nakamura, C. E., Bioconversion of a fermentable carbon source to 1, 3-propanediol by a single microorganism. Google patents, Vol. 5,686,276. United States Patent, USA, 1997.
- Landick, R., Carey, J., Yanofsky, C., 1985. Translation activates the paused transcription complex and restores transcription of the *trp* operon leader region. *Proceedings of the National Academy of Sciences of the United States of America*. 82, 4663-4667.
- Lee, N., Francklyn, C., Hamilton, E. P., 1987. Arabinose-induced binding of AraC protein to *araI*₂ activates the *araBAD* operon promoter. *Proceedings of the National Academy of Sciences of the United States of America*. 84, 8814-8818.
- Leon, L. L., Miranda, C. C., De Souza, A. O., Durán, N., 2001. Antileishmanial activity of the violacein extracted from *Chromobacterium violaceum*. *Journal of Antimicrobial Chemotherapy*. 48, 449-450.
- Li, Y., Chen, G. K., Tong, X. W., Zhang, H. T., Liu, X. G., Liu, Y. H., Lu, F. P., 2012. Construction of *Escherichia coli* strains producing L-serine from glucose. *Biotechnology Letters*. 34, 1525-1530.

- Machover, D., 1997. A comprehensive review of 5-fluorouracil and leucovorin in patients with metastatic colorectal carcinoma. *Cancer*. 80, 1179-1187.
- Maier, T., Flinspach, R., 2005. European Patent Application 1496111A2.
- Makrides, S. C., 1996. Strategies for achieving high-level expression of genes in *Escherichia coli*. *Microbiological Reviews*. 60, 512-538.
- Mandenius, C. F., Brundin, A., 2008. Bioprocess optimization using design-of-experiments methodology. *Biotechnology Progress*. 24, 1191-1203.
- Martínez-Gómez, K., Flores, N., Castañeda, H. M., Martínez-Batallar, G., Hernández-Chávez, G., Ramírez, O. T., Gosset, G., Encarnación, S., Bolivar, F., 2012. New insights into *Escherichia coli* metabolism: carbon scavenging, acetate metabolism and carbon recycling responses during growth on glycerol. *Microbial Cell Factories*. 11, 46.
- Martinez-Morales, F., Borges, A. C., Martinez, A., Shanmugam, K. T., Ingram, L. O., 1999. Chromosomal integration of heterologous DNA in *Escherichia coli* with precise removal of markers and replicons used during construction. *Journal of Bacteriology*. 181, 7143-7148.
- Martins, D., Costa, F. T. M., Brocchi, M., Durán, N., 2011. Evaluation of the antibacterial activity of poly-(D, L-lactide-co-glycolide) nanoparticles containing violacein. *Journal of Nanoparticle Research*. 13, 355-363.
- Martins, D., Frungillo, L., Anazzetti, M. C., Melo, P. S., Durán, N., 2010. Antitumoral activity of L-ascorbic acid-poly-D, L-(lactide-co-glycolide) nanoparticles containing violacein. *International Journal of Nanomedicine*. 5, 77-85.
- Mathers, C. D., Boschi-Pinto, C., Lopez, A. D., Murray, C. J. L., 2001. Cancer incidence, mortality and survival by site for 14 regions of the world. Geneva: World Health Organization. 8.
- Matz, C., Webb, J. S., Schupp, P. J., Phang, S. Y., Penesyan, A., Egan, S., Steinberg, P., Kjelleberg, S., 2008. Marine biofilm bacteria evade eukaryotic predation by targeted chemical defense. *PLoS ONE*. 3.

May, G., Brummer, B., Ott, H., Treatment of prophylaxis of polio and herpes virus infections – comprises admin. of 3-(1,2-dihydro-5-(5-hydroxy-1H-indol-3-yl)-2-oxo-3Hpyrrole-3-ylidene)-1,3-dihydro-2H-indol-2-one. German patent, DE 3935066, 1991.

Mazumdar, S., Blankschien, M. D., Clomburg, J. M., Gonzalez, R., 2013. Efficient synthesis of L-lactic acid from glycerol by metabolically engineered *Escherichia coli*. *Microbial Cell Factories*. 12, 7.

McClellan, K. H., Winson, M. K., Fish, L., Taylor, A., Chhabra, S. R., Camara, M., Daykin, M., Lamb, J. H., Swift, S., Bycroft, B. W., Stewart, G. S. A. B., Williams, P., 1997. Quorum sensing and *Chromobacterium violaceum*: exploitation of violacein production and inhibition for the detection of N-acylhomoserine lactones. *Microbiology*. 143, 3703-3711.

Mendes, A. S., de Carvalho, J. E., Duarte, M. C. T., Durán, N., Bruns, R. E., 2001. Factorial design and response surface optimization of crude violacein for *Chromobacterium violaceum* production. *Biotechnology Letters*. 23, 1963-1969.

Moat, A. G., Foster, J. W., Spector, M. P., 2003. *Microbial physiology*. John Wiley & Sons, New York.

Mojib, N., Philpott, R., Huang, J. P., Niederweis, M., Bej, A. K., 2010. Antimycobacterial activity in vitro of pigments isolated from Antarctic bacteria. *Antonie Van Leeuwenhoek*. 98, 531-540.

Nakamura, Y., Asada, C., Sawada, T., 2003. Production of antibacterial violet pigment by psychrotropic bacterium RT102 strain. *Biotechnology and Bioprocess Engineering*. 8, 37-40.

Nakamura, Y., Sawada, T., Morita, Y., Tamiya, E., 2002. Isolation of a psychrotrophic bacterium from the organic residue of a water tank keeping rainbow trout and antibacterial effect of violet pigment produced from the strain. *Biochemical Engineering Journal*. 12, 79-86.

Neidhardt, F. C., Curtiss, R., Ingraham, J. L., Lin, E. C. C., Low, K. B., Magasanik, B., Reznikoff, W. S., Riley, M., Schaechter, M., Umberger, H. E., 1996.

Escherichia coli and *Salmonella*: cellular and molecular biology. ASM Press, Washington, D. C.

Olano, C., Lombó, F., Méndez, C., Salas, J. A., 2008. Improving production of bioactive secondary metabolites in actinomycetes by metabolic engineering. *Metabolic Engineering*. 10, 281-292.

Pantanella, F., Berlutti, F., Passariello, C., Sarli, S., Morea, C., Schippa, S., 2007. Violacein and biofilm production in *Janthinobacterium lividum*. *Journal of Applied Microbiology*. 102, 992-999.

Park, J. H., Lee, K. H., Kim, T. Y., Lee, S. Y., 2007. Metabolic engineering of *Escherichia coli* for the production of L-valine based on transcriptome analysis and in silico gene knockout simulation. *Proceedings of the National Academy of Sciences of the United States of America*. 104, 7797-7802.

Parkin, D. M., 2001. Global cancer statistics in the year 2000. *The Lancet Oncology*. 2, 533-543.

Patjanasontorn, B., Boonma, P., Wilailackana, C., Sittikesorn, J., 1992. Hospital acquired *Janthinobacterium lividum* septicemia in Srinagarind hospital. *Journal of the Medical Association of Thailand*. 75, 6-10.

Patnaik, R., Liao, J. C., 1994. Engineering of *Escherichia coli* central metabolism for aromatic metabolite production with near theoretical yield. *Applied and Environmental Microbiology*. 60, 3903-3908.

Patnaik, R., Spitzer, R. G., Liao, J. C., 1995. Pathway engineering for production of aromatics in *Escherichia coli*: confirmation of stoichiometric analysis by independent modulation of AroG, TktA, and Pps activities. *Biotechnology and Bioengineering*. 46, 361-370.

Pemberton, J. M., Vincent, K. M., Penfold, R. J., 1991. Cloning and heterologous expression of the violacein biosynthesis gene cluster from *Chromobacterium violaceum*. *Current Microbiology*. 22, 355-358.

Rettori, D., Durán, N., 1998. Production, extraction and purification of violacein: an antibiotic pigment produced by *Chromobacterium violaceum*. *World Journal of Microbiology & Biotechnology* 14, 685-688.

Rodrigues, A. L., Göcke, Y., Bolten, C. J., Brock, N. L., Dickschat, J. S., Wittmann, C., 2012. Microbial production of the drugs violacein and deoxyviolacein – analytical development and strain comparison. *Biotechnology Letters*. 34, 717-720.

Rodrigues, A. L., Trachtmann, N., Becker, J., Lohanatha, A. F., Blotenberg, J., Bolten, C. J., Korneli, C., de Souza Lima, A. O., Porto, L. M., Sprenger, G. A., Wittmann, C., 2013. Systems metabolic engineering of *Escherichia coli* for production of the antitumor drugs violacein and deoxyviolacein. *Metabolic Engineering*. 20, 29-41.

Rüffer, N., Heidersdorf, U., Kretzers, I., Sprenger, G. A., Raeven, L., Takors, R., 2004. Fully integrated L-phenylalanine separation and concentration using reactive-extraction with liquid-liquid centrifuges in a fed-batch process with *E. coli*. *Bioprocess and Biosystems Engineering*. 26, 239-248.

Saïda, F., Uzan, M., Odaert, B., Bontems, F., 2006. Expression of highly toxic genes in *E. coli*: special strategies and genetic tools. *Current Protein and Peptide Science*. 7, 47-56.

Sambrook, J., Russell, D. W., 2001. *Molecular Cloning: a laboratory manual*. Cold Spring Harbor Laboratory Press, New York.

Sánchez, C., Braña, A. F., Méndez, C., Salas, J. A., 2006. Reevaluation of the violacein biosynthetic pathway and its relationship to indolocarbazole biosynthesis. *ChemBioChem*. 7, 1231-1240.

Sarovich, D. S., Pemberton, J. M., 2007. pPSX: A novel vector for the cloning and heterologous expression of antitumor antibiotic gene clusters. *Plasmid*. 57, 306-313.

Sawada, K., Zen-In, S., Wada, M., Yokota, A., 2010. Metabolic changes in a pyruvate kinase gene deletion mutant of *Corynebacterium glutamicum* ATCC 13032. *Metabolic Engineering*. 12, 401-407.

- Shen, T., Liu, Q., Xie, X., Xu, Q., Chen, N., 2012. Improved production of tryptophan in genetically engineered *Escherichia coli* with TktA and PpsA overexpression. *Journal of Biomedicine and Biotechnology*. 2012, 1-8.
- Shinoda, K., Hasegawa, T., Sato, H., Shinozaki, M., Kuramoto, H., Takamiya, Y., Sato, T., Nikaidou, N., Watanabe, T., Hoshino, T., 2007. Biosynthesis of violacein: a genuine intermediate, protoviolaceinic acid, produced by VioABDE, and insight into VioC function. *Chemical Communications*. 2007, 4140-4142.
- Shirata, A., Tsukamoto, T., Yasui, H., Hata, T., Hayasaka, S., Kojima, A., Kato, H., 2000. Isolation of bacteria producing bluish-purple pigment and use for dyeing. *Japan Agricultural Research Quarterly*. 34, 131-140.
- Sieradzki, K., Roberts, R. B., Haber, S. W., Tomasz, A., 1999. The development of vancomycin resistance in a patient with methicillin-resistant *Staphylococcus aureus* infection. *New England Journal of Medicine*. 340, 517-523.
- Sprenger, G. A., 1995. Genetics of pentose-phosphate pathway enzymes of *Escherichia coli* K-12. *Archives of Microbiology*. 164, 324-330.
- Sprenger, G. A., 2007. Aromatic amino acids. In: Wendisch, V. F., (Ed.), *Amino acid biosynthesis – pathways, regulation and metabolic engineering*. vol. 5. Springer, Berlin Heidelberg, pp. 93-127.
- Sprenger, G. A., Schörken, U., Sprenger, G., Sahm, H., 1995. Transketolase A of *Escherichia coli* K12. *European Journal of Biochemistry*. 230, 525-532.
- Thomason, L. C., Costantino, N., Court, D. L., 2007. *E. coli* genome manipulation by P1 transduction. *Current Protocols in Molecular Biology*. 79, 1.17.1-1.17.8.
- Ti, T. Y., Tan, W. C., Chong, A. P. Y., Lee, E. H., 1993. Nonfatal and fatal infections caused by *Chromobacterium violaceum*. *Clinical Infectious Diseases*. 17, 505-507.
- Trouiller, P., Olliaro, P., Torreele, E., Orbinski, J., Laing, R., Ford, N., 2002. Drug development for neglected diseases: a deficient market and a public-health policy failure. *The Lancet*. 359, 2188-2194.

References

- Tyo, K. E. J., Kocharin, K., Nielsen, J., 2010. Toward design-based engineering of industrial microbes. *Current Opinion in Microbiology*. 13, 255-262.
- Vivanco, I., Sawyers, C. L., 2002. The phosphatidylinositol 3-kinase-AKT pathway in human cancer. *Nature Reviews Cancer*. 2, 489-501.
- Wacker, M., Linton, D., Hitchen, P. G., Nita-Lazar, M., Haslam, S. M., North, S. J., Panico, M., Morris, H. R., Dell, A., Wren, B. W., 2002. N-linked glycosylation in *Campylobacter jejuni* and its functional transfer into *E. coli*. *Science*. 298, 1790-1793.
- Wang, H., Jiang, P., Lu, Y., Ruan, Z., Jiang, R., Xing, X. H., Lou, K., Wei, D., 2009. Optimization of culture conditions for violacein production by a new strain of *Duganella* sp. B2. *Biochemical Engineering Journal*. 44, 119-124.
- Weiner, M., Albermann, C., Gottlieb, K., Sprenger, G. A., Weuster-Botz, D., 2014. Fed-batch production of L-phenylalanine from glycerol and ammonia with recombinant *Escherichia coli*. *Biochemical engineering journal*. 83, 62–69.
- WHO, 2012a. Global tuberculosis report 2012.
- WHO, Poliomyelitis - Fact sheet N°114. World Health Organisation, 2012b.
- Wittmann, C., 2007. Fluxome analysis using GC-MS. *Microbial Cell Factories*. 6, 6.
- Wittmann, C., Kiefer, P., Zelder, O., 2004. Metabolic fluxes in *Corynebacterium glutamicum* during lysine production with sucrose as carbon source. *Applied and Environmental Microbiology*. 70, 7277–7287.
- Wittmann, C., Kim, H. M., John, G., Heinzle, E., 2003. Characterization and application of an optical sensor for quantification of dissolved O₂ in shake-flasks. *Biotechnology Letters*. 25, 377-380.
- Wittmann, C., Weber, J., Betiku, E., Krömer, J., Böhm, D., Rinas, U., 2007. Response of fluxome and metabolome to temperature-induced recombinant protein synthesis in *Escherichia coli*. *Journal of Biotechnology*. 132, 375-384.
- Yang, C., Jiang, P., Xiao, S., Zhang, C., Lou, K., Xing, X. H., 2011. Fed-batch fermentation of recombinant *Citrobacter freundii* with expression of a violacein-

synthesizing gene cluster for efficient violacein production from glycerol. *Biochemical Engineering Journal*. 57, 55-62.

Yang, F., Hanna, M. A., Sun, R., 2012. Value-added uses for crude glycerol - a byproduct of biodiesel production. *Biotechnology for Biofuels*. 5, 13.

Yang, L. H., Xiong, H., Lee, O. O., Qi, S. H., Qian, P. Y., 2007. Effect of agitation on violacein production in *Pseudoalteromonas luteoviolacea* isolated from a marine sponge. *Letters in Applied Microbiology*. 44, 625-630.

Yee, L., Blanch, H. W., 1992. Recombinant protein expression in high cell density fed-batch cultures of *Escherichia coli*. *Nature Biotechnology*. 10, 1550-1556.

Zeppenfeld, T., Larisch, C., Lengeler, J. W., Jahreis, K., 2000. Glucose transporter mutants of *Escherichia coli* K-12 with changes in substrate recognition of IICBGlc and Induction behavior of the *ptsG* gene. *Journal of Bacteriology*. 182, 4443-4452.

Zhang, W., Li, F., Nie, L., 2010. Integrating multiple 'omics' analysis for microbial biology: application and methodologies. *Microbiology*. 156, 287–301.

Zhang, Y., Shang, X., Lai, S., Zhang, G., Liang, Y., Wen, T., 2012. Development and application of an arabinose-inducible expression system by facilitating inducer uptake in *Corynebacterium glutamicum*. *Applied and Environmental Microbiology*. 78, 5831-5838.

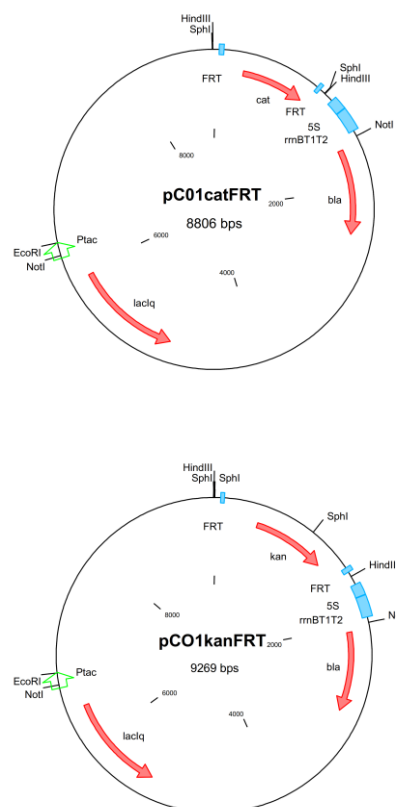
7 Appendix

All the work described in this section was carried out by the group of Prof. Sprenger at the University of Stuttgart, Institute of Microbiology.

7.1. Supplementary Information

7.1.1. Construction of strains TRP1 to TRP6

If not stated otherwise, all strains are based on *E. coli* BW25113 and were obtained by the λ red recombination method (Datsenko and Wanner, 2000). Primers for amplification of gene cassettes (Cm^R or Km^R from plasmids pCO1catFRT or pCO1kanFRT see Suppl. Figure 1) and for verification of



Suppl. Figure 1. Maps of plasmids pCO1catFRT and pCO1kanFRT with relevant features for the present study. Both plasmids are based on vector pJF119EH (Fürste et al., 1986). NotI restriction sites (custom-synthesized by GeneArt, Regensburg, Germany) were introduced by site-directed mutagenesis 5'upstream of the P_{TAC} promoter and 3'downstream of the transcription terminator sequence, 5S $rrmBT1T2$ to obtain vector pF113. Cm^R and Km^R gene cassettes, respectively, were equipped on both ends with FRT sites and HindIII restriction sites, respectively (Degner and Sprenger, unpublished results).

chromosomal insertions, deletions, or disruptions are listed in Supplementary Table 1. If antibiotic resistance cassettes were integrated, P1-mediated transduction could be used to transfer the respective gene disruptions to other strains e.g. *E. coli* MG1655, a parent strain of BW25113 (Datsenko and Wanner, 2000).

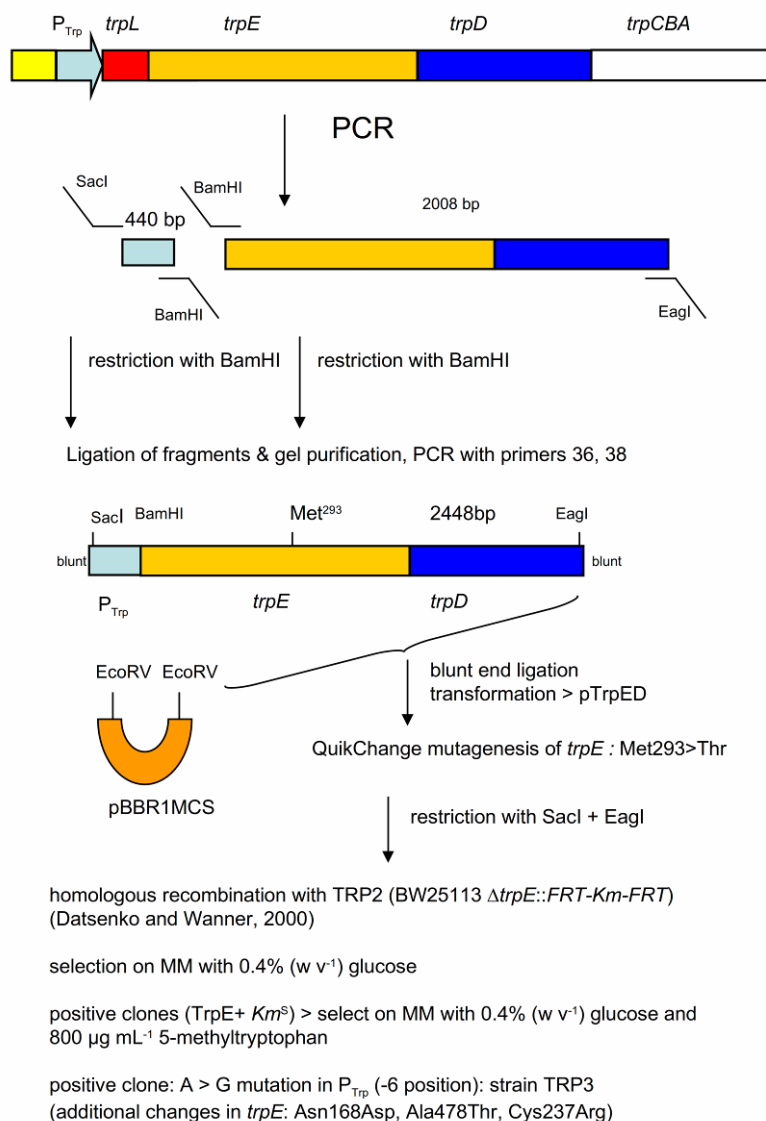
Supplementary Table 1. Primers used.

Primer ID	Primers (5'->3')	Target
27	CAGTCATAGCCGAATAGCCTCTC	K1 primer (inside of <i>Km^R</i> cassette)
28	TGGATAATGTTTTTTCGCGCCGACATCATAACG GTTCTGGCAAATATTCTGAAATGTTGTGTAGG CTGGAGCTGCTTCG	deletion of the <i>trpE</i> gene
29	ATCGGTTGTACAAAACTTTCAGTGCCGCCA GCATTTTCTCTGGCTCATTAATATCATATGAAT ATCCTCCTTAGTTC	
30	TATTCGACATGTTTAAGGTGGGGATTGGTCC CTCATCTTCCCATATGTGTAGGCTGGAGCTG CTTCG	deletion of the <i>sdaA</i> gene
31	TCACACTGGACTTTGATTGCCAGACCACCGC G-TGAGGTTTCCATATGAATATCCTCC TTAGTTC	
32	GCGGTGGCAATAGCGCGCAGTAC	
33	TTTTGAGCTCTGCGCGAGGAACTCACACATTA G	screening of the <i>trpE</i> deletion
34	GGCCTATTTCCCTAAAGGGTTTATTGAG	cat-screen (inside of <i>cat-</i> cassette)
35	TCGCGCCAGTGAAGATGAAGTCTCGG	screening of the <i>sdaA</i> deletion
36	TTTTGAGCTCTGCGCGAGGAACTCACACATTA G	deletion of the <i>trpL</i> sequence (amplification of left fragment) <i>SacI</i> restriction site is underlined
37	TTTTGGATCCCGTGAAGTGGTACTAGTTAA C	deletion of the <i>trpL</i> sequence (left fragment amplification) engineered <i>Bam</i> HI restriction site is underlined
38	TTAAACCGGCCGGAATGTTACTGCCAACCAG CG	deletion of the <i>trpL</i> sequence (amplification of right fragment) engineered <i>EagI</i> restriction site is underlined
39	TTTTGGATCCATTAGAGAATAACAATGCAAAC AC	deletion of the <i>trpL</i> sequence (right fragment amplification) underlined - <i>Bam</i> HI restriction site
40	GAGTAATCCCAGCCCGTACACGTTTTTTATGC AGGATAATG	QuikChange mutagenesis (Met293Thr exchange) of <i>trpE</i> gene
41	CATTATCCTGCATAAAAAACGTGTACGGGCTG GGATTACTC	
42	TTAGTACAGCAGACGGGCGCGAATGGTACCC GGAATAGCTTTCATTGCCTCATATGAATATCC TCCTTAGTTC	deletion of the <i>serA</i> gene
43	AAGGTATCGCTGGAGAAAGACAAGATTAAGT	

Appendix

	TTCTGCTGGTAGAAGGCGTTTGTGTAGGCTG GAGCTGCTTCG	
44	TTTTGAGCTCATGGCAAAGGTATCGCTGGAG AAAG	cloning of the <i>serA</i> gene as well as screening of <i>serA</i> deletion
45	TTTTGTGCGACTTAGTACAGCAGACGGGCGCG	
46	CGCGCAATATCTGCAAGATTCCGCCAGATG GG	QuikChange mutagenesis of the <i>serA</i> gene Thr372Asp
47	CCCATCTGGGCGGAATCTTGCAGATATTGCG CG	
48	GACGAACTGGTGTGGGTAAGCGTATGGAAG AGCACTTGCCTTTTCCGCCTGCTCAAGGCG CACTCCCGTTCTGG	integration of <i>serA</i> into <i>xyI</i> -locus
49	ATTAAAGCTGGGACATTGCTCAGGGTTAATTT CGCGGCCAGACAATCCCAC CAGGGTTATTGTCTCATGAGCG	integration of <i>serA</i> into <i>xyI</i> -locus
50	TGTCCTCACGTAAAGAGCTTGCCAATGCTATT CGTGCGCTGATTGTGTAGGCTGGAGCTGCTT CG	
51	TGCCGGAGCAGATTCACCGAAGGTGGTCATA CCGACGATAGCACATATGAATATCCTCCTTAG TTC	deletion of the <i>tktA</i> gene
52	GGCTGACCGTTGATATTGTTGCCTAGC	screening of <i>tktA</i> disruption
53	TGCAGGCATGAAACCGCGTCTTTTTTCAGATA AAAAGCGCAATCAGTCGCTCAAGGCGCACTC CCGTTCTGG	
54	TAACATTACTCAGCAATAAACTGATATTCCGT CAGGCTGGAATAAGGATGGCCTTCTGCTTAA TTTGATGCCTG	integration of <i>tktA</i> gene into <i>gal</i> locus
55	TTTCACACAGGAAAGCATATGTCGAGCTCGG TACCCGGGGATCCTC	QuikChange mutagenesis of vector pJF119EH- EcoRI >NdeI
56	GGGTACCGAGCTCGACATATGCTTTCCTGTG TGAAATTGTTATCCGCTC	
57	TTTCACACCGCATACGGTGCACTCTCAGTACA ATCTGCTCTG	QuikChange mutagenesis of vector pJF119EH - deletion of NdeI site at position 2421
58	CTGAGAGTGCACCGTATGCGGTGTGAAATAC CGCAC	
59	TCACACAGGAGATATACATATGTCGAGCTCG GTACCCGGG	QuikChange mutagenesis of pJF119E ΔNdeI– modification of sequence between P _{TAC} promoter and start codon to yield pJNNmod
60	CTCGACATATGTATATCTCCTGTGTGAAATTG TTATCCGCTCACAATTC	
61	TTAAACCGGCCGGAATGTTACTGCCAACCAG CG	amplification of P _{TRP} <i>trpE</i> fragment for sequencing
62	TTTTGAGCTCTGCGCGAGGAACTCACACATTA G	
63	CCA GCG AGT GAT AAC GCG CCA C	sequencing of P _{TRP} <i>trpE</i> fragment
64	ACGGCCAGTTAAGCCATTCATGCCAG	screening of the <i>tktA</i> deletion
65	CTCAGCGCACGAATAGCATTGGCAAGC	
66	CCACACGCCACGGTGCGCTTTAG	
67	GAG GTG CAA AGG GTG AGT AGA ATG TTC	screening of the <i>tktA</i> integration

Strain TRP1 (BW25113 $\Delta sdaA::FRT-Cm-FRT$; Table 2): The disruption of gene *sdaA* (encoding a L-serine dehydratase) was accomplished by primers 30 and 31 (encompassing homologous DNA 5' upstream and 3' downstream of *sdaA*) to amplify the Cm^R cassette from pCO1catFRT plasmid. Verification of chromosomal integration was by PCR using primers 34 and 35.



Suppl. Figure 2. Deletion of *trpL* gene and mutagenesis of *trpE* gene in the chromosome of strain BW25113. The strain TRP2 (BW25113 $\Delta trpE::FRT-Km-FRT$) was constructed using the λ red recombination method (Datsenko and Wanner, 2000). Disruption of the *trpE* gene was by insertion of an amplified Km^R cassette from plasmid pCO1kanFRT (Suppl. Figure 1; Degner and Sprenger, unpublished results) and primers 28 and 29.

Strain TRP2 (BW25113 $\Delta trpE::FRT-Km-FRT$, Table 2): The disruption of gene *trpE* (encoding a subunit of anthranilate synthase) was accomplished by primers

28 and 29 (encompassing homologous DNA 5' upstream and 3' downstream of *trpE*) to amplify the Km^R cassette from pCO1kanFRT plasmid. Verification of chromosomal integration was by PCR using primers 32 and 33. Strain TRP2 is tryptophan auxotroph.

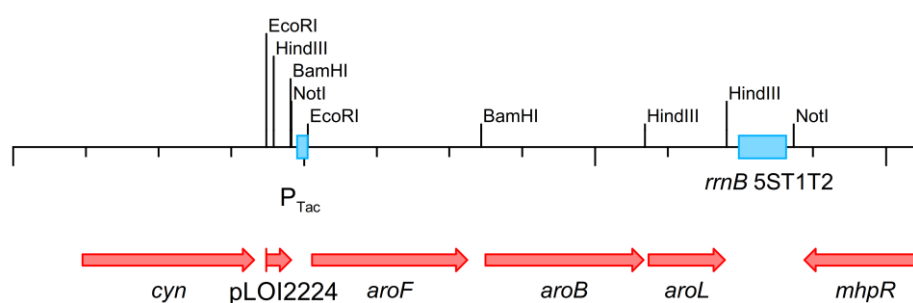
Strain TRP3 (BW25113 $\Delta trpL$, $trpE^{fr}$): Deletion of the *trpL* sequence was carried out by replacing the Km^R cassette in strain TRP2 by a $P_{TRP}\Delta trpL$ - $trpE^{fr}$ - $trpD'$ fragment. This fragment was created by PCR-splicing (see Suppl. Figure 2 for illustration).

The left fragment (440 bp) was PCR-amplified using primers 36 and 37. The fragment contains the promoter of the *trp* operon but lacks the leader peptide coding *trpL* region. A *SacI* restriction site was introduced at the 5', and a *Bam*HI site at the 3' end. The right fragment (2008 bp) was amplified using the primers 38 and 39. This DNA fragment contains the complete *trpE* gene and a 5' portion of the *trpD* gene. A *Bam*HI site was introduced at the 5', and an *EagI* site at its 3' end. Next, both DNA fragments were digested with *Bam*HI, purified and excised from an agarose gel, and ligated in a 1:1 molar ratio. This ligation mix was used as template for the next PCR which was performed with the primers 36 and 38. The resulting fragment (2448 bp) was purified from a 0.8% ($w v^{-1}$) agarose gel, and blunt-end ligated with pBBR1MCS vector DNA (Kovach et al., 1994) that had been linearized with *EcoRV*, to result in plasmid pTrpED. pTrpED DNA was used as template for QuikChange mutagenesis (QuikChange® Site-Directed Mutagenesis Kit, Stratagene, San Diego, USA) to obtain a feedback-resistant variant of anthranilate synthase, encoded by $trpE^{fr}$. QuikChange mutagenesis (Hogrefe et al., 2002) was carried out with the primers 40 and 41 to change the codon for Met in position 293 to Thr (Caligiuri and Bauerle, 1991). The resulting mutant plasmid was designated pTrpED-M293. DNA sequencing revealed additional changes which lead to the following amino acid alterations: Asn168Asp, Cys237Arg, and Ala478Thr. According to literature, these changes are not detrimental to enzyme structure or activity of anthranilate synthase.

For the replacement of the Km^R cassette in strain TRP2 (BW25113 $\Delta trpE::FRT$ - Km - FRT), TrpED-M293 plasmid DNA was digested with *EagI* and *SacI* and used for homologous λ red recombineering with strain TRP2 (transiently carrying pKD46 plasmid) as recipient. As TRP2 is tryptophan-auxotroph, selection was done on minimal medium agar plates containing 0.4% ($w v^{-1}$) glucose and 20

$\mu\text{g mL}^{-1}$ thiamine but lacking L-tryptophan. The resulting clones should have exchanged the residing $\Delta\text{trpE}::\text{FRT-Km-FRT}$ by the incoming $\Delta\text{trpL-trpE}^{\text{fr}}$ version. To test for feedback-resistant clones, colonies were plated on mineral medium (MM) agar plates containing the antimetabolite, 5-methyl-tryptophan (5MT). Initially, all tryptophan-prototroph clones showed reduced growth on MM agar (0.4% (w v⁻¹) glucose and 20 $\mu\text{g mL}^{-1}$ thiamine) containing 800 $\mu\text{g mL}^{-1}$ 5MT. After 2-3 days, papillae arose which could grow in the presence of 5MT. One of these papillae was picked and colony-purified. Its chromosomal DNA was isolated and a region encompassing the P_{TRP} promoter and the *trpE* gene was amplified by PCR with primers 61 and 62. DNA sequencing (with primer 63) revealed that P_{TRP} operator (*trpO*) region carries a mutation (transition A > G in position -6 relative to the transcription start), presumably leading to constitutive and increased transcription of the *trp* operon message. This mutant strain was termed TRP3 (BW25113 $\Delta\text{trpL, trpE}^{\text{fr}}$).

Strain TRP4 (F52 $\Delta\text{lac}::\text{P}_{\text{TAC}}\text{aroFBL-FRT-Km-FRT}$) is based on an *E. coli* K-12 W3110 derivative F52 which was from an unrelated study (Trachtmann and Sprenger, unpublished results) and which had obtained the artificial operon encoding the *aroFBL* genes from *E. coli* by P1-mediated transduction from strain F144 (Orf and Bongaerts, unpublished results). Relevant markers for the present study are the artificial *aroFBL* operon under control of P_{TAC} promoter. For illustration see Suppl. Figure 3.



Suppl. Figure 3. Chromosomal integration of *E. coli* *aroFBL* genes as an artificial operon under control of a P_{TAC} promoter (Orf and Bongaerts, unpublished results) replacing the resident *lacIZYA* gene cluster. For the DNA sequence of the respective region see Suppl. Figure 4 and text.

The DNA sequence was established and is presented in Suppl. Figure 4. The artificial operon is essentially based on plasmid-borne *aroFBL* genes of *E. coli* as present on vector pF81 (Rüffer et al., 2004) which were assembled under control

of P_{TAC} promoter on vector pF113 (see legend of Suppl. Figure 1). Therefrom, a NotI fragment containing $P_{TAC}aroFBL$ and the termination sequence *rrnB5ST1T2* was excised. Suicide vector pLOI2224 (Km^R ; (Martinez-Morales et al., 1999) gene sequence in Genbank AF172934) was digested with NotI, treated with Klenow polymerase to fill-in overlapping sequences and religated. This pLOI2224 Δ NotI plasmid DNA was double digested with EcoRI plus BamHI and ligated to upstream and downstream sequences of the *lacIZYA* gene cluster from *E. coli*. As well, FRT sites were introduced adjacent to a kanamycin resistance marker and to oriR6K of pLOI2224 and a unique NotI site was engineered. Finally the NotI fragment containing $P_{TAC}aroFBL$ was ligated to yield vector pC102 (Orf and Bongaerts, unpublished results). The vector was introduced into strain W3110 wildtype

```
5' ATGATTCAGTCACAAATTAACCGCAATATTCGTCTTGATCTTGCCGATGCCATTTTGCTCAGCAAAGCTAA
AAAAGATCTCTCATTTGCCGAGATTGCCGACGGCACCGGTCTGGCAGAAGCCTTTGTAACCGCGGCTTTGCTG
GGTCAGCAGGCGCTTCCTGCCGACGCCGCCCGCTGGTCGGGGCGAAGCTGGATCTCGACGAAGACTCCATTC
TACTGTTGCAGATGATTCCACTGCGTGGCTGCATTGATGACCGTATTCCAACGATGATATCGTTT
CTATGAAATGTTGCAGGTGTACGGTACAACCCTGAAAGCGTTGGTTCATGAGAAATTTGGCGATGGCATTATT
AGCGCGATTAACCTTCAAACGACGTTAAGAAAGTGGCGGACCCGGAAGGTGGCGAACGTCGCGTATCACCCT
TAGATGGTAAATATCTGCCGACCAAACCGTTCTGACAGCCATGCGCAACCATCAAAAGACGTTACAGATGCTG
CTGGTACTGGTGCTGATTGGTCTTAATATGCGACCACTGCTCACCTCCGTCGGGCCACTGCTACCGCAATTGC
GCCAGGCGAGCGGAATGAGCTTTAGCGTGGCTGCCCTGTTGACCGCTCTGCCGGTGGTTACCATGGGCGGGCT
GGCGCTGGCCGGAAGCTGGCTTCATCAGCATGTCAGCGAACGTCGCAGTGTGCCATCAGTCTGTTGCTGATT
GCCGTCGGTGCATTGATGCGTGAGCTTTACCCGCAAAGTGCCTGCTGCTTAGCAGCGCACTGCTTGGTGGGG
TGGGGATCGGCATCATTACAGGCGGTGATGCCTTCGGTGATTAACGGCGGTTTCAGCAGCGCACGCCACTGGT
GATGGGGCTGTGGTCCGCGGCTCTGATGGGCGGCGGTGGGCTTGGTGCCGCCATAACGCCCTGGTTAGTTCAA
CATAGCGAAACCTGGTATCAAACACTCGCCTGGTGGGCGCTGCCTGCCGTTGTTGCGCTCTTTGCCCTGGTGGT
GGCAAAGCGCCCGCAGGTGCGCTCTTCCACAAGACAACAACCACTCCGGTTCGCGTGGTATTCACTCCCCG
CGCGTGGACGCTGGGTGTTTACTTCGGTCTGATTAACGGCGGTTACGCCAGCCTGATTGCCTGGTTACCCGCT
TTCTATATTGAGATTGGTGCCAGCGCGCAGTACAGCGGTTCCCTTACTGGCATTGATGACGCTTGGGCAAGCCG
CAGGAGCTTTGCTGATGCCTGCTATGGCTCGCCATCAGGATCGGCGCAAACGTTAATGCTGGCGCTGGTGT
ACAACGGTGGGGTTCGCGGCTTTATCTGGCTGCCGATGCAATTGCCGGTATTGTGGGCGATGGTGTGTGGG
TTAGGTCTGGGCGGCGCGTTCGCTCTGTTTGTGCTGGCGCTCGATCACTCTGTGCAACCGGCTATTGCTG
GCAAGCTGGTGGCGTTTATGCAGGGAATCGGTTTTATCATCGCCGGGCTTGCCCCGTGGTTTTCTGGCGTGT
CGGTAGTATCAGCGCAATTACCTGATGGACTGGGCAATTCATCGCTGTGCGTGTGCGTGTGGGCTGATGATCATA
ACCTCGGTTTTTGACCAAGTACGTTTTCCGCGAGCTGTGGTCAAAGAGGCGATGATGCGACGCTGTTCTCCGCG
CTTTGTTTACGCCGATGCGGCTAATGTAGATCGCTGAACCTGTAGGCTGATAAGCGCAGCGGAATTCGGT
CTCCCTATAGTGAGTCGTATTAATTTGATAAGCCAGATCAAGCTTGTGCGACCAATTCGAAGTTCTTATACTT
TCTAGAGAATAGGAACCTCCGGGATCAATTCATCGCGGAATTAATTCGAGCTCGGGAAGATCTTCCGGAAAGAT
CTTCCCCGGGGATCCGCGGCCGCATCATAACGGTTCTGGCAAATATTCTGAAATGAGCTGTTGACAATTAATC
ATCGGCTCGTATAATGTGTGGAATTGTGAGCGGATAACAATTTACACAGGAAACAGAATTCGAGCATAAAACA
GGATCGCCATCATGCAAAAAGACGCGCTGAATAACGTACATATTACCGACGAACAGGTTTTAATGACTCCGGA
ACAACGAAGGCCGCTTTTCCATTGAGCCTGCAACAAGAAGCCAGATTGCTGACTCGCGTAAAAGCATTTCA
GATATTATCGCCGGGCGGATCCTCGTCTGCTGGTAGTATGTGGTCCCTGTTCCATTGATGATCCGAAACTG
CTCTGGAATATGCTCGTGCATTTAAAGCCCTTGCCGCGAGAGGTCAGCGATAGCCTCTATCTGGTAATGCGCGT
CTATTTTGAAAACCCCGTACCCTGTCGGCTGGAAAGGGTTAATTAACGATCCCCATATGGATGGCTCTTTT
GATGTAGAAGCCGGGCTGCAGATCGCGCGTAAATTGCTGCTTGAGCTGGTGAATATGGGACTGCCACTGGCGA
CGGAAGCGTTAGATCCGAATAGCCCGCAATACCTGGGCGATCTGTTTAGCTGGTCAGCAATTTGGTGCTCGTAC
AACGGAATCGCAAACCTCACCGTGAAATGGCCTCCGGGCTTTCCATGCCGGTGGTTTTAAAAACGGCACCGAC
GGCAGTCTGGCAACAGCAATTAACGCTATGCGCGCCGCCAGCCGACCGTTTTTGTGGCATTAACCAGG
CAGGGCAGGTTGCGTGTGTACAAACTCAGGGGAATCCGGACGGCCATGTGATCCTGCGCGGTGGTAAAGCGCC
GAACTATAGCCCTGCGGATGTTGCGCAATGTGAAAAAGAGATGGAACAGGCGGGACTGCGCCCGTCTCTGATG
GTAGATTGCAGCCACGGTAATTCGAATAAAGATTATGCGCGTCAGCCTGCGGTGGCAGAATCCGTGGTTGCTC
AAATCAAAGATGGCAATCGCTCAATTATTGGTCTGATGATCGAAAGTAATATCCACGAGGGCAATCAGTCTTC
```

CGAGCAACCGCGCAGTGAATGAAATACGGTGTATCCGTAACCGATGCCTGCATTAGCTGGGAAATGACCGAT
 GCCTTGCTGCGTGAAATTCATCAGGATCTGAACGGGCAGCTGACGGCTCGCGTGGCTTAAGAGGTTTATTATG
 GTTGCTGAATTGACCGCATTACCGGATCAAATTGATGAAGTCGATAAAGCGCTGCTGAATTTATTAGCGAAGC
 CCCGGGGGATCCGTAATTAAGGTGGATGTCGCGTTATGGAGAGGATTGTCGTTACTCTCGGGGAACGTAGTTA
 CCCAATTACCATCGCATCTGGTTTGTTTAATGAACCAGCTTCATTCCTTACCCTGAAATCGGGCGAGCAGGTC
 ATGTTGGTCACCAACGAAACCTGGCTCCTCTGTATCTCGATAAAGTCCGCGGGCTACTTGAACAGGCGGGTG
 TTAACGTCGATAGCGTTATCCTCCCTGACGGCGAGCAGTATAAAAGCCTGGCTGTACTCGATAACCGTCTTTAC
 GCGTGTGTACAAAAACCGCATGGTTCGCGATACTACGCTGGTGGCGCTTGGCGGGCGGCTAGTGGGCGATCTG
 ACCGGCTTCGCGGGCGAGTTATCAGCGCGGTGTCCTGTTTCATTCAAGTCCCAGACGTTACTGTCCGAGG
 TCGATTTCCGTTGGCGGCAAACTGCGGTCAACCTCCCTCGGTAAAAACATGATTTGGCGGCTTCTACCA
 ACCTGCTTCAGTGGTGGTGGATCTCGACTGCTGAAAACGCTTCCCCCGCGTGAGTTAGCGTCGGGGCTGGCA
 GAAGTCATCAAATACGGCATTATTTCTTGACGGTGCCTTTTTTAACTGGCTGGAAGAGAATCTGGATGCGTTGT
 TGCGTCTGGACGGTCCGGCAATGGCGTACTGTATTTCGCCGTTGTTGTGAAGTGAAGGCAGAAGTTGTCGCCGC
 CGACGAGCGCAAAACCGGGTTACGTGCTTTACTGAACTGGGACACACCTTTGGTCATGCCATTGAAGCTGAA
 ATGGGGTATGGCAATTGGTTACATGGTGAAGCGTTCGTCGGGGTATGGTGATGGCGGGCGGGACGTCGGAAC
 GTCTCGGGCAGTTTAGTTCTGCCGAAACGCAGCGTATTATAACCTGCTCAAGCGGGCTGGGTTACCGGTCAA
 TGGGCCGCGCAAAATGTCGCGCAGGCGTATTTACCGCATATGCTGCGTGACAAGAAAGTCTTGGCGGAGAG
 ATGCGCTTAATTTCTCCGTTGGCAATTGGTAAGAGTGAAGTTCGCAGCGGGCTTTCGCACGAGCTTGTCTTA
 ACGCCATTGCCGATTGTCAATCAGCGTAACAACAAGAAAGCTTCTATTGGGGAAAACCCACGATGACACAACC
 TCTTTTTCTGATCGGGCTCGGGGCTGTGGTAAAACAACGGTTCGGAATGGCCCTTGGCGATTTCGCTTAACCGT
 CGGTTTGTGCGATAACCGATCAGTGGTTGCAATCACAGCTCAATATGACGGTTCGCGGAGATCGTCGAAAGGGAAG
 AGTGGGCGGGATTTTCGCGCCAGAGAAAACGGCGGGCGTGGAAAGCGGTAACCTGCGCCATCCACCGTTATCGCTAC
 AGGCGGGCGGCATTATTTCTGACGGAAATTTAATCGTCACTTCATGCAAAATAACGGGATCGTGGTTTATTTGTGT
 GCGCCAGTATCAGTCTGGTTAACCGACTGCAAGCTGCACCGGAAGAAGATTTACGGCCAACCTTAACGGGAA
 AACCGCTGAGCGAAGAAGTTCAGGAAGTGTGGAAGAACCGGATGCGCTATATCGCGAAGTTGCGCATATTTAT
 CATCGACGCAACAAACGAACCCAGCCAGGTGATTTCTGAAATTCGCAGCGCCCTGGCAGACAGATCAATTTGT
 TGATTTTCGAGCGCAAGCTTCTGTTTTGGCGGATGAGAGAAGATTTTCAGCTGATACAGATTAATTAAGAAC
 GCAGAAGCGGTCTGATAAAAACAGAATTTGCCGCGGAGTAGCGCGGTGGTCCCACCTGACCCCATGCCGAA
 CTCAGAAGTGAACGCCGTAGCGCCGATGGTAGTGTGGGGTCTCCCCATGCGAGAGTAGGGAACCTGCCAGGCA
 TCAAATAAAAACGAAAGGCTCAGTCGAAAAGACTGGGCCCTTTCGTTTTATCTGTTGTTTGTGCGGTGAACGCTCTC
 CTGAGTAGGACAAAATCCGCCGGGAGCGGATTTGAACGTTGCGAAGCAACGGCCCGGAGGGTGGCGGGCAGGAC
 GCCCGCCATAAACTGCCAGGCATCAAATTAAGCAGAAGGCCATCTGACGGATGGCCCTTTTTCGCTTCTACA
 AACTCTTTTGTATTTTCTAAATACATTCAAATATGCGGCCGCCCTGAATTGACTCTCTTCCGGGCGCTATC
 ATGCCATAACCGAAAGGTTTTCGCGCATTCGATGGTGTCAACGTAATGCATGCCGCTTCGCCTTCCGGCCA
 CCAGAATAGCCTGCGATTCAACCCCTTCTTCGATCTGTTTTGCTACCCGTTGTAGCGCCGGAAGATGCTTTTC
 CGCTGCCTGTTCAATGGTCAATTGCGCTCGCCATATACACCAGATTCAGACAGCCAATCACCCGTTGTTCACTG
 CGCAGCGGTACGGCGATAGAGGCGATCTTCTCCTCCTGATCCCAGCCGCGGTAGTTCTGTCCGTAACCCCTTT
 TGCGCGCGCGCCAGAATGGCTTCCAGCTTTAACGGTTCCCGTGCCAGTTGATAGTCATCACCGGGGCGGGA
 GGCTAACATTTTCGATTAATTTCTTGGCGTCTTGTTCGGGGCAAAAGGCCAGCCAGGTCAGGCCCGAGGCGGTT
 TTCAGAAGCGGCAAAACGTCGCCCGACCATTTGCCCGGTGAAAGGATAAGCGGCTGAAACGGTGAGTGGTTTCGC
 GTACCACCATTCATCAACATCCAGCGTGGACACATCTGTCCGGCATAACCACTTCGCGCAACAGATCGCCCAG
 CAGTGGGGCCCGAGTGCAGAAATCCACTGTTTCGTCACGAAATCCTTCGCTTAATTGCCGCACTTTGATGGTC
 AGTCGAAAATATCATCGGAGGGGCTACGGCGGACATATCCCTCTTCTGACGCGTCTCCAGCAGTCGCCGCA
 CAGTGGTGCATGCAGGCCGCTGAGTTCCGCCAGCAGCCCGACGCTGGCACCGCCATCAAGTTTATTTAACAT
 ATTTAATAACATTAGACCGCGGGTTAAGCCGCGCACGGTTTTGTATTCCGTCGCTCATTGTTCTGCAT3'

Suppl. Figure 4. DNA sequence of chromosomal $P_{TAC}aroFBL$ region.

(LJ110; (Zeppenfeld et al., 2000)) and selection was on resistance against kanamycin. Km^R recombinants were screened for loss of the chromosomal *lacZYA* genes (lactose-negative phenotype) and verified by PCR. Using phage P1-assisted transduction, the chromosomal region could be transferred to other *E. coli* recipient strains. To remove the Km^R cassette, the FLP recombination method using plasmid pCP20 (Cherepanov and Wackernagel, 1995) was used. Suppl. Figure 3 depicts the chromosomal gene order after FLP recombination. The DNA

sequence of the chromosomal region $\Delta lac::P_{TAC}aroFBL-FRT-Km-FRT$ was finally verified by DNA sequencing. The sequence is given in Suppl. Figure 4.

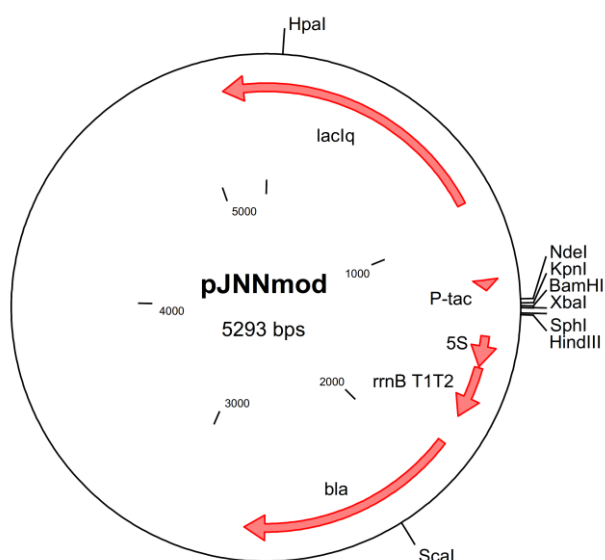
Strain TRP5 (BW25113 Ara⁺ $\Delta tktA$ $\Delta gal::P_{TAC}tktA-FRT-Cm-FRT$): First, strain BW25113 strain was made arabinose-positive by P1-mediated transduction using a P1 lysate grown on strain LJ110 (Zeppenfeld et al., 2000). Selection was carried out on plates with MM and 0.4% (w v⁻¹) L-arabinose. This strain was termed BW25113Ara⁺. Next, the residing *tktA* gene was deleted using the *Km*^R cassette from plasmid pCO1kanFRT (Suppl. Figure 1) and using the primers 50 and 51. The PCR amplicon was introduced by electroporation into strain BW25113Ara⁺ and selection was for *Km* resistance. The disruption was confirmed by PCR using primers 52 and 27. Removal of the *Km*^R cassette was carried out by FLP recombinase with transient transformation by plasmid pCP20 to give strain BW25113Ara⁺ $\Delta tktA$. Verification of the deletion was performed with PCR using primers 64 and 65. Wild type *tktA* gene from *E. coli* K-12 (Sprenger et al., 1995) was cloned on plasmid pF113 to give plasmid pC18 (Degner and Sprenger, unpublished results). A *Cm*^R cassette from pCO1catFRT (Suppl. Figure 1) was prepared by HindIII digestion and gel purification and ligated to vector pC18 (linearized with HindIII), downstream of the *tktA* gene. This gene construct was then PCR amplified using primers 53 and 54 which contain homologous DNA sequences to the *gal* locus of *E. coli* chromosome. The resulting PCR amplicon was used to transform strain BW25113Ara⁺ $\Delta tktA$ to resistance against chloramphenicol. *Cm*^R transformants were checked for their Tkt-positive phenotype and verified by PCR using primers 66 and 67.

Strain TRP6 (BW25113 $\Delta serA$ $\Delta xyl::P_{TAC}serA^{fr}-FRT-Km-FRT$): Deletion of the chromosomal *serA* gene was carried out by the replacement of the gene with the *Km*^R cassette which had been PCR-amplified from pCO1kanFRT plasmid with primers 42 and 43. *Km*^R clones were verified by PCR screening with primers 44 and 45. For chromosomal integration of a *serA* gene encoding a feedback-resistant 3-phosphoglycerate dehydrogenase (*serA*^{fr}), pJA-*serA* plasmid was constructed first. The *serA* gene was PCR amplified from the LJ110 chromosome using the primers 44 and 45 and cloned into SacI and Sall restriction site in the pJF119EH vector (Fürste et al., 1986) under control of the P_{TAC} promoter. A feedback resistance of the protein was engineered by QuikChange mutagenesis (Hogrefe et al., 2002). The codon for Thr at position 372 was changed to encode

Asp (Thr372Asp) to yield an enzyme (3-phosphoglycerate dehydrogenase) which is feedback-resistant against L-serine (Maier and Flinspach). Site-directed PCR mutagenesis was performed with the primers 46 and 47 (pJF119serA^{fr}). The *Km*^R cassette from pCO1kanFRT was ligated to pJF119serA^{fr} (linearized with HindIII) downstream of the *serA*^{fr} gene to yield pJF119serA^{fr}-FRT-Km-FRT. For chromosomal integration, the *xyl* locus was chosen and strain BW25113Δ*serA* was the recipient. The _{P_{TAC}}*serA*^{fr}-FRT-Km-FRT region was PCR-amplified from pJF119serA^{fr}-FRT-Km-FRT plasmid with primers 48 and 49. The selection was carried out on plates with LB and *Km*. *Km*^R clones were tested on MacConkey agar with 1% (w v⁻¹) xylose (pale colonies due to loss of xylose catabolism) and on MM agar containing kanamycin and glucose.

7.1.2. Cloning of vector pJNNmod

Plasmid vector pJNNmod is based on plasmid pJF119EH (Fürste et al., 1986). First, an EcoRI site (in the polylinker region) of pJF119EH was changed to NdeI site by QuikChange mutagenesis with primers 55 and 56. Next, the resident



Suppl. Figure 5. Map of plasmid pJNNmod. The plasmid is based upon pJF119EH (Fürste et al., 1986). The multiple cloning site has been changed to contain restriction sites for the following enzymes: NdeI-KpnI-BamHI-XbaI-SphI-HindIII. (Trachtmann and Sprenger, unpublished results).

NdeI site was removed by QuikChange mutagenesis with primers 57 and 58 to yield pJNN plasmid. To optimize the distance between the P_{TAC} promoter and the start codon, this region was also modified by the QuikChange method using 59 and 60 as primers for this step. Ultimately, the pJNNmod vector (Suppl. Figure 5) was constructed.